INFORMATION TO USERS

This material was produced from a microfilm copy of the original document. While the most advanced technological means to photograph and reproduce this document have been used, the quality is heavily dependent upon the quality of the original submitted.

The following explanation of techniques is provided to help you understand markings or patterns which may appear on this reproduction.

1. The sign or "target" for pages apparently lacking from the document photographed is "Missing Page(s)". If it was possible to obtain the missing page(s) or section, they are spliced into the film along with adjacent pages. This may have necessitated cutting thru an image and duplicating adjacent pages to insure you complete continuity.

2. When an image on the film is obliterated with a large round black mark, it is an indication that the photographer suspected that the copy may have moved during exposure and thus cause a blurred image. You will find a good image of the page in the adjacent frame.

3. When a map, drawing or chart, etc., was part of the material being photographed the photographer followed a definite method in "sectioning" the material. It is customary to begin photoing at the upper left hand corner of a large sheet and to continue photoing from left to right in equal sections with a small overlap. If necessary, sectioning is continued again – beginning below the first row and continuing on until complete.

4. The majority of users indicate that the textual content is of greatest value, however, a somewhat higher quality reproduction could be made from "photographs" if essential to the understanding of the dissertation. Silver prints of "photographs" may be ordered at additional charge by writing the Order Department, giving the catalog number, title, author and specific pages you wish reproduced.

5. PLEASE NOTE: Some pages may have indistinct print. Filmed as received.

Xerox University Microfilms
300 North Zeeb Road
Ann Arbor, Michigan 48106

Downloaded from SHAREOK. Persistent Handle URL: https://hdl.handle.net/11244/3639

74-6959

KILLION, Jerald Jay, 1942-
THE EFFECT OF CONCANAVALIN A ON THE GROWTH AND ELECTRICAL PROPERTIES OF TUMOR CELLS.

The University of Oklahoma, Ph.D., 1973
Biophysics, medical

University Microfilms, A XEROX Company, Ann Arbor, Michigan

© 1973

JERALD JAY KILLION

ALL RIGHTS RESERVED

THIS DISSERTATION HAS BEEN MICROFILMED EXACTLY AS RECEIVED.

THE UNIVERSITY OF OKLAHOMA

GRADUATE COLLEGE

THE EFFECT OF CONCANAVALIN A ON THE GROWTH AND ELECTRICAL PROPERTIES OF TUMOR CELLS

A DISSERTATION

SUBMITTED TO THE GRADUATE FACULTY

in partial fulfillment of the requirements for the

degree of

DOCTOR OF PHILOSOPHY

BY

JERALD JAY KILLION

Oklahoma City, Oklahoma

1973

THE EFFECT OF CONCANAVALIN A ON THE GROWTH

AND ELECTRICAL PROPERTIES

OF TUMOR CELLS

APPROVED BY

Roger Thies

Bernard Rabinovitch

Paul B. McCay

Jack Kyle

DISSERTATION COMMITTEE

TO MY WIFE AND DAUGHTER

CATHY AND JULIE

ACKNOWLEDGMENTS

I wish to thank my major advisor, Dr. Tushar Chowdhury, Department of Physiology and Biophysics, for his assistance during the course of my studies. I am very grateful to the Oklahoma Medical Research Foundation for their generous support the past two years. Appreciation is also extended to the members of my Graduate Committee for their help in preparing this dissertation.

A special debt of gratitude belongs to Dr. Mark Kollmorgen, Cancer Section, OMRF. He provided and sustained an atmosphere of untiring guidance and encouragement throughout the completion of this research. The dedication, productivity, and integrity with which he approaches any task has been a valuable experience. His curiosity, questions, criticism, and suggestions have been as unselfish as his help in the laboratory.

I want to thank Dave Erwin for endless hours of helpful discussions and Joyce Phillips for her patience with my fickle mind as she typed this manuscript.

It would be impossible to express the many, many thoughts of appreciation I have for my wife, Cathy, and daughter, Julie. Suffice it to know that my graduate studies could not have been accomplished without their warm love.

TABLE OF CONTENTS

Page

LIST OF TABLES..... vi

LIST OF ILLUSTRATIONS..... viii

Chapter

I. INTRODUCTION
- Membrane Properties of Tumor Cells..... 1
- The Cell Surface, Ions, and Growth Regulation..... 5
- The Transmembrane Potential and Cell Growth..... 9
- Concanavalin A and Some Of Its Biological Effects..... 12
- Specific Aims..... 16

II. MATERIALS AND METHODS
- Tissue Culture..... 17
- Agglutination Studies..... 22
- Microelectrode Studies..... 25
- Electrical Recording System..... 28
- Measurement of the TMP and MR of Tissue-Culture Cells..... 29
- Statistical Analysis of Data..... 33

III. RESULTS
- Physico-chemical Factors of Agglutination..... 34
- Growth Parameters of the 3T3 and PY3T3 Cell Lines..... 53
- Agglutination Studies on the 3T3 and PY3T3 Cells..... 62
- Differential Effect of Native and TRYP-Con A on Cell Growth..... 70
- Growth Parameters of the Chronic TRYP-Con A Treated PY3T3 Cell Line..... 74
- Microelectrode Properties and Cell Penetration..... 83
- The Effect of Cell Density, Ions, and Temperature on the Transmembrane Potential and Resistance..... 89
- The Effect of Acute and Chronic TRYP-Con A Treatment on the TMP and MR..... 99

IV. DISCUSSION
- Physico-chemical Factors of Agglutination..... 105
- Effects of External Ions on the Transmembrane Potential and Membrane Resistance..... 110
- Electrical Properties of 3T3 and PY3T3 Cells..... 123
- The Effect of TRYP-Con A on the TMP and MR..... 127
- Summary..... 132

BIBLIOGRAPHY..... 135

LIST OF TABLES

Table		Page
1.	Composition of Solutions.....	20
2.	Composition of Solutions used for Agglutination Studies.....	23
3.	Composition of Solutions used for Microelectrode Studies.....	32
4.	Concentration of Con A Required for 75% Cell Agglutination.....	42
5.	Test of D-Mannitol for Hapten-Inhibition of Agglutination.....	42
6.	Concentration of α-methyl-D-Mannoside Required for Hapten-Inhibition of Agglutination at Regular and Low Ionic Strength.....	49
7.	The Irreversible Nature of Agglutination at Low Ionic Strength using Con A.....	49
8.	Agglutination of Cells Incubated at Regular Ionic Strength with Con A, Followed by Assay at Low Ionic Strength with No Con A.....	51
9.	Agglutination of Cells Incubated at Regular Ionic Strength with Con A, Followed by Assay at Low Ionic Strength with Con A.....	51
10.	Agglutination of Cells Incubated at Low Ionic Strength with Con A, Followed by Incubation at Regular Ionic Strength with No Con A.....	52
11.	Mixed Agglutination of Cells when Incubated at Different Ionic Strengths.....	52
12.	Specificity of Agglutination of L5178Y Cells by Con A using Hapten-Inhibitors.....	54
13.	The Minimum Concentration of Con A Required to Yield a Score of 1+.....	55
14.	The Degree of Agglutination of 3T3 Cells with Con A.....	65
15.	Agglutination of 3T3 Cells at Various Ionic Strengths using 25 μg/ml Con A.....	65

LIST OF TABLES-continued

Table		Page
16.	Agglutination of 3T3 Cells at Various Ionic Strengths	67
17.	Agglutination of 3T3 Cells at Various Ionic Strengths using 50 and 200 µg/ml Con A	68
18.	The Degree of Agglutination of PY3T3 Cells with Con A	69
19.	Degree of Agglutination of PY3T3 Cells at Low Ionic Strength with Con A	71
20.	Growth Parameters and Agglutinability of 3T3, PY3T3, and PY3T3CCA Cells	80
21.	The Effects of External Ions on the Transmembrane Potential and Membrane Resistance of 3T3 Cells	95
22.	The Effects of External Ions on the Transmembrane Potential and Membrane Resistance of PY3T3 Cells	96
23.	The Effect of Temperature on the Transmembrane Potential and DC Membrane Resistance of 3T3 and PY3T3 Cells	100

LIST OF ILLUSTRATIONS

Figure		Page
1.	The Basic Protocol used for Agglutination Studies.....	26
2.	Basic Electronic Instrumentation used for the Microelectrode Studies.....	30
3.	Degree of Agglutination as a Function of Time.....	35
4.	Degree of Agglutination as a Function of Time Semi-log Plot.....	36
5.	Degree of Agglutination as a Function of the Con A Concentration.....	38
6.	Degree of Agglutination as a Function of the Cell Density.....	39
7.	Degree of Agglutination as a Function of the Con A Concentration, Semi-log Plot.....	40
8.	Degree of Agglutination as a Function of the Ionic Strength.....	44
9.	Degree of Agglutination as a Function of the Ionic Composition of the Solution.....	45
10.	Percent of Cells Agglutinated as a Function of Diluting Mannoside.....	47
11.	Normalized Plot of the Percent of Cells Agglutinated as a Function of Diluting Mannoside.....	48
12a.	3T3 Cells in Sparse Culture, 300x.....	57
12b.	3T3 Cells at Confluency, 300x.....	57
13a.	PY3T3 Cells in Sparse Culture, 300x.....	58
13b.	PY3T3 Cells at Saturation Density, 300x.....	58
14.	Growth of 3T3 Cells.....	60
15.	Growth of PY3T3 Cells.....	61
16.	The Percent of ^{3}H-labeled 3T3 Cells with Time.....	63
17.	The Percent of ^{3}H-labeled PY3T3 Cells with Time.....	64
18.	Growth of L5178Y Cells with native Con A.....	72

LIST OF ILLUSTRATIONS-continued

Figure		Page
19.	Growth of L5178Y Cells with TRYP-Con A	73
20a.	PY3T3CCA Cells after 2 Months, 300x	75
20b.	PY3T3CCA Cells after 4 Months, 300x	75
20c.	PY3T3CCA Cells after 6 Months, 300x	76
21.	Growth of PY3T3CCA Cells after 1, 2, and 3 Months	78
22.	Growth of PY3T3CCA Cells after 4,5, and 6 Months	79
23.	Growth of PY3T3 Cells Following Acute Treatment with TRYP-Con A	81
24.	The Percent of ^{3}H-labeled Cells with Time Following Acute Treatment with TRYP-Con A	82
25.	Change in Tip Potential as a Function of the Tip Potential	84
26.	Change in Tip Resistance as a Function of the Tip Resistance	85
27.	Change in Tip Resistance as a Function of the Tip Potential	87
28.	Example of a Successful Cell Puncture	88
29.	The Transmembrane Potential as a Function of Cell Density	91
30.	The DC Membrane Resistance as a Function of Cell Density	92
31.	Histograms of the Transmembrane Potential as a Function of Cell Density	93
32.	Histograms of the DC Membrane Resistance as a Function of Cell Density	94
33.	The Effect of a One-Hour Incubation with TRYP-Con A on the Transmembrane Potential and DC Membrane Resistance in PY3T3 Cells	101

LIST OF ILLUSTRATION-continued

Figure		Page
34.	The Effect of Chronic TRYP-Con A on the Transmembrane Potential and DC Membrane Resistance of PY3T3 Cells	103
35.	The Transmembrane Potential of 3T3 and PY3T3 Cells as a Function of External Potassium	112
36.	The Value of $\exp(E_m F/RT)$ for 3T3 Cells as a Function of External Potassium	114
37.	The Value of $\exp(E_m F/RT)$ for PY3T3 Cells as a Function of External Potassium	115
38.	A Comparison of the Theoretical Curve for the Equation $0.24\sqrt{(K)_o}-0.014(K)_o-0.24$ and Data	116
39.	The Permeability Ratio P_{Na}/P_K as a Function of External Potassium, as derived from the Modified Goldman Equation	118

THE EFFECT OF CONCANAVALIN A ON THE GROWTH AND ELECTRICAL PROPERTIES OF TUMOR CELLS

CHAPTER I

INTRODUCTION

Membrane Properties of Tumor Cells

Studies on the membrane properties of tumor cells have been motivated by the necessity to quantitate differences between normal and neoplastic cells. The study of cellular events following neoplastic transformation has been aided by the use of *in vitro* cell lines. However, the limited life-span and karyotypic changes associated with the culture of normal cells limits the reproducibility and conclusions of such studies (1).

Transformed cells in tissue culture have several distinguishing characteristics compared to their nontransformed counterparts. Most tumor cell lines do not possess the same degree of "density-dependent growth control" that is observed for nontransformed cell cultures. This property is often referred to as contact inhibition of growth (1-4, 17). The saturation density (expressed as cells/cm^2) is usually an order of magnitude higher for tumor cells than in the normal cells. This is primarily due to the presence of multi-layered clones (5,6,17). This ability of tumor cells to grow in macroscopic clones was examined by

Abercrombie (7) who offered an explanation for the metastatic properties of tumors based on cell adhesion to endothelial tissue. Cell-cell interaction in vitro was studied using microcinematography (8). Normal fibroblasts would either change direction or cease migration upon contacting a neighboring cell. However, sarcoma cells would overlap each other, pile up in several layers, and demonstrated a marked decrease in contact inhibition. Normal cells usually grow to a confluent monolayer with a marked decrease in proliferative activity upon reaching confluency (9,10). Evidence that this loss of growth regulation in vitro is related to in vivo growth comes from examining the transplantability of in vitro transformed cells into animals. When 3T3 mouse fibroblasts are transformed by simian or polyoma virus, the ability of these cells to induce tumor is directly correlated with their in vitro saturation densities (11), i.e., the tumorigenicity is proportional to the loss of in vitro density-dependent growth. Some transformed cell lines do demonstrate contact inhibition of growth, so this property is not unique to the neoplastic state (12).

The morphology of transformed cells is strikingly different from the nontransformed cells. When chick embryo fibroblasts in vitro were infected with the oncogenic Rous sarcoma virus (RSV), the cells became rounded, loosely attached both to cells and the substratum, and grew to much higher saturation densities compared to non-infected cultures (1). Mouse 3T3 cells transformed in vitro developed a spectrum of morphological cell type, ranging from the normal-appearing small, flat, cell to giant, multi-nucleated cells having long psuedopodia (9). Similar morphological changes are observed in vivo (12,13).

The electrophoretic mobility (EPM) of cells is a measure of the average charge density of the cell surface (21), and was once thought to express a clear difference between normal and transformed cells. Ambrose measured the EPM of hamster kidney cells to be about 6 X 10^{-3} cm/sec/volt/meter compared to homologous tumor cells which had an EPM of 12 X 10^{-3} (14). Purdom showed that as methylcholanthrene-induced mouse sarcoma cells were grown under in vivo conditions that enhanced invasiveness, the EPM increased (13). However, studies on embryonic (15) and regenerating liver cells (16,18,109) suggested that increased surface charge density may be associated with growth in general, and not specifically with malignancy. Other work has demonstrated that changes in surface sialic acid and electrophoretic mobility occur during the cell cycle (19, 20). The main contribution to surface charge density is from the ionized carboxyl groups of sialic acid. Therefore, it was natural to propose that the EPM was correlated with an increase in sialic acid at the electrokinetic surface of the cell, and further, that this increase could account for the invasiveness of tumor cells in surrounding tissue (7). Since other surface moieties can contribute to the electrophoretic mobility (21,22), this generalization may not be true for all tumors (23).

Phytoagglutinins have consistently shown differences in the surface architecture between normal and transformed cells (24-27). Even though several studies have shown that the amount of agglutinin bound to the normal and transformed cell is usually the same, the transformed cells have a different distribution of the carbohydrates involved in binding the agglutinin molecule which leads to differences in agglutinability (28-30). Agglutinability of nontransformed and transformed cells

is the same after the nontransformed cells have been briefly treated with proteolytic enzymes (24,25,30). This suggests that some Concanavalin A (Con A) binding sites on the surface of nontransformed cells may be of a cryptic nature (17). This idea was further strengthened by Burger's observation that 3T3 cells, during mitosis, have the same pattern of bound fluorescent-labeled Con A as the polyoma virus-transformed 3T3 cell (PY-3T3) (5). This observation lead Burger to postulate that neoplastic transformation involves the continued presence of a surface configuration found on the cell during mitosis, and that lack of proper "feedback signals" from the cell surface to intracellular systems may lead to unchecked growth (5,17). This thought is interesting since many cell lines display a higher electrophoretic mobility during mitosis (16), a time during which cell surface sialic acid is elevated. These observations on the surface properties of mitotic, nontransformed cells may correlate with the reports of higher amounts of sialic acid at the surface of transformed cells. The properties of Con A are discussed on page 12.

The assays used for the agglutinability of nontransformed and transformed cells vary with respect to experimental conditions and until many of the physico-chemical factors that influence agglutination with Con A are examined, conclusions about the nature of surface changes following neoplastic transformation of cells may be premature.

Transformed cells <u>in vitro</u> and <u>in vivo</u> display surface changes associated with antigens that are unique to the neoplastic state (31-34). The role of these antigens in maintaining the tumorous tissue <u>in vivo</u> is unknown, although biochemical changes in the plasma membrane of transformed cells have been demonstrated in several laboratories.

Using labeled precursors, Warren et al. observed that RSV-transformed chick embryo fibroblasts contained much more carbohydrate-rich surface protein than the normal cells (35). Further studies by the same group showed that sialic acid at the cell surface increased from 2-11 times compared to the non-infected cultures and this increase was due to a high activity of a sialyl transferase enzyme (36).

Since the structure of components found at the surface of these transformed cells is unknown, it remains to be shown whether these glycoproteins are also involved with the increased agglutinability using carbohydrate-specific wheat germ agglutinin (WGA) and Con A (24-27). Certainly other structural changes occur at the cell surface, since 3T3 cells show a marked simplification of ganglioside pattern following polyoma virus infection (37). In this case, the amount of enzyme-released sialic acid from glycolipid remained the same as nontransformed 3T3 cells, but the distribution of sialic acid was altered, being found in one particular fraction of lipid compared to four fractions before infection. Many architectural changes probably occur at the cell surface following neoplastic transformation, since PY3T3 cells are highly agglutinable with Con A, but Con A binding is not inhibited by a hapten-reaction with sialic acid (38). Poduslo et al. showed that a large molecular weight group of polypeptides (>150,000) appeared in the plasma membrane fraction of hamster kidney fibroblasts after in vitro transformation with RSV (39). This group stained as glycoproteins, demonstrating the trend of increased carbohydrates in the plasma membrane of transformed cells.

The Cell Surface, Ions, and Growth Regulation

Neoplasia has been described in terms of a loss of growth regu-

lation of cells (5,6,10,17,40) and numerous findings indicate the cell surface plays a key role in cellular growth control (5,6,41-43). In fact, current evidence suggests that there may be a common feature underlying the diversity of neoplasia, namely, that alterations in one or more of their membrane systems is a regular feature of tumor cells (40). Although alterations in many subcellular membrane systems occur following transformation (40,44-66), many biochemical and behavioral events of cells may be directly affected by the composition and structure of the cell surface.

Investigations on the stimulation of growth following cell surface alterations have frequently used confluent cultures of nontransformed cells or cultures of peripheral, small lymphocytes. Confluent cultures have minimal mitotic activity and lymphocytes normally do not divide unless stimulated by mitogens, such as antigens.

When confluent mouse 3T3 cells and chick embryo fibroblasts were treated with trypsin (<10 minutes, 0.0025%) this resulted in initiation of cell division and a subsequent higher cell density of the cultures (1,47). Other enzymes, such as pronase, ficin, and neuraminidase gave a similar effect. Stimulation of cell division in confluent cultures could also be shown by layering L1210 murine leukemic lymphoblasts onto 3T3 cells, suggesting that proteolytic enzymes may be on or near the surface membrane of malignant cells (34). Rubin suggests that some proteolytic factors may be released from the cells in transformed cultures resulting in continued surface modification leading to high proliferative activity (1). Support for this line of thought was increased by the demonstration that the saturation density of PY3T3 cell cultures could be lowered by

adding protease inhibitors to the culture medium (48). Since the onset of DNA synthesis and subsequent cell division in enzyme-stimulated confluent 3T3 cultures was preceded by a decrease in intracellular cyclic-AMP levels, Burger suggested that proteolytic enzymes may affect membrane-bound enzyme systems such as adenyl cyclase (34).

Cyclic-AMP levels may affect the expression of in vitro growth regulation, since addition of adenosine-3',5'-cyclic monophosphate and its derivatives to transformed cell cultures yield morphological and growth behavior changes that resemble normal cell cultures (49-51). The intracellular level of cyclic-AMP is chiefly determined by the balance between its formation from 5'-ATP by adenyl cyclase and its degradation to 5'-ATP by a specific 3',5'-cyclic phosphodiesterase (52). The pathway which leads to alteration of cyclic-AMP levels in transformed cells can not be generalized, but one report demonstrated that adenyl cyclase activity in simian virus-transformed cells (SV_{40}3T3) was 50% less than the nontransformed 3T3 cells (53).

Besides demonstrating specific surface changes in transformed cells, Con A is also a potent mitogen for lymphocyte stimulation (54-57). Rat thymocytes and human lymphocytes were shown to have changes in adenyl cyclase activity following mitogenic stimulation (58,59). Con A altered the adenyl cyclase activity of isolated fat cells and directly interacted with insulin receptors on the cell surface (60). In addition to changes observed in cyclic-AMP levels when a cell population increases proliferative activity, other membrane events may accompany changes in intracellular metabolic systems.

Following mitogenic stimulation of lymphocytes, Husler reported

the existence of low-resistance pathways between mitogen-agglutinated cells (61). The onset of this phenomenon was rapid following stimulation, and this may correspond to the increase in potassium and calcium fluxes reported by several workers. Lymphocyte stimulation was dependent upon the influx of K^+ into the cell (62) and addition of ouabain, the cardiac glycoside which inhibits Na^+-K^+ dependent ATPase, prevented the lymphocytes from entering the DNA synthetic phase (63). There is evidence that calcium is a principal stimulatory regulator of cell proliferation both *in vivo* and *in vitro* (59,110). Cone demonstrated that Chinese hamster ovary cells could be blocked from mitosis by substituting Na^+ with K^+ (64). This effect was reversible by restoring the proper ion balance. Similarly, the growth rate of hamster kidney cells could be manipulated by altering the concentration of external potassium, with optimal growth at a value of 64 mM/l (65). Levels above or below this value resulted in a decreased growth rate, which is interesting since normal tissue culture media usually contains 5 to 8 mM/l potassium. The activity of Na^+-K^+ ATPase was found to be 50% lower in SV_{40}3T3 cells compared to their nontransformed counterparts (53). These observations suggest a role for membrane permeability to ions and membrane-bound enzyme systems in the growth regulation of cells (111).

The ionic conductance of cell membranes was studied by Lowenstein in primary and transplanted rat liver cancers (66). The normal liver cells communicated freely with each other (as measured by cell-cell junctional ionic conductance), whereas the hepatoma cells had a very low ionic conductance between them. The computed junctional conductance was about three orders of magnitude less for the tumorous tissue compared to

the normal controls. This cellular communication has been thought to be important for density-dependent growth inhibition (1). It has also been shown that serum factors in tissue culture medium could affect this intercellular communication (67). Histological examination revealed that unlike the normal cells, virus-transformed hamster cells lacked tight junctions (desmosomes) between cells and an increase in ruthenium-red staining was observed. This latter finding suggests that the increase in mucopolysaccharides at the cell surface may affect ionic permeability (68). Lowenstein described the effect of Ca^{++} upon junctional membrane permeability using measurements of ionic conductance (69). Since raising Ca^{++} to 10^{-2} M caused a rapid decrease in membrane permeability, he proposed that junctional permeabilities may be regulated by external Ca^{++} levels. Many morphological and metabolic features of cells are dependent upon the amount of contact between cells (70).

The Transmembrane Potential and Cell Growth

Measurement of the transmembrane potential and ionic conductance across the plasma membrane allows investigation of a physiological meaningful parameter with little manipulation of the cell system, especially with controlled conditions afforded by *in vitro* systems.

Mammalian cells have a potential difference across the plasma membrane, the interior of the cell being negative with respect to the extracellular bathing solution. Most definitive studies on the transmembrane potential (TMP) and DC membrane resistance (MR) have used excitable cells, such as squid axons, primary explants of nervous tissue, and cultured embryonic heart fibroblasts.

Most measurements on non-excitable cells yield a much lower TMP

(magnitude) than that found for excitable cells (71). The reason for the high magnitude of potentials in excitable cells is the high relative permeability of the membrane to K^+ compared to Na^+, i.e. the ratio P_{Na}/P_K <<1 (71-73). Since the ionic gradients across the membranes of these two kind of cells are not that different, and the distribution of chloride seems to be passive, the low TMP observed for non-excitable cells is probably due to an increase in the P_{Na}/P_K ratio. Whether this increase results from a lowering of the absolute K^+ permeability or an increase in absolute Na^+ permeability compared to excitable membranes has not been resolved (74,75) and may vary with cell type. There is little evidence for "electrogenic pumping" of ions in contributing to the resting membrane potential of non-excitable cells (71).

Measurements of the TMP and MR of non-excitable cells are scarce, mainly because of the technical difficulties associated with impaling cells having diameters less than 50 microns and yet assuming no cell damage. Therefore, some studies required techniques that selected for large, non-dividing cells (76) or immobilized cells following detachment from the substrate (77). These inherent difficulties probably explain the different values obtained by several workers for the TMP of Ehrlich ascites tumor cells and HeLa cells. Johnstone (78) reported a TMP of -5 to -10 mV for Ehrlich ascites cells, whereas Aull (79) reported a mean value of -11.2 mV, and Smith (80) reported the value of -8.3 mV. Lassen (81) obtained a potential of -24 mV for the same cell line provided the TMP was measured within 10 milliseconds of penetration. A mean value for the TMP of HeLa cells of -17 mV was obtained by Borle (82), in contrast to Okada's measurement of -48 mV (83).

There are numerous studies which indicate that malignant cells are less electronegative than normal cells and have a higher membrane resistance. Tokonka obtained a mean potential of -34 mV for normal gastric epithelial tissue, compared to -24 mV for gastric carcinoma cells (84). Chowdhury and Chou obtained -31.5 and -18.5 mV potentials for the respective normal and chemically induced anaplastic carcinoma cells of murine skin (85). Furthermore, the tumorous cells had an average membrane resistance of 6.5 MegOhms compared to the 3.0 MegOhms resistance for normal cells. Both studies above were done in situ.

Striking changes of the transmembrane potential was observed by Fritz and Nahmias following infection of human laryngeal tumor cells with herpes virus, in vitro (77). The TMP changed from an average value of -20 mV to + 12 mV fourteen hours after infection. They attributed this to an increase in permeability to sodium, based on the histological observation of cell swelling. It is interesting to note that no data have appeared on the TMP of cells following infection with known oncogenic viruses.

A series of studies by Cone suggest that the TMP may, in fact, reflect the proliferative activity of a cell population, rather than neoplastic transformation (64,86-90). He advanced an attractive hypothesis regarding the relation of the TMP and intracellular physiology (86). Briefly, the interactions between membrane permeability, transmembrane potential, and intracellular events may be pictured as a cyclic feed-back process where changes in any one of the parameters affects the others. Membrane permeability may be altered through structural and compositional changes of the cell membrane, alterations in enzymatic systems, or changes

in ionic conditions. In turn, mitotic activity and intracellular enzyme systems may be altered by changes in membrane permeability. Support for this hypothesis comes from a variety of sources. A recent report has shown that the incorporation of thymidine into hamster kidney cells can be directly correlated with the level of the transmembrane potential (65). The higher magnitude of the TMP for tumor cells may indeed reflect their proliferative rate, rather than the malignancy.

Concanavalin A and Some of Its Biological Effects

Con A was the first phytoagglutinin isolated in pure form, in 1936 (91). It is a carbohydrate-binding protein and the binding is specific for sugars of the α-D-Mannose configuration (38,92,93). The three-dimensional structure of Con A was recently proposed by Edelman and his colleagues (94). It exists as a dimer composed of two identical subunits below pH 6.0. Above this pH, mixtures of dimers and tetramers exist, along with some molecular species formed by a naturally occurring fragment of the Con A molecule. The subunit has a molecular weight of about 27,000 daltons, and calcium and manganese are required co-factors for binding activity (94-96). The molecule contains no carbohydrate and does not react with human blood-group antigens, as do other agglutinins (93). Inhibition data for dextran-binding suggest that unmodified hydroxyl groups at the C-3, C-4, and C-6 positions of the D-glucopyranose (or D-Mannopyranose) ring are essential for binding to the active sites of the molecule (92). Although crystallized Con A appears to be uniform in biological activity, isoelectric focusing reveals at least eight species of molecules, depending upon pH, with most sugar-reactive moieties between pH 6.6 and 7.1 (107). Trypsinized Con A (TRYP-Con A) contains a

heterogeneous population with respect to molecular weight. Depending upon the conditions of treatment, amount of trypsin, and the amount of Con A, fragments ranging from 10,000 to 200,000 daltons can be present in the solution (96). Edelman could not reproduce the homogeneous, monovalent species which Burger has reported following trypsinization of Con A (17).

The biological effects of Con A are numerous, and only the literature most relevant to the present study will be considered. The most frequently reported use of Con A is as a mitogen for lymphocytes. For this reason (and the high specificity of Con A-carbohydrate binding), the interaction of Con A with lymphocytes is considered an excellent model for antigen-antibody interactions (54-57). The binding of Con A to lymphocytes is concentration dependent, and at a level of 50 µg/ml, about 10^7 molecules are bound per cell (97). Moller demonstrated that both B and T lymphocytes bind about the same amount of Con A per cell, but only T lymphocytes are stimulated to divide by soluble Con A. Just as agglutination seems to be dependent upon the surface distribution of Con A binding, so does the phenomenon of lymphocyte stimulation (56,97).

If incubated with lymphocytes before an antigenic stimulation, Con A prevents the fluidity of immunoglobulin receptors which normally lead to the formation of the polar cap (98). Con A inhibits phagocytosis in polymorphonuclear leukocytes (99). This protein also inhibits tumor cell migration, which may be important for the ability of a tumor to metastasize (100,108).

Con A has also been used to select cells with particular membrane characteristics from malignant cell lines, <u>in vitro</u>. The intact molecule is preferentially cytotoxic (<200µg/ml) to tumor cells, probably due to

the cross-linkages formed on the cell surface (17). Ozanne and Sambrook isolated Con A-resistant SV_{40}3T3 cells by repeated exposure of the cultures to the cytotoxic, native Con A (101). Less agglutinability was observed using these cells and morphology was similar to the nontransformed 3T3 cells. No karyotypic changes from the parent line were observed and the viral T-antigen was still present. Con A-resistant Chinese hamster cells isolated by Wright (102) were more sensitive to various agents including ouabain, testosterone, glucose, cyclic-AMP, and sodium butyrate than untreated cells. Ultrastructure, morphology, and extent of contact inhibition of growth for Con A-resistant PY3T3 cells were similar to the nontransformed 3T3 cells studied by McNutt (103). Most reports have dealt with qualitative comparisons of Con A-selected cells to the untreated, transformed cells.

To investigate the effect upon in vitro growth regulation of transformed cells following modification of the cell surface, Burger demonstrated that the binding of fragments from TRYP-Con A to PY3T3 cells lowered the saturation density of the cell culture (17). This effect was dose-dependent, and restoration of the saturation density to that observed for 3T3 cells required the continuous presence of 75 μg/ml TRYP-Con A. This was shown to be a reversible effect upon PY3T3 growth, since removal of the TRYP-Con A from the growth medium abrogated the observed decrease in saturation density. In addition, incubating the TRYP-Con A with α-methyl-D-Mannoside also prevented the effect as the sugar is a potent inhibitor of Con A binding (92,93). To relate the surface alteration produced by the binding of TRYP-Con A, studies will need to be done that examine membrane parameters following this treat-

ment. A recent study has shown that the activities of Na^+-K^+ATPase and adenyl cyclase of SV_{40}3T3 cells is shifted to near the values obtained for the nontransformed 3T3 cells, following treatment of the transformed cells with 70 µg/ml TRYP-Con A (53). The growth rates of SV_{40}3T3 and 3T3 cells were observed to be inhibited when external potassium was increased, the 3T3 cells being less sensitive. This insensitivity to changes in external potassium of normal cells compared to transformed cells has been reported by other workers (65,90). Using 70 µg/ml TRYP-Con A, the SV_{40}3T3 cells also decreased their sensitivity to changes in external potassium, which was correlated with the change observed in Na^+-K^+ ATPase activity (53). Although the interactions between this enzyme system, ion distribution, TMP, and intracellular metabolic pathways is not known, Burger suggests the effect of TRYP-Con A is mediated by changes in adenyl cyclase (104). Yoshikawa-Fudaka suggests the effect of TRYP-Con A upon tumor cell growth is mediated by changes in Na^+-K^+ ATPase activity (53).

Other cell surface modifications lead to similar changes in growth of tumor cells. The addition of dextran sulfate also lowered the saturation density of SV_{40}3T3 cells (43). Using 200 mM urea, Weston and Hendricks reduced the cell-cell interaction normally observed in cultures of untreated mouse fibroblasts (105). Ambrose observed that a wheat germ lipase (WGL) inhibited in vitro tumor cell growth (42). This action of the lipase was specific in the sense that the effect could be abrogated by incubating the lipase with a hapten-inhibitor of WGL action, N-acetyl-glucosamine. This inhibition of tumor cell growth was later shown to be due to an impurity in the lipase preparation which was wheat germ ag-

glutinin (106). Both wheat germ agglutinin and Con A have been used to demonstrate surface changes accompanying malignant transformation of cells (24-27). Since their sugar-binding specificities are different, and they show a similar effect upon tumor cell growth, it is likely that many modifications of the cell surface can lead to similar observations.

Specific Aims of This Study

With the preceding review of pertinent literature in mind, it is evident that the cell surface plays more than a passive role in the regulatory events of cell growth and behavior.

The specific questions to be answered by this study are:

1. What are some of the physico-chemical factors that influence agglutination of transformed and nontransformed cells using Concanavalin A?

2. Are there changes in the transmembrane potential and membrane resistance as the *in vitro* cell density increases?

3. Do the transformed cells differ from the nontransformed cells with respect to the TMP and MR?

4. What is the likely basis for any observed differences in these electrical parameters?

5. Since TRYP-Con A-treated tumor cells resemble the nontransformed cells with respect to growth and morphology, does this treatment also cause the TMP and MR to change toward the corresponding values observed in the nontransformed cell system?

CHAPTER II

MATERIALS AND METHODS

Tissue Culture

Cell Lines

The cell lines used in the present study were the L5178Y murine leukemic lymphoblast, 3T3 Swiss Albino mouse fibroblast, and the polyoma virus-transformed 3T3 mouse fibroblast (PY3T3). All lines were carried *in vitro*.

The L5178Y cells were a gift from the laboratory of Dr. Leonard Miller, VA Hospital, OUHSC. They were grown in suspension culture using Fischer's Medium for Leukemic Cells (138), supplemented with 10% horse serum, 100 units penicillin, and 100 μg streptomycin per milliter of complete medium (All chemicals obtained from Grand Island Biological Company). The cells were maintained at 35°C, in 125 ml glass flasks, using 20 ml of medium. The pH was held between 6.9 and 7.2 using 8% CO_2 in air, and the cultures were split 1:5 every 72 hours to maintain logarithmic growth. Routine trypan blue staining showed more than 95% viable cells at any time while in tissue culture.

The 3T3 Swiss Albino mouse fibroblasts were obtained from the American Type Culture Collection (CCL92). They were used between the third and 40th passage in this laboratory.

The PY3T3 cell line was a gift from the laboratory of M. M.

Burger, Princeton University. They were used between the fifth and 35th passage.

Both cell lines were maintained in tissue culture using plastic T-25 flasks (Falcon Plastics). They were incubated at 37°C, and grown on Dulbecco's Modified Eagle's Medium (DMEM), supplemented with 10% fetal calf serum, 100 units penicillin, and 100 µg streptomycin per milliliter complete medium (139). The pH was maintained between 6.8 and 7.2 using 8% CO_2 in air. Cells in sparse culture, ($<10^5$ cells/cm^2) received 3 ml of fresh medium every 72 hours, while more confluent flasks, ($>10^5$ cells/cm^2) received 4 ml. Depending upon experimental conditions, optimal growth was maintained using a 1:1 dilution of conditioned medium with fresh medium.

Preparation of Conditioned Medium

For experiments involving measurements of incorporation of ^3H-thymidine, it was desirable to use conditioned DMEM medium, as this avoids the lag observed in cell growth due to the addition of fresh medium (17).

Conditioned medium was prepared by pouring off medium from logarithmic-growing cultures ($<10^5$ cells/cm^2) after 36 hours, and diluting this with the addition of 30% fresh medium (by volume). This solution was filtered using laboratory grade filter paper, and sterilized by filtration through a 0.20 micron Millipore filter.

Routine Assays for Contamination

All media were tested for mold, yeast, and bacterial contamination before use. This was done by plating 0.3 ml medium onto Sabouraud Dextrose and NIH agar (Difco) growth medium in small plastic Petri

dishes, followed by incubation at 37°C. Tests were considered negative if no colony growth appeared within 5 days. In addition, cultures were tested in the same manner, and any that showed contamination were discarded.

The 3T3 and PY3T3 cell lines were free of mycoplasma contamination when obtained by this laboratory.

Solutions Used During Tissue Culture

Routine tissue culture of these lines required use of Puck's Buffer, Puck's Buffer with 0.5 mM ethylenedinitrilotetraacetic acid (EDTA, tetrasodium), normal saline, and Dulbecco's phosphate-buffered saline (PBS). The composition of these solutions are given in Table 1.

Cell Growth Measurements

3T3 or PY3T3 cells were seeded into T-25 flasks at the appropriate cell density and 3 ml of fresh DMEM added. Beginning twenty-four hours later, flasks were sacrificed at daily intervals for counting. The cells were taken up with a rubber policeman, following a 10 minute rinse with 0.5 mM EDTA solution. Duplicate counts were made using a hemocytometer. Optimal growth conditions were maintained using a 1:1 dilution of the conditioned medium with fresh medium.

Duplicate cultures were prepared for photography by rinsing the flasks twice with normal saline and adding 3 ml of the methanol:glacial acid fixative for 12 minutes. All staining was done with Giemsa diluted 1:1 with PBS, for 12 minutes.

Trypan Blue Stain for Viable Cell Counts

This procedure followed the protocol outlined by Merchant (120).

TABLE 1

COMPOSITION OF SOLUTIONS

	Component	mg/l
Normal Saline	NaCl	9000
Dulbecco's PBS	NaCl	8000
	KCl	200
	Na_2HPO_4	1150
	KH_2PO_4	200
	$CaCl_2$(anhyd.)	100
	$MgCl_2 \cdot 6H_2O$	100
Puck's Buffer	NaCl	8000
	KCl	400
	$NaHCO_3$	1875
	Phenol Red	5
Puck's Buffer with EDTA	NaCl	8000
	KCl	400
	$NaHCO_3$	1875
	Phenol Red	5
	EDTA	200

The use of trypan blue is based on the ability of viable cells to exclude the dye. A 0.4% Trypan blue stock solution was prepared in Puck's buffer and stored at room temperature. 0.5 ml of cell suspension was mixed with 0.1 ml of the trypan blue solution in a 12 X 75 mm tube. This was allowed to stand for 5 minutes before filling a hemocytometer for counting. A total cell count and a count of unstained cells was made, counting at least 200 cell Assuming those cells which were unstained to be viable, the percent viable cells were computed.

Autoradiography

Cells in log-phase growth were seeded into 150 mm plastic Petri dishes containing 5, 13 X 54 mm coverslips, and 15 mls of DMEM medium was added. The cells were allowed to grow for 36 hours to attain the proper cell density. The dishes were placed in a CO_2 incubator at 37°C, with 10% CO_2 in air.

TRYP-Con A was added to the appropriate dishes, at a final concentration of 40 µg/ml. Three hours later, ^{3}H-thymidine (specific activity 18 Ci/mMole, No. 027X, New England Nuclear) at an activity of 0.3 µCi/ml in conditioned medium was added to the cultures.

At appropriate times, coverslips were lifted from the dishes under aseptic conditions, rinsed twice in normal saline, and fixed for 12 minutes in fixative composed of 3 parts methanol, 1 part glacial acetic acid (filtered). After air-drying, the slides were dipped into nuclear track emulsion (NTB-2, KODAK), and allowed to stand for 24 hours. They were then placed into a light-tight slide box and stored at 4°C for 72 hours.

The emulsion was developed using KODAK photographic chemicals.

The slides were rinsed for 20 minutes in doubly-distilled water, and allowed to dry. Slides were then stained using 1 part Giemsa with 1 part phosphate-buffered saline for 12 minutes. Counts were made of labeled and unlabeled cell nuclei, counting 500 cells per slide.

Preparation of Trypsinized-Concanavalin A

This solution was prepared according to the method of Burger (17). Concanavalin A (Grade III, Twice crystallized, Lot. No. 91C-5420, Sigma) in saturated NaCl was added to Dulbecco's phosphate-buffered saline at 2.0 mg/ml. Bovine pancreatic trypsin (Type I, 2X crystallized, Lot No. 20C-8035, Sigma) was added at 2.0 mg/ml. This solution was incubated for 5 hours at 37°C. Trypsin inhibitor (Soybean, Type IS, Lyophilized, Lot No. 22C-8340, Sigma) was added at 2.0 mg/ml for two hours. The solution contained a light precipitate, and was sterilized by filtration via a 0.2 micron Millipore filter.

Agglutination Studies

Salt Solutions

For experiments involving different ionic strengths, the solutions listed in Table 2 were used. Ionic strength referred to in this study is defined by the relation $I = \frac{1}{2}(\Sigma c_i z_i^2)$ where c_i is the concentration in mM/l of the ith ion having valence z_i. Ionic strength for uni-univalent salts may be expressed in mEq/l.

Concanavalin A Solutions

Con A from the same Lot number as given above was dissolved in Dulbecco's PBS, or in the D-Mannitol solution. Although a precipitate

TABLE 2

COMPOSITION OF SOLUTIONS USED FOR

AGGLUTINATION STUDIES

	(All values mM/l)			
	NaCl	KCl	D-Mannitol	$CaCl_2$
Solution 1	145	5	20	-
Solution 2	120	5	70	-
Solution 3	95	5	120	-
Solution 4	45	5	220	-
Solution 5	0	0	320	-
Solution A	150	0	20	-
Solution B	125	25	20	-
Solution C	100	50	20	-
Solution D	50	100	20	-
Solution E	0	150	20	-
Solution F	80	70	20	-
Solution G	40	110	20	-
Solution H	10	140	20	-
Solution I	-	-	317	1
Solution J	-	-	305	5
Solution K	-	-	290	10
Solution L	-	-	275	15

formed and was subsequently filtered, the amount of protein lost from the 2 mg/ml solution was less than 5%, as determined by a Lowry protein assay (141).

Inhibitor Solutions

Inhibition studies were done using known hapten-inhibitors of Con A binding, α-methyl-D-Mannoside, α-methyl-D-Glucoside (Sigma), and sucrose (92-94). These were made up as 320 mM/l solutions, then diluted with the Con A solutions thirty minutes prior to use. For the ionic strength studies, α-methyl-D-Mannoside was dissolved in PBS or D-Mannitol solutions at a final concentration of 20 mM/l.

Agglutination Assay

Unless otherwise indicated, the following basic procedure was used for agglutination studies. L5178Y cells were pooled and counted. Since the PY3T3 and 3T3 cells grow attached to the flask surface, they were incubated in 0.5 mM EDTA solution for 20-30 minutes, followed by gentle aspiration to give a single-cell suspension. No difference in the agglutinability of these cells was observed using EDTA, or by scraping the cells free with a rubber policeman.

The cells were washed twice in either serum-free medium, or Dulbecco's PBS, using 12 ml glass centrifugation tubes. The cells were resuspended in the appropriate solution, at a final cell density between 5 to 10 X 10^5 cells/ml. Con A was added at the proper concentration, and the final working volume was either 1.0 or 2.0 ml. This was split into replicates, and the tubes placed on a horizontal shaker table (Eberbach, W. H. Curtin Co.) for 30 minutes at a frequency of 150 per

minute. The tubes were poured into petri dishes, allowed to settle for 2 to 4 minutes, and the dish scanned using phase-contrast optics. Agglutination was scored by the following scheme (122), which defines the degree of agglutination.

0 = no cell clumps

1+ = occasional clumps

2+ = 3-10 cell clumps predominate

3+ = 10-30 cell clumps predominate

4+ = 30-100 cell clumps predominate

5+ = 100+ cell clumps, with free cells

5++ = large, 100+ clumps, no free cells.

For calculation of the percent cells agglutinated, several microscopic fields of view were chosen. Taking the average clump size, the number of clumps were counted and multiplied by the average clump size. The free cells were counted and the percent cells agglutinated computed.

For agglutination studies where the cells were incubated in a given solution for 30 minutes, then resuspended in a different solution, Figure 1 shows the basic protocol used for those experiments.

Microelectrode Studies

Preparation of Glass Tubing

All microelectrodes used in the present study were fabricated from Kimax glass capillary tubes (Kimax, Art. No. 46485, O.D. 1.2-1.5 mm, wall 0.2 mm, Fisher Scientific Co.). The tubing was cut to 15 cm in length and boiled in distilled water for thirty minutes, followed by drying at 100°C for 24 hours.

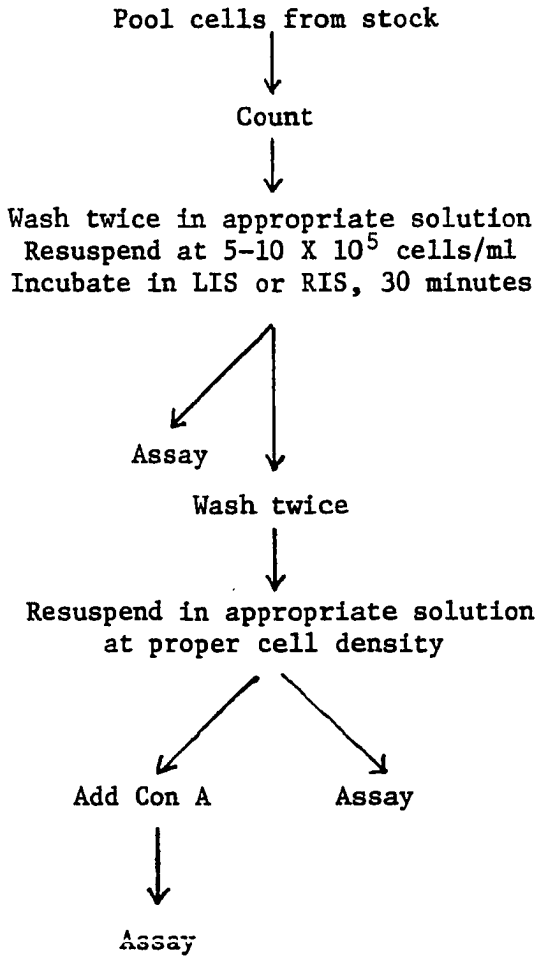

Figure 1. The basic protocol used for agglutination studies. All experiments were performed at least three times, using duplicates. The usual working volume was 1.0 ml. Cells tested were in logarithmic-phase growth.

Fabrication of Microelectrodes

Microelectrodes were pulled on a Chowdhury Pipette-Puller (123). This horizontal puller yields microelectrodes that have greater mechanical rigidity and finer tips than conventional pullers. Microelectrodes were filled immediately after fabrication, to avoid any dust-contamination from storage.

Filling of Microelectrodes

Low tip potentials (<10 mV) were most consistently obtained by the following procedure, which is a modification of the one described by Chowdhury (123).

1. The microelectrodes were mounted on plastic holders and completely immersed into 15% ethanol for 48 to 72 hours, at 35^{0}C. During this time, most microelectrodes would fill by capillary action above the tapered portion of the tip (approximately 3mm). The beaker was covered with plastic film as a dust cover at all times.

2. Just before use, the microelectrodes were immersed in a 1M NaCl solution. The solution was placed under reduced pressure at room temperature for about one hour. This would fill completely many electrodes, requiring no further handling. Those that still had a small air bubble trapped near the taper were filled by removal of the bubble with a stainless steel wire.

3. The microelectrodes were used within 48 hours of filling. Tip potentials ranged from 0 mV to about 15 mV, with tip resistances from 20 to 60 MegOhms.

Estimated Change in Tip Potential and Resistance Upon Insertion Into HiK^+ - $LoNa^+$

Since it is not known how the tip potential or resistance of a microelectrode may change when the microelectrode goes from an environment having low K^+ and high Na^+ concentrations to the cell interior where the situation is reversed, these changes were estimated. Thirty-two microelectrodes were fabricated and filled with 1 M NaCl according to the procedure described above. Two solutions were prepared as follows: 1) 140 mM NaCl-10 mM KCl and 2) 10 mM NaCl-140 mM KCl.

The microelectrodes were immersed for 5 minutes into Solution #1, the tip potential and resistance measured, then immersed into Solution #2, followed by immediate measurement of potential and resistance.

Using the relationships obtained from this study, corrections were made on all individual measurements of single-cell impalements. Most studies used microelectrodes requiring no correction for intracellular potential or membrane resistance values.

Electrical Recording System

Microelectrodes were positioned by a Narishige micromanipulator. The potential difference between the indifferent electrode and the microelectrode was measured by an electrometer (Model M4A, W. P. Instruments) coupled to the electrodes via a calomel half-cell and a saturated KCl salt-bridge. The high-impedance probe of the electrometer and calomel cells were kept inside a Faraday cage to minimize electrical noise.

The output of the electrometer preamplifier was connected to the input of a low-level DC amplifier (Model 5P1, Grass Electronics)

which was used to drive the final DC amplifier before display on a chart recorder.

Resistance measurements were made using the built-in bridge circuit of the electrometer. Current was passed between the electrodes and the resistance was displayed as a voltage drop on the chart recorder.

The recording system is shown schematically in Figure 2.

Measurement of the TMP and MR of Tissue-Culture Cells

Mechanics of Cell Penetration

The entire microscope room was warmed to 35°C before use. The top of the T-25 flask was removed, the medium poured off, the appropriate bathing solution added, and the flask positioned on the stage of a Nikon, inverted, phase-contrast microscope. Most impalements were visualized at 320X magnification.

The pH of the bathing solution was adjusted by blowing 100% CO_2 across the top of the flask when required. All solutions used phenol red for an indicator of pH. The microelectrode was immersed into the bathing solution, and the indifferent electrode lowered into the solution and held fixed. The tip potential and resistance was measured, usually running the recorder at a chart speed of 1 - 2.5 mm/sec.

The tip of the microelectrode was positioned next to the cell selected for impalement, and cell penetration was accomplished by moving the microscope stage the final 1-2 microns.

Criteria of Valid Measurements

Most punctures were unsuccessful due to cell damage upon insertion of the electrode. This was manifested by a rapid decay in the

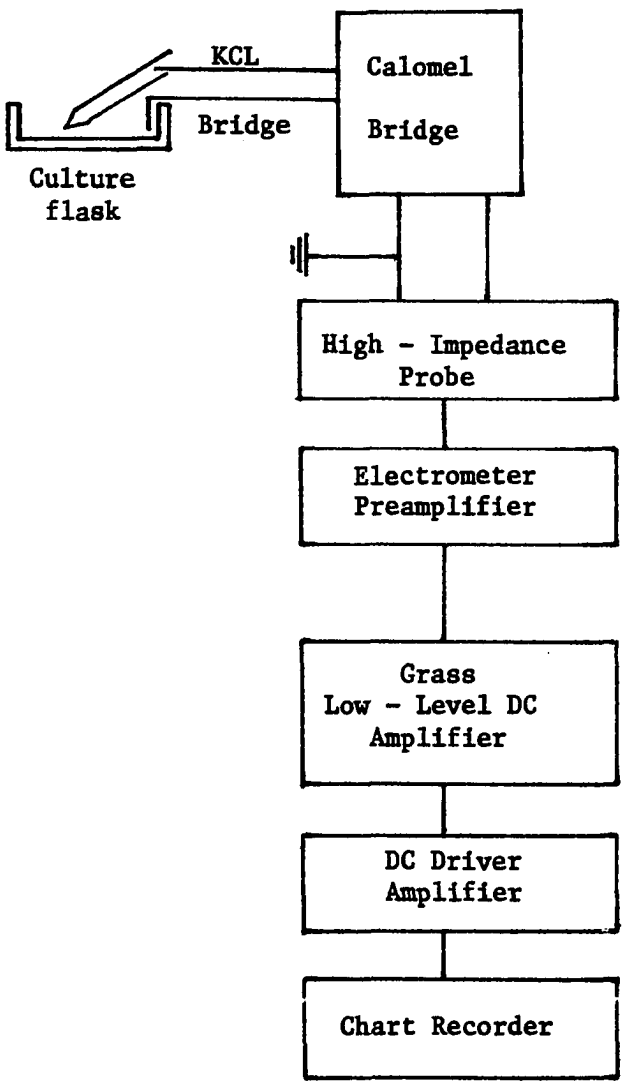

Figure 2. Basic electronic instrumentation used for micro-electrode studies. The electrometer probe and bridges were enclosed in a Faraday cage to minimize noise.

TMP. The following criteria were considered to give valid measurements of the TMP and MR.

1. The inherent tip potential, of the microelectrode must be less than 10 mV in magnitude.

2. Upon insertion into the cell, the recorder must display a sharp drop in potential, and remain stable until the measurement of membrane resistance is completed (about 5-10 seconds).

3. Upon removal, the recorder must return to the value displayed prior to impalement, and the tip resistance must return to it's prior value.

4. All punctures must be preceded by a measurement of tip potential and resistance.

5. The final values of the TMP and MR must be corrected for estimated changes in tip potential and resistance.

Bathing Solutions Used for Electrical Studies

The electrical studies were done in a reference salt solution, so that known variations of ionic constituents could be accomplished. The reference salt solution (KRSS) was prepared using the same ionic composition of Dulbecco's Modified Eagle's Medium, leaving out serum, amino acids, and antibiotics.

Changes in external potassium, sodium, and chloride were done by using the basic KRSS formula. These solutions are listed in Table 3.

When measuring the TMP and MR upon changing the external bathing solution, the T-25 flask was mounted on the microscope stage as described and a suction pipette immersed. A 10 ml burette was used to add the new solution. The procedure was as follows:

TABLE 3
COMPOSITION OF SOLUTIONS USED FOR MICROELECTRODE STUDIES

	(All values mM/l)										
	Mannitol	NaCl	KCl	$CaCl_2$	$MgSO_4$	NaH_2PO_4	$NaHCO_3$	$N(CH_3)_4Cl$	NH_4HCO_3	Glucose	Na_2SO_4
KRSS	-	109.5	5.4	1.8	0.8	1.0	44.0	-	-	20.0	-
Solution K_1	-	95.5	20.7	1.8	0.8	1.0	44.0	-	-	20.0	-
Solution K_2	-	64.0	52.5	1.8	0.8	1.0	44.0	-	-	20.0	-
Solution K_3	-	23.0	92.5	1.8	0.8	1.0	44.0	-	-	20.0	-
Solution Na_1	-	43.0	5.4	1.8	0.8	1.0	44.0	66.0	-	20.0	-
Solution Na_2	-	0.0	5.4	1.8	0.8	1.0	44.0	109.0	-	20.0	-
Solution Na_3	-	0.0	5.4	1.8	0.8	1.0	11.0	109.0	33.0	20.0	-
Solution Na_4	-	0.0	5.4	1.8	0.8	1.0	-	109.0	44.0	20.0	-
Solution Cl_1	30.0	43.0	5.4	1.8	0.8	1.0	44.0	-	-	20.0	33.0
Solution Cl_2	43.0	22.0	5.4	1.8	0.8	1.0	44.0	-	-	20.0	43.0
Solution Cl_3	54.0	6.0	5.4	1.8	0.8	1.0	44.0	-	-	20.0	50.0

1. The microelectrode, indifferent electrode, suction pipette, and addition burette were all positioned in the flask.

2. The cells were incubated for 5 minutes in 3 ml of KRSS solution.

3. 2 mls of KRSS was withdrawn by suction and the burette opened.

4. 3 mls of the new solution was added, and 3 mls was withdrawn simultaneously from the opposite end of the flask.

5. This was continued until 2 ml of the new solution remained in the flask. This procedure required 20-30 seconds.

6. Cell impalements were started immediately, since positioning the microelectrode had already been accomplished.

Although several attempts were made to change the bathing solution with the microelectrode inside a cell, this was not accomplished.

Statistical Analysis of Data

All computations were performed on a programmed Olivetti 101 calculator. The Student's t-test was used to determine significance between any two means used in this study (124). A probability of less than 5% for chance was considered significant ($P<.05$). Plots of linear regression curves were accepted if the linear regression coefficient was greater than 0.80.

In situations where the degrees of freedom for comparison between two means ($n_1 + n_2 -2$) did not match the published tables, the next lower value was used.

CHAPTER III

RESULTS

Physico-Chemical Factors of Agglutination

The agglutination of L5178Y cells using Con A was found to be dependent upon time, cell density, concentration of Con A, and ionic strength when holding the pH, temperature, and shaker table frequency constant.

Figure 3 shows the degree of agglutination (DOA) as a function of time, in minutes. The three curves were generated by using 200, 500, and 1000 μg/ml Con A, at a constant cell density of 2 X 10^5 cells/ml. All control values (no Con A) were scored zero up to 60 minutes of incubation. It was observed that some non-specific aggregation of the L5178Y cells would occur when incubated for longer than 60 minutes. The three curves reached a plateau at about 30 minutes of incubation on the shaker table. During the first 15 to 30 minutes, the DOA changes as a function of time.

A semi-log plot, where the DOA is plotted against the logarithm of time shows that the average clump size was independent of the Con A concentrations, since the three curves have essentially the same slope. This is demonstrated in Figure 4.

The cell density chosen for an agglutination assay affects both

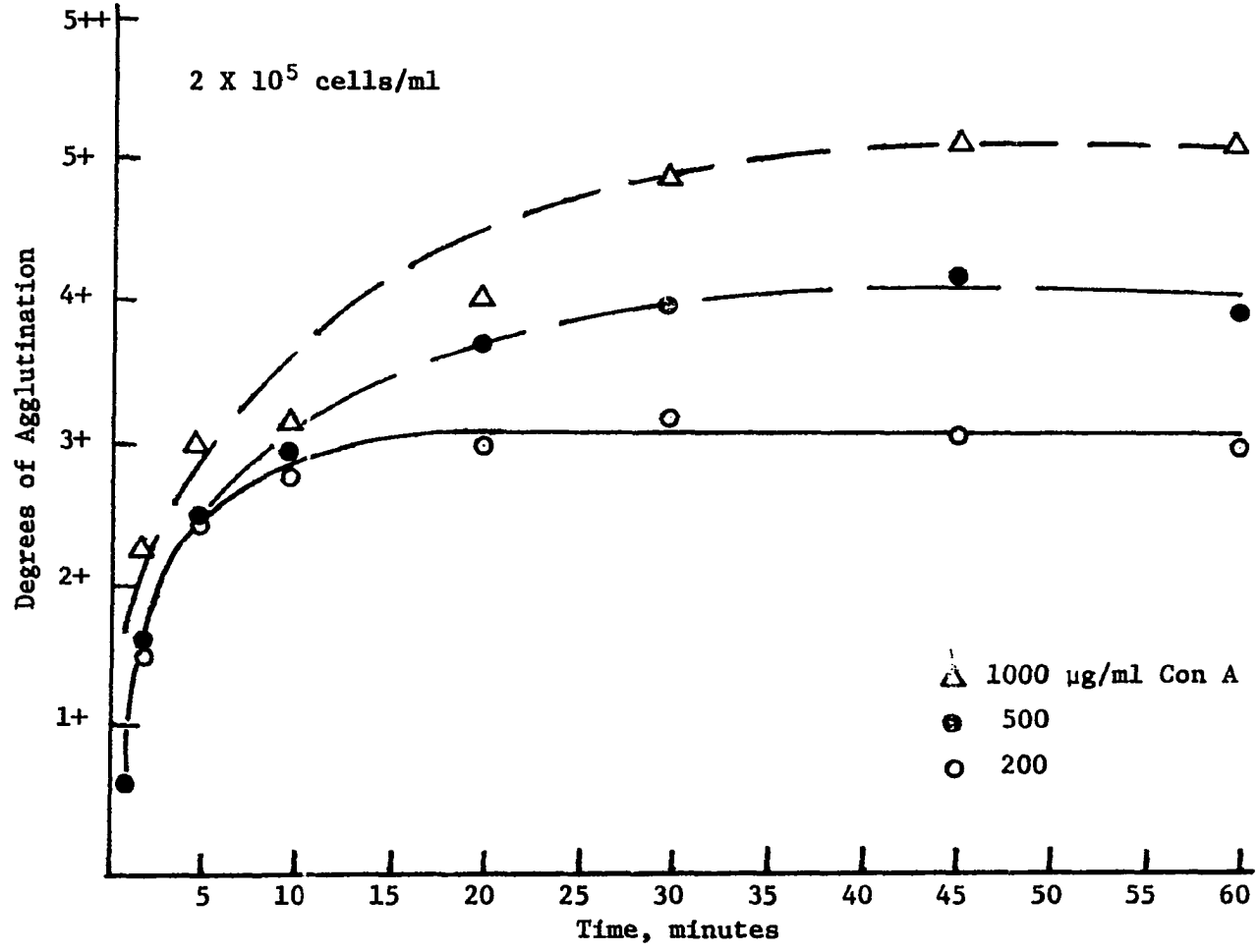

Figure 3. The degree of agglutination of L5178Y cells as a function of time. Scoring was based on the average of at least three experiments, done with duplicates.

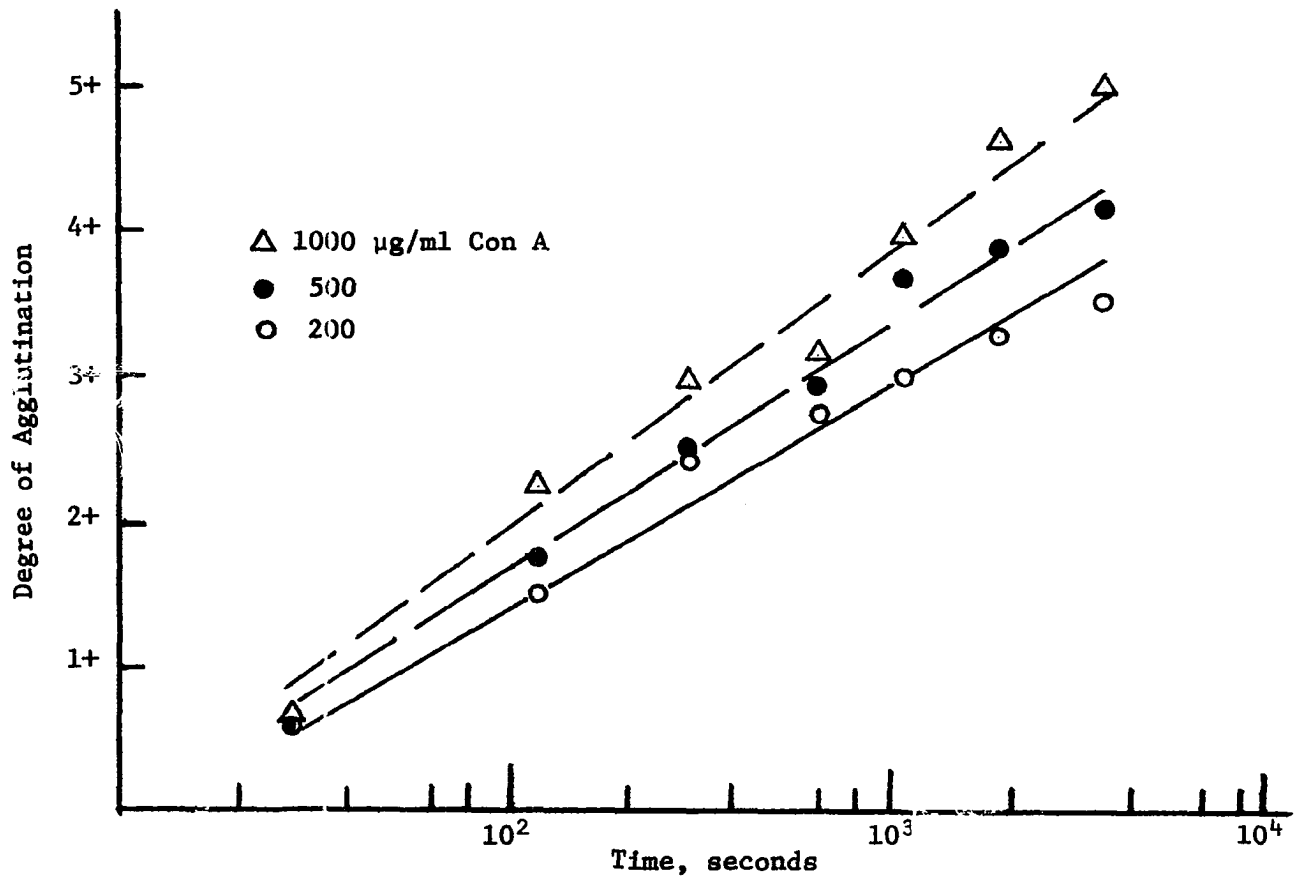

Figure 4. The data of Figure 3 plotted against the logarithm of time, in seconds. This graph demonstrates that for fixed cell density, the increase in agglutination with time is independent of the Con A concentration. All curves are drawn to their respective plateau regions (30 minutes).

the degree of agglutination as well as the reproducibility of the scoring. Figure 5 shows the effect of cell density, where the DOA is plotted against the Con A concentration, in μg/ml. The five curves were obtained by using cell densities of 10^3, 10^4, 10^5, 10^6, and 10^7 cells/ml.

At low cell densities ($<10^5$) and low concentrations of Con A (<200 μg/ml), scoring ranged from zero to 1+ (10^3 cells/ml) and 1+ to 2+ (10^4 cells/ml). High cell densities ($>10^6$ cells/ml) yield DOA scores that rise rapidly at comparable Con A values. The most reproducible assay was when 10^5 to 10^6 cells/ml were used. In all of the experiments, the control values were zero.

This effect is more clearly demonstrated in Figure 6 where the DOA is plotted against the logarithm of cell density, for fixed concentrations of Con A. The slopes of the family of curves are similar, as is the amount of displacement between curves. This indicates that cell density and Con A concentration play equally important roles in determining the degree of agglutination. The change in average clump size, for a fixed Con A concentration, was determined by the cell density. Conversely, as demonstrated by the following experiment, the average clump size varies with Con A concentration, using given cell densities.

The degree of agglutination as a function of the Con A concentration is shown in Figures 5 and 7. The average clump size is an exponential function of the Con A concentration. Using the L5178Y cells, 100% of the cells were agglutinated with about 600 μg/ml Con A at a cell density of 10^7 cells/ml. Using 10^6 cells/ml, all of the cells could not be agglutinated, even at a Con A concentration of 1000 μg/ml.

The semi-log plot of Figure 7 shows that an increase of the

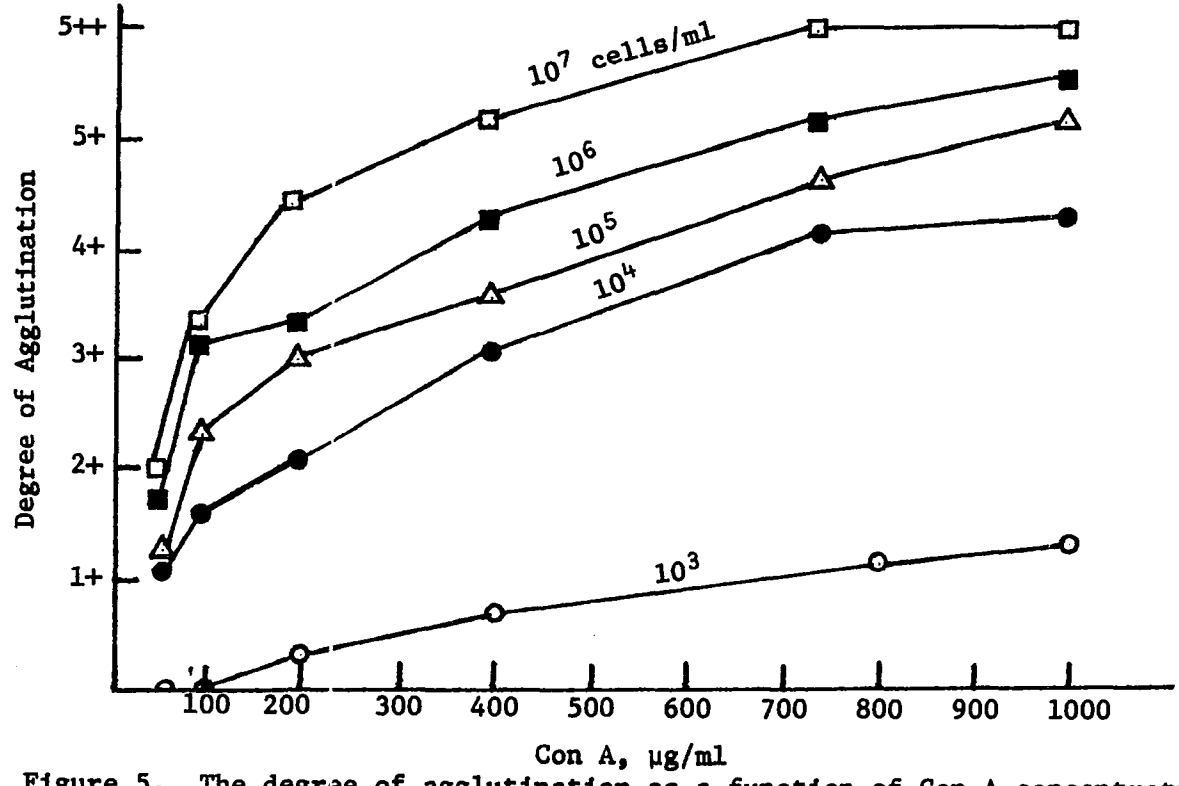

Figure 5. The degree of agglutination as a function of Con A concentration, µg/ml. The family of curves were generated by using the cell densities indicated.

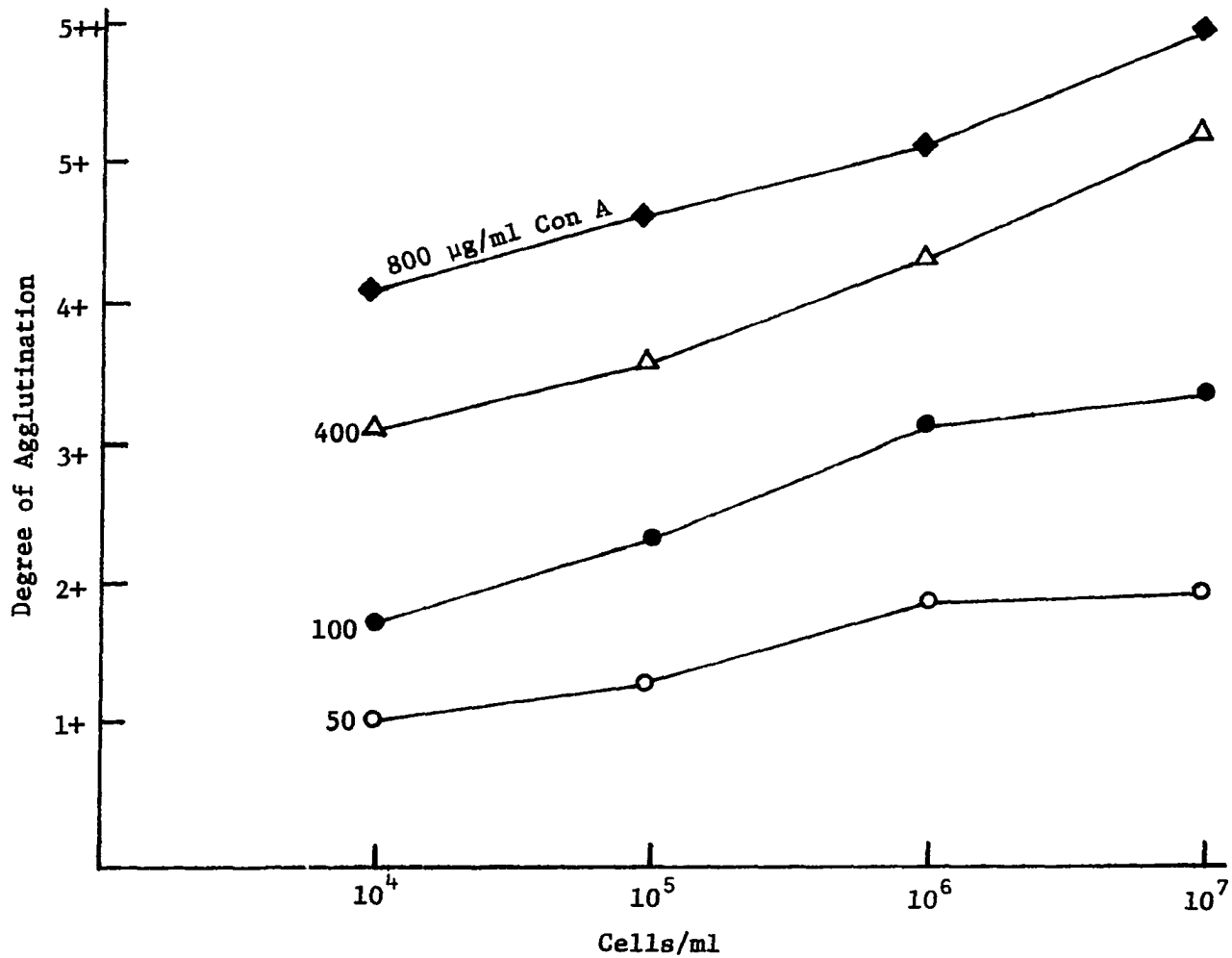

Figure 6. The degree of agglutination as a function of cell density. The curves are for different concentrations of Con A. Data is the same as Figure 5.

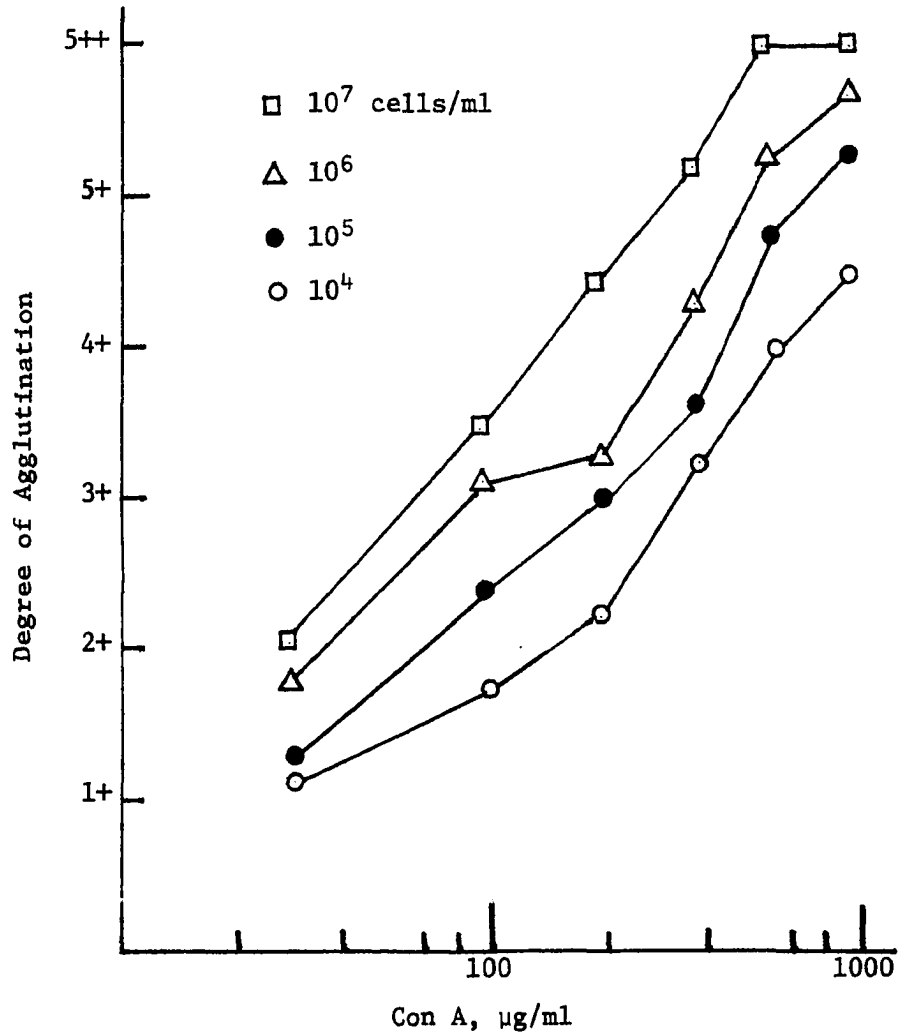

Figure 7. The degree of agglutination as a function of the Con A concentration. Data is the same as Figure 5. For fixed cell densities, the increase in agglutination is a function only of the Con A concentration.

average clump size by a factor of three (a DOA score of 1 unit) required the Con A concentration to be doubled. This relationship appears to be independent of cell density, as shown by the similar slopes of the curves. Table 4 gives the concentrations of Con A required to agglutinate approximately 75% of the cells. These values are expressed for the different cell densities using the DOA score of 4+. This score gave the most consistent results for 75% cell agglutination, using the L5178Y cell line.

D-Mannitol and sucrose are commonly used to maintain proper osmolarity of incubation media when ionic constituents are removed. Sucrose is a potent inhibitor of Con A binding to cells (92), hence it was decided to use D-Mannitol. To confirm that D-Mannitol would not interfere with the agglutination assay, a stock solution of Con A, at 2 mg/ml was prepared in 320 mM D-Mannitol (C_m).

Table 5 gives the results of agglutination assays using the C_m solution. C_1 was prepared using Con A dissolved in PBS and C_2 was 320 mM D-Mannitol, with no Con A. For 100, 200, and 500 µg/ml of Con A, it was observed that there was no inhibition of agglutination. No differences in cell morphology and percent cells agglutinated were found when using either C_m or C_1.

The effect of ionic strength upon agglutination was determined using solutions one through five listed on page 23. The ionic strengths of these solutions were computed to range from 150 to 0 mEq/1. An ionic strength of 150 mEq/1 was denoted regular ionic strength (RIS) while the zero ionic strength solution was designated low ionic strength (LIS). A Con A concentration of 100 µg/ml and a cell density of 5×10^5 cells/ml

TABLE 4

CONCENTRATION OF CON A REQUIRED FOR 75% CELL AGGLUTINATION

Cell Density (cells/ml)	Con A (µg/ml)
10^4	800
10^5	400
10^6	275
10^7	175

TABLE 5

TEST OF D-MANNITOL FOR HAPTEN-INHIBITION OF AGGLUTINATION

Con A (µg/ml)	C_m [a]	C_1 [b]	C_2 [c] Mannitol
100	+ +	+ +	0
200	+ +	+ +	0
500	+ + +	+ + +	0

[a] C_m = 320 mM D-Mannitol plus Con A

[b] C_1 = PBS plus Con A

[c] C_2 = 320 mM D-Mannitol with no Con A

was used for these ionic strength experiments. All controls were scored zero, using the same solutions with no Con A. Incubation times varied between 0, 30, and 45 minutes in the appropriate solution before assay of agglutination.

Figure 8 shows the relation between the DOA and ionic strength, in mEq/1. There was a marked enhancement of agglutination by lowering the ionic strength from 150 mEq/1. Prior incubation of the cells for 30 or 45 minutes in the low ionic strength solutions increased the effect upon average clump size. RIS gave a score of 2+ using 100 μg/ml Con A, but 45 minutes incubation in LIS solution before adding the Con A resulted in 100% of the cells being agglutinated. No morphological changes of the cells were observed when incubated in either LIS or RIS solutions.

This enhancement of agglutination using LIS incubation medium was studied in greater detail. Figure 9 shows the effect of removing sodium chloride and potassium chloride, using solutions A through H. It was found that there was no change in the agglutinability of L5178Y cells when either the concentration of NaCl or KCl was altered. The ionic strength was held constant at 150 mEq/1. In addition, using solutions I through J for increasing the $CaCl_2$ content of the incubation medium, no difference in agglutinability was obtained. The enhancement noted in Figure 7 for the $CaCl_2$ values was due to the low ionic strength of the medium but was independent of the $CaCl_2$ content. The normal calcium content of Fischer's medium is about 2 mM/1 and the experimental variation ranged from 1 to 15 mM/1.

Quantitative data on the LIS enhancement of agglutination was obtained by hapten-inhibition of agglutination using α-methyl-D-Mannoside.

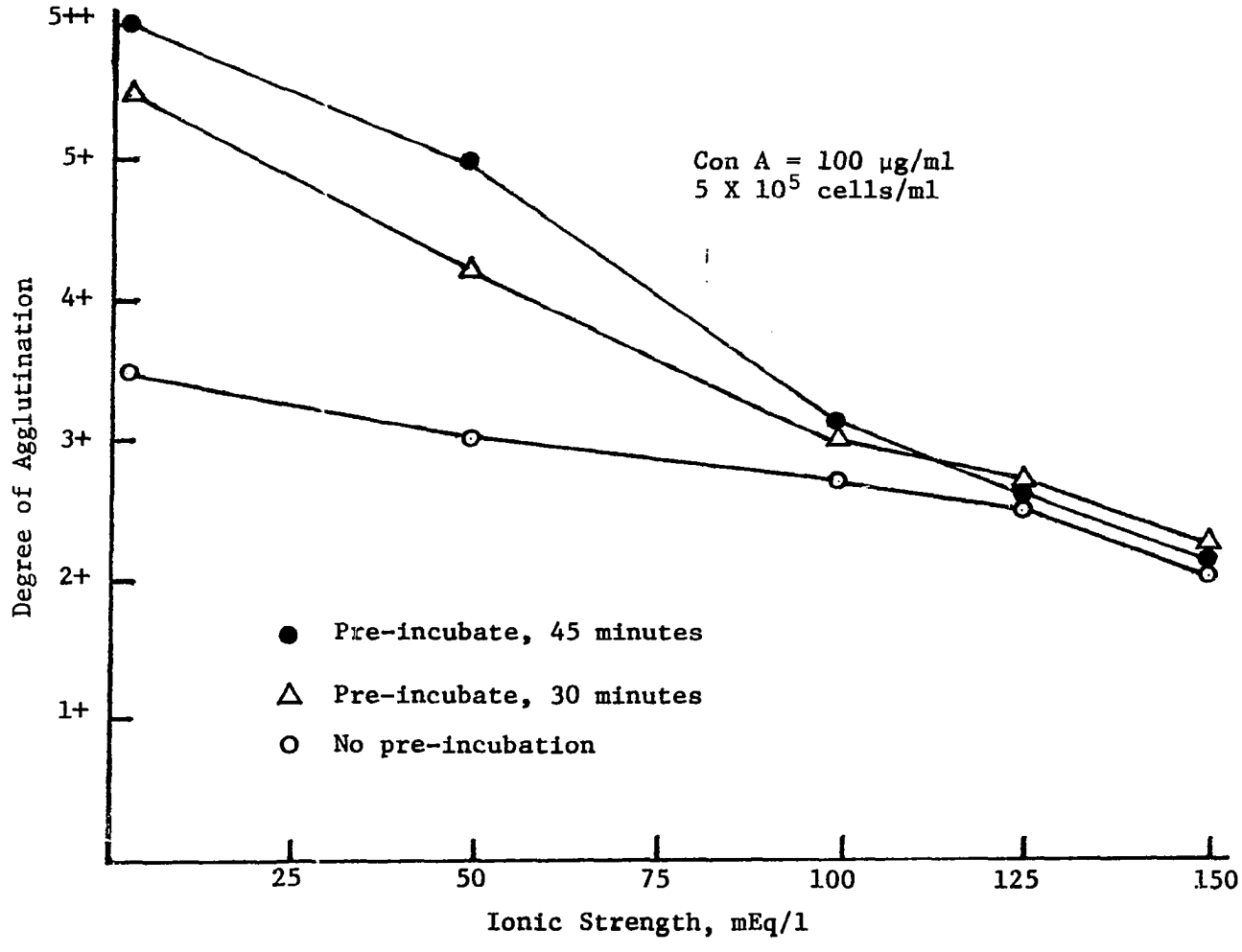

Figure 8. Degree of agglutination as a function of the ionic strength. Pre-incubation of the cells before assay enhances agglutinability. All controls (no Con A) were zero. Each point is the average of at least three experiments. Osmolarity was held constant using D-Mannitol.

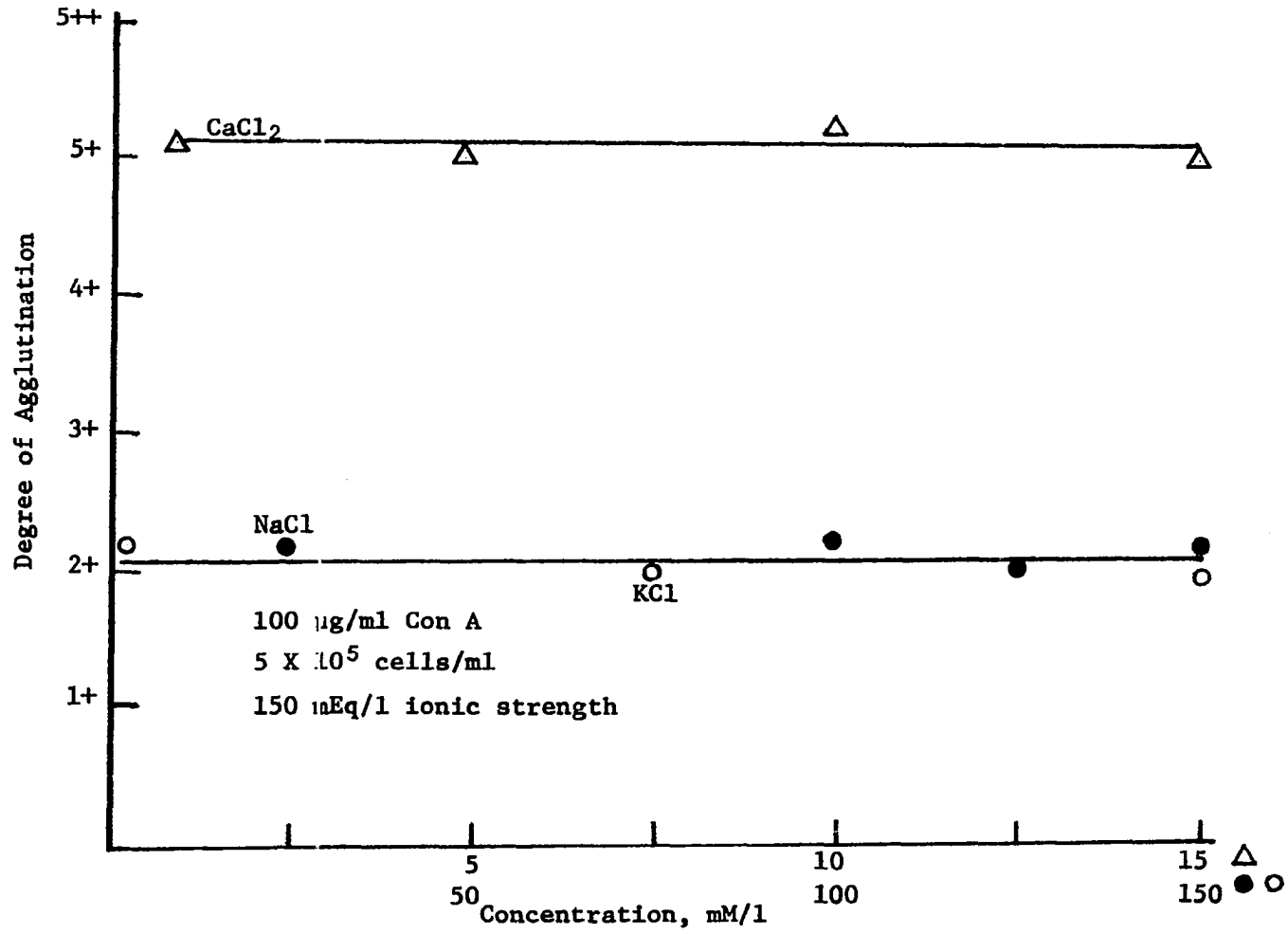

Figure 9. The agglutinability as a function of the three ionic constituents of the incubation media used for these studies. Enhanced DOA from $CaCl_2$ is due to low ionic strength.

The sugar was added to LIS and RIS solutions at a final concentration of 20 mM/l. Identical solutions containing the inhibitor and 200 μg/ml Con A were also prepared. The cells were incubated in either LIS or RIS solutions for 30 minutes, then resuspended in different dilutions of the stock LIS and RIS solutions and assayed for agglutination. The results are shown in Figures 10 and 11 where the percentage of cells agglutinated is plotted as a function of dilutions of the 20 mM/l inhibitor solution. All assays used control solutions containing no Con A and had less than 5% agglutination. As shown in Figure 8, both curves intercept the abscissa near the same value, indicating that a 1.5:1 dilution of 20 mM α-methyl-D-Mannoside completely inhibits agglutination. This corresponds to an inhibitor concentration of about 13 mM/l. Infinite dilution of the inhibitor solutions was different for RIS and LIS and can be examined more clearly by normalization of the two curves, since LIS allowed about 90% cell agglutination compared to 75% for the RIS solution.

Figure 11 shows the same data plotted as normalized curves to 100% agglutination. The curves diverge from a similar intercept and by extrapolating values for the inhibitor concentration required for 0, 25, 50, 75, and 100 percent inhibition, comparisons can be made between the LIS and RIS solutions. These values are shown in Table 6. The LIS solution required the presence of about forty times more inhibitor than the RIS solution for the onset of inhibiting agglutination.

Table 7 demonstrates the irreversibility of the agglutination using 100 μg/ml Con A and the LIS solution. The cells were incubated for 30 minutes in the LIS medium with Con A, washed twice in LIS medium with no Con A, then assayed for agglutination. The cells were then re-

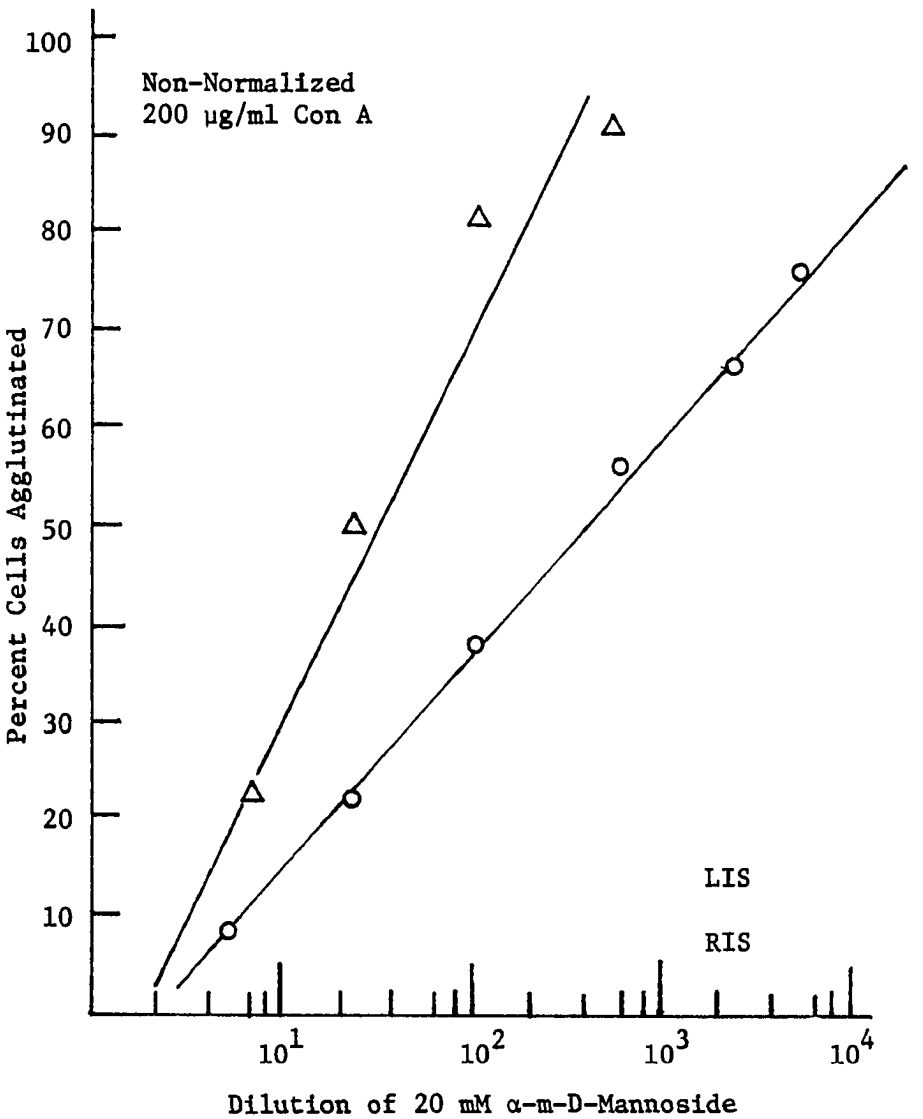

Figure 10. The percentage of cells agglutinated is plotted against dilutions of the inhibitor, α-m-D-Mannoside. Both curves have linerar regression coefficients >0.95. Each point is the mean of three experiments.

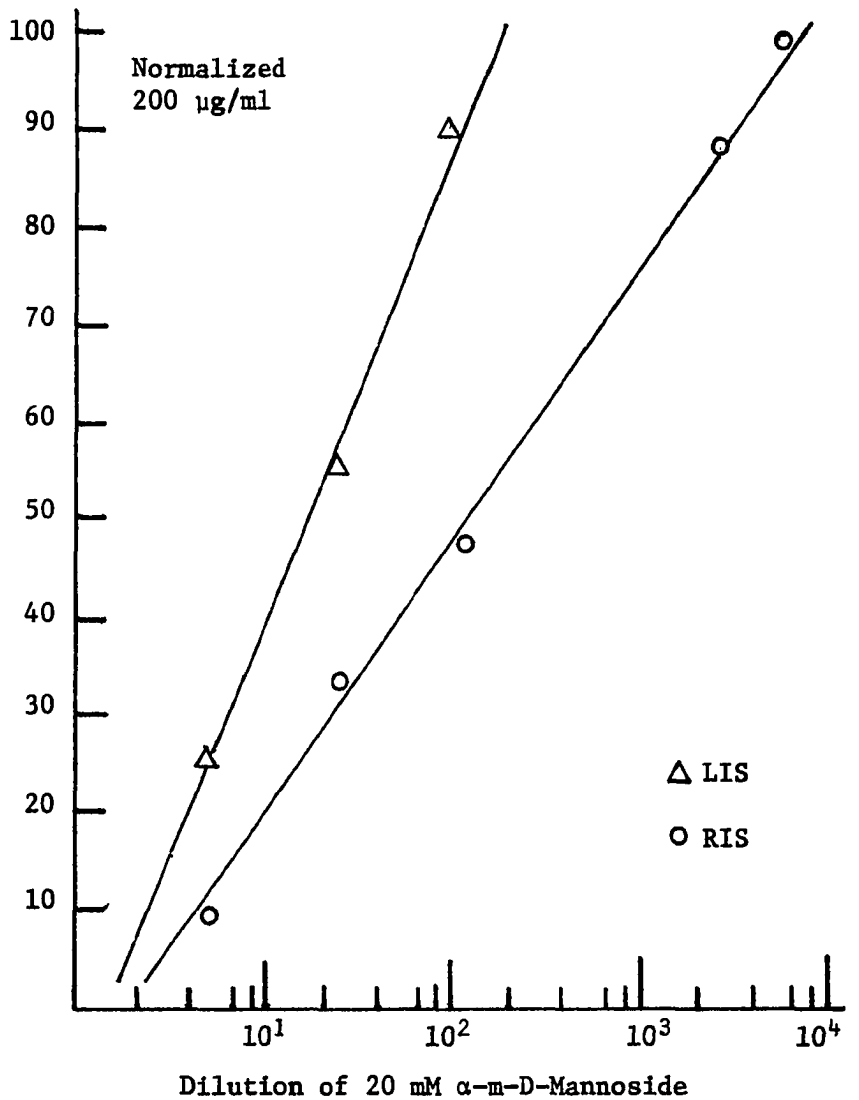

Figure 11. A normalized plot of the data in Figure 10. For LIS, "infinite" dilution occurs at about 0.1 mM, compared to .0025 mM using RIS.

TABLE 6

CONCENTRATION OF α-METHYL-D-MANNOSIDE REQUIRED FOR HAPTEN-INHIBITION OF AGGLUTINATION AT REGULAR AND LOW IONIC STRENGTH

Ionic Strength		
150 mEq/l	0 mEq/l	Percent Inhibition[a]
0.0025 mM	0.1 mM	0
0.020	0.33	25
0.15	1.1	50
1.1	4.0	75
8.5	13.0	100

[a] 200 µg/ml Con A, 5 X 10^5 cells/ml

TABLE 7

THE IRREVERSIBLE NATURE OF AGGLUTINATION AT LOW IONIC STRENGTH USING CON A

Time (hours)	LIS[a]	Control [b]
0.5	3.0[c]	0
1.0	3.0	0
2.0	3.1	0
3.0	3.1	0.7

[a] 320 mM D-Mannitol with 100 µg/ml Con A

[b] 320 mM D-Mannitol with No Con A

[c] Average DOA scores from three experiments

suspended as single cells, washed twice, and assayed in this same manner for three hours with no additional Con A being added. The control solution was 320 mM D-Mannitol with no Con A added. The values of the degree of agglutination represent the average of three experiments, each experiment using duplicate samples.

The following experiments allowed determination of when the cells must be present in LIS medium for the observed enhancement of agglutination. Table 8 shows the results of incubating 5 X 10^5 cells/ml with 100 µg/ml Con A (this cell density and Con A concentration was used in all of the following experiments) in RIS for 30 minutes, followed by resuspension of the cells in LIS with no additional Con A and assayed for agglutination. The control values were zero and the Table demonstrates the DOA score of 2+ was not changed using this procedure as the cells went from RIS to LIS incubation solutions.

Table 9 shows the results of the above experiment when repeated, but adding 100 µg/ml Con A after resuspension of the cells at low ionic strength. The enhancement was then observed, as the DOA score changed from 2+ at RIS to 5+ when the cells were then assayed at LIS with Con A.

When the order of incubation solutions was reversed from that described above, the LIS effect was observed. Table 10 shows that when the cells were first incubated in LIS medium, the DOA score was 5+. After resuspension of these cells in RIS medium with no additional Con A, the degree of agglutination was unchanged. This effect was confirmed in a different manner by taking equal proportions of cells incubated under different circumstances. Cells were incubated in RIS medium with 100 µg/ml Con A, washed, and combined with cells that had incubated in LIS

TABLE 8

AGGLUTINATION OF CELLS INCUBATED AT REGULAR IONIC STRENGTH WITH CON A, FOLLOWED BY ASSAY AT LOW IONIC STRENGTH WITH NO CON A

Incubation Conditions	Degree of Agglutination[a]
Regular Ionic Strength with Con A	+ +
After transfer to Low Ionic Strength, no Con A	+ +

[a] All controls zero, scores are the means of three experiments using 5 X 10^5 cells/ml, 100 µg/ml Con A

TABLE 9

AGGLUTINATION OF CELLS INCUBATED AT REGULAR IONIC STRENGTH WITH CON A, FOLLOWED BY ASSAY AT LOW IONIC STRENGTH WITH CON A

Incubation Conditions	Degrees of Agglutination [a]
Regular Ionic Strength with Con A	+ +
After transfer to low ionic strength with Con A	+ + + + +

[a] All controls zero, scores are the means of three experiments using 5 X 10^5 cells/mo, 100 µg/ml Con A

TABLE 10

AGGLUTINATION OF CELLS INCUBATED AT LOW IONIC STRENGTH WITH CON A, FOLLOWED BY INCUBATION AT REGULAR IONIC STRENGTH WITH NO CON A

Incubation conditions	Degree of Agglutination[a]
Low ionic strength with Con A	+ + + + +
After transfer to regular ionic strength with no Con A	+ + + + +

[a] All controls zero, scores are the means of three experiments using 5 X 10^5 cells/ml, 100 µg/ml Con A

TABLE 11

MIXED AGGLUTINATION OF CELLS WHEN INCUBATED AT DIFFERENT IONIC STRENGTHS

Incubation Conditions	Degree of Agglutination
Low ionic strength with no Con A	0
Regular ionic strength with Con A	+ +
After combining the above cell suspensions, washed free of excess Con A	+ + +

[a] All controls zero, scores are the means of three experiments. All final cell densities were 5 X 10^5 cells/ml, 100 µg/ml Con A.

medium having no Con A present. Table 11 shows that this mixed agglutination assay resulted in an increase of the degree of agglutination. This enhancement was without the presence of additional Con A after mixing.

The specificity of Con A-mediated agglutination of L5178Y cells is shown in Table 12. Each inhibitor was used at 20 mM/l and the Con A concentration was 100 µg/ml. The control solutions having no Con A scored zero, while the control solutions having no sugars scored 2+. In addition, when cell clumps were mixed with 10 mM α-m-D-Mannoside, the agglutinated cells were dispersed after 30 minutes of gentle agitation. Hence, the agglutination of cells could be blocked by prior addition of the sugar or by adding the inhibitor after the cells were aggregated with Con A.

The minimum concentration of Con A required to yield an agglutination score of 1+ was also determined. This score represents about 25% of the cells being agglutinated. Results shown in Table 13 indicate that about 4.0 µg/ml Con A was sufficient to agglutinate the L5178Y cell line.

Growth Parameters of the 3T3 and PY3T3 Cell Lines

Morphology

Sparsely-seeded cultures ($<10^4$ cells/cm^2) of the 3T3 cell line grow as single, isolated cells. The cells grow attached to the substratum, detaching only during mitosis after rounding up. Most cells are flat, about 50 microns across, with occasional pseudopodia extending 10 to 20 microns. The cytoplasm contains some granules surrounding the nucleus, being transparent under phase-contrast microscopy, and vacuoles

TABLE 12

SPECIFICITY OF AGGLUTINATION OF L5178Y CELLS BY CON A USING HAPTEN-INHIBITORS

Incubation Solution[a]	Degree of Agglutination[b]
Sucrose	0
α-m-D-Glycoside	0
α-m-D-Mannoside	0
PBS, No Con A	0
PBS, with Con A, no sugars	+ +

[a] All inhibitors used at 20 mM/l in PBS

[b] Assays used 5 X 10^5 cells/ml, 100 μg/ml Con A

TABLE 13

THE MINIMUM CONCENTRATION OF CON A REQUIRED TO YIELD A SCORE OF 1+

Con A (μg/ml)	Degree of Agglutination[a]
0.5	0
1.0	0
1.5	0
2.0	0
2.5	0
3.0	±[b]
4.0	+
5.0	+
7.5	+
10.0	+
15.0	+
50.0	+ +

[a] All controls zero, each score is the average of three experiments. Assay used 1 X 10^6 cells/ml.

[b] Mixed scores of zero and occasional doublets

may be observed with the nucleus of some cells. The 3T3 cells at low density and at confluency are shown in Figures 12a and 12b, respectively. These photographs are at 300x magnification, the cells being fixed in methanol:glacial acetic acid and stained with Giemsa.

This cell line exhibits contact inhibition of growth when cultured under the proper conditions. As the cells form small clones, they assume a cuboidal shape, withdraw any extended pseudopodia, decrease in size (surface area), and do not overlap the neighboring cells. As mitosis within a clone occurs, the mitotic cells detach, float, and re-attach in a space not occupied by cells. This process continues until the cells reach a confluent monolayer. The confluent culture exhibits a marked decrease in proliferation, since the cells grow only as a single layer, do not overlap, and mitotic figures are rarely present. The entire culture takes on a "cobblestone" appearance, with the cells having the same morphological appearance. When maintained at confluency for more than 48 hours (or following a change of medium) the number of mitotic figures increase and rounding up of some cells can be observed. If left in this state, these cells will escape the density-dependent inhibition of growth.

In contrast to the nontransformed cells described above, the PY-3T3 cell line has a spectrum of morphology. Most PY3T3 cells grow as attached, fibroblastic, elongated, refractile cells. Long, thin pseudo-podia reaching 50 to 200 microns in length can be observed, though the body of most cells are about 30 to 50 microns across. The PY3T3 cells are shown in a sparse culture ($<10^5$ cells/cm^2) in Figure 13a. The isolat-ed cells frequently overlap each other which results in small "islands"

Figure 12a. 3T3 cells in sparse culture. Photographs on this page were taken at 300x magnification. The cells were fixed with methanol and stained with Giemsa.

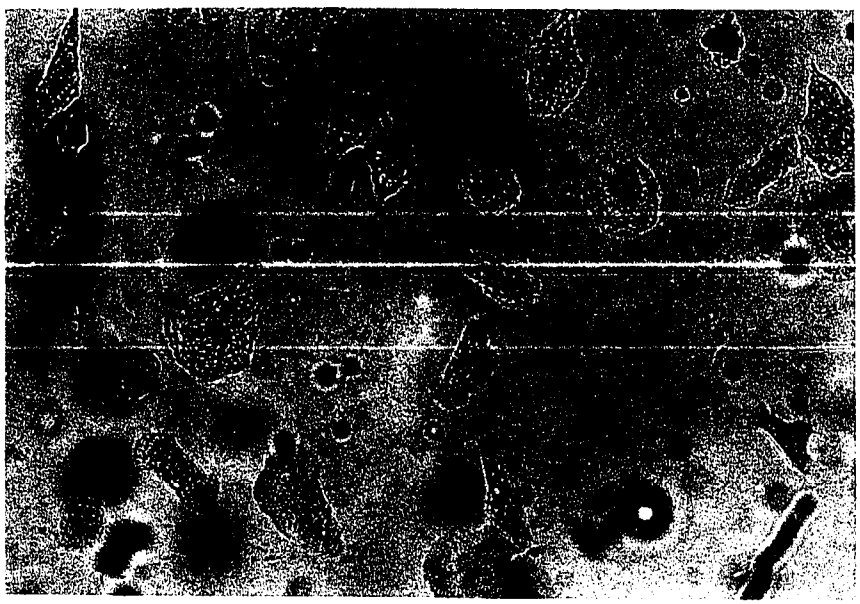

Figure 12b. 3T3 cells at confluency. When cultured at the proper density, little or no cell overlap is observed. The heavily-stained nuclei are prominent.

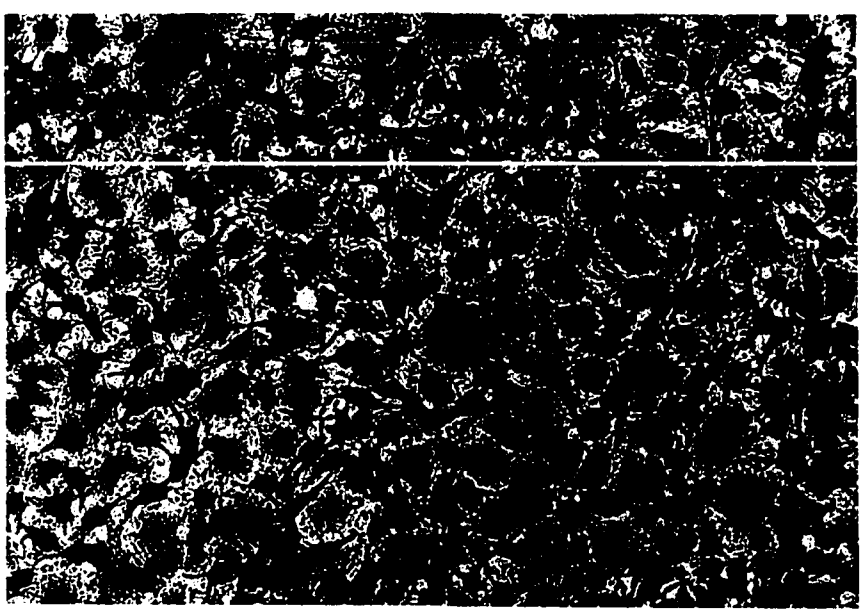

Figure 13a. PY3T3 cells in sparse culture. Photographs on this page are at 300x magnification. The extended pseuopodia are visible and the nature of how these cells overlap can be observed.



Figure 13b. PY3T3 cells at saturation density. The dense center of the clone is due to the piling up of the cells. The criss-cross pattern seen at the periphery is common for transformed cells.

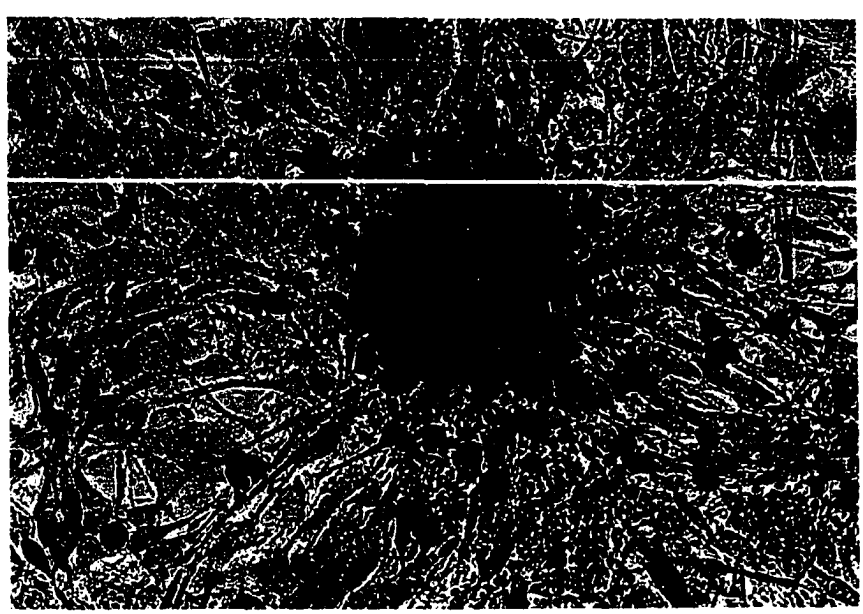

of cells at this stage of culture growth. Large, flat cells are common, reaching up to 200 microns across and being very transparent using phase-contrast microscopy. These cells rarely extend pseudopodia, appearing more as a thin "web", and are often multi-nucleated with the nuclei taking up 60 to 80% of the apparent cell volume.

Large, macroscopic clones are visible as the culture approaches saturation density ($\simeq 10^6$ cells/cm^2). The center of a clone is shown in Figure 13b. It is many cell layers thick, the cells being loosely packed in a criss-cross pattern at the periphery, until the very center is observed, where the cells are very dense and is opaque under light microscopy. This type of clone allows the high saturation density of the PY3T3 cell cultures with the cells demonstrating a much less degree of density-dependent growth behavior compared to the 3T3 cells.

Doubling Time and Saturation Density of the 3T3 and PY3T3 Cell Lines

The growth curve of 3T3 cells in logarithmic-phase growth is shown in Figure 14. The cell number per cm^2 is given as a function of culture time, in days. This curve shows that the average doubling time of 3T3 cultures is 23.5 ± 0.1 hours, using four experiments with duplicates. The saturation density is 6.4 ± 0.2 X 10^4 cells/cm^2.

A similar plot for PY3T3 cells is shown in Figure 15. The average doubling time of 29.1 ± 0.6 hours was obtained with three experiments, done with duplicates. The saturation density is more than an order of magnitude higher than 3T3 cultures, being 8.6 ± 0.2 X 10^5 cells/cm^2. This saturation density has been maintained for several weeks in culture, with frequent changes of medium.

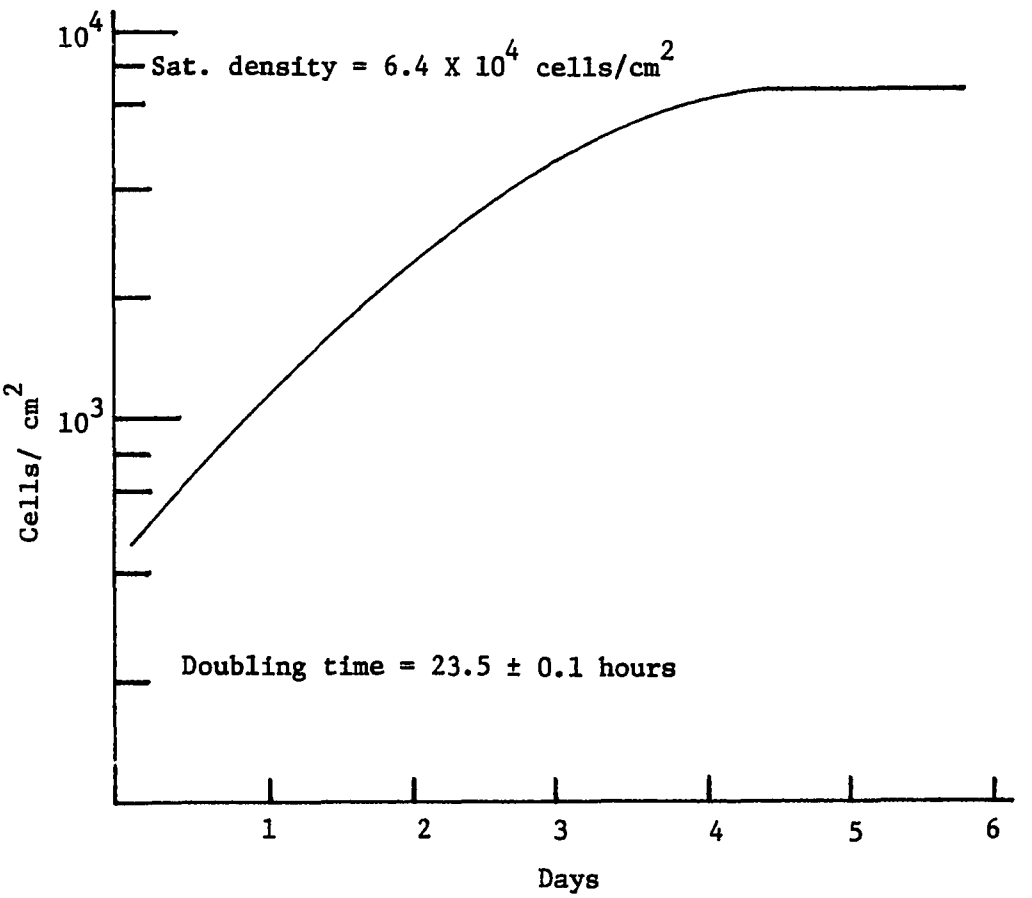

Figure 14. Growth of 3T3 Swiss Albino fibroblasts in culture. The curve was generated by the mean of four experiments.

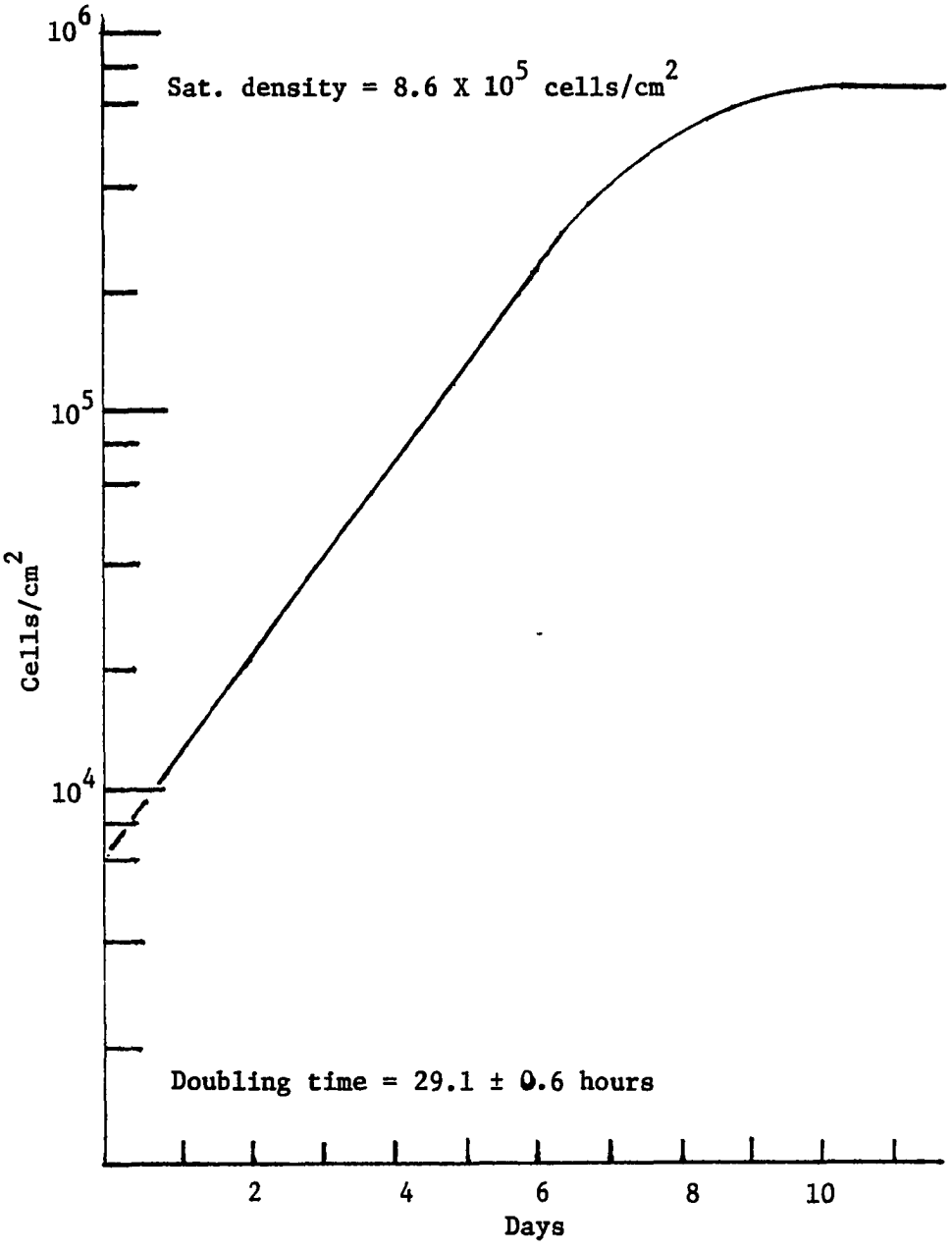

Figure 15. Growth of polyoma virus-transformed 3T3 cells in culture. The curve was generated by the mean of three experiments.

The growth curves were obtained by averaging the slopes of best-fit linear plots to individual experiments, and the average regression coefficient was 0.985.

Proliferative Pool, Initial Fraction in DNA Synthesis, Flow Rate Across G_1-S, and Cell Cycle Time for the 3T3 and PY3T3 Cell Lines

The results of the continuous labeling experiments using 0.3μCi/ml ^{3}H-thymidine are shown in Figures 16 and 17. The percentage of labeled cells is plotted as a function of time, in hours. The curves indicate that both cell lines have about 40% of their cell populations in DNA synthesis at any given time. The slope of the two curves are the same and shows that the flow rate of 3T3 and PY3T3 cells across the G_1-S border of the cell cycle is about 3% of the cell population per hour. The plateau of both curves indicate the percentage of the cells that are in the proliferative pool, i.e. those cells that contribute to the growth of the culture. Since both cell lines demonstrate that at least 95% of the cells are labeled, then the cell cycle times are extremely close to the doubling times of the cultures. Hence, the average cell cycle times are about 23 and 29 hours for the 3T3 and PY3T3 cell lines, respectively.

Agglutination Studies on the 3T3 and PY3T3 Cell Lines

Except where indicated, all assays used the standard procedures and solutions given in Materials and Methods.

The degree of agglutination of 3T3 cells as a function of the Con A concentration is given in Table 14. The average clump size increased from a score of 1+ at 100 μg/ml Con A to 2+ using 600 μg/ml. Approximately 70% of the cells are agglutinated using 600 μg/ml Con A.

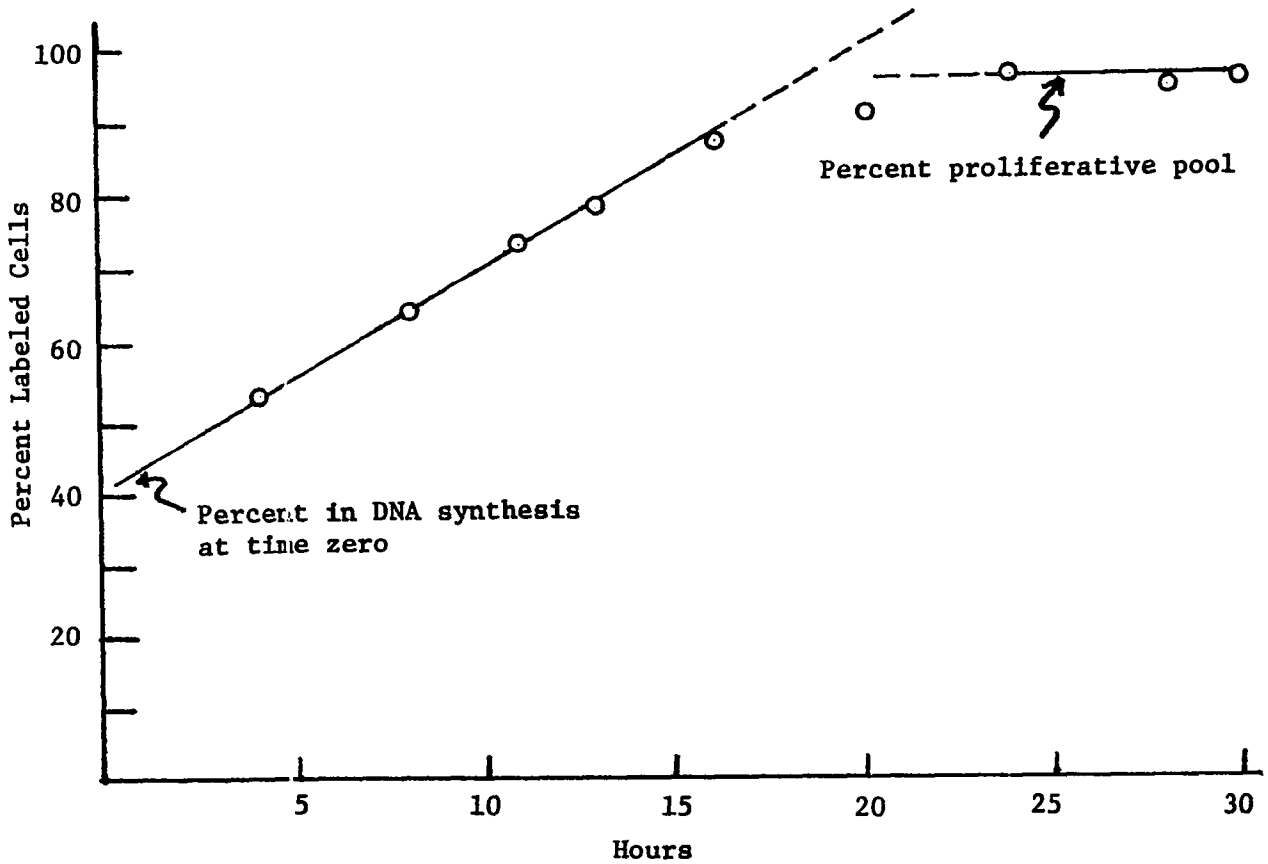

Figure 16. The percent of ^{3}H-labeled 3T3 cells with time. About 40% are in the S phase of the cell cycle. The flow rate across the G_1-S border is about 3% per hour. Final labeling indicates that about 95% of the cells are in the proliferative pool.

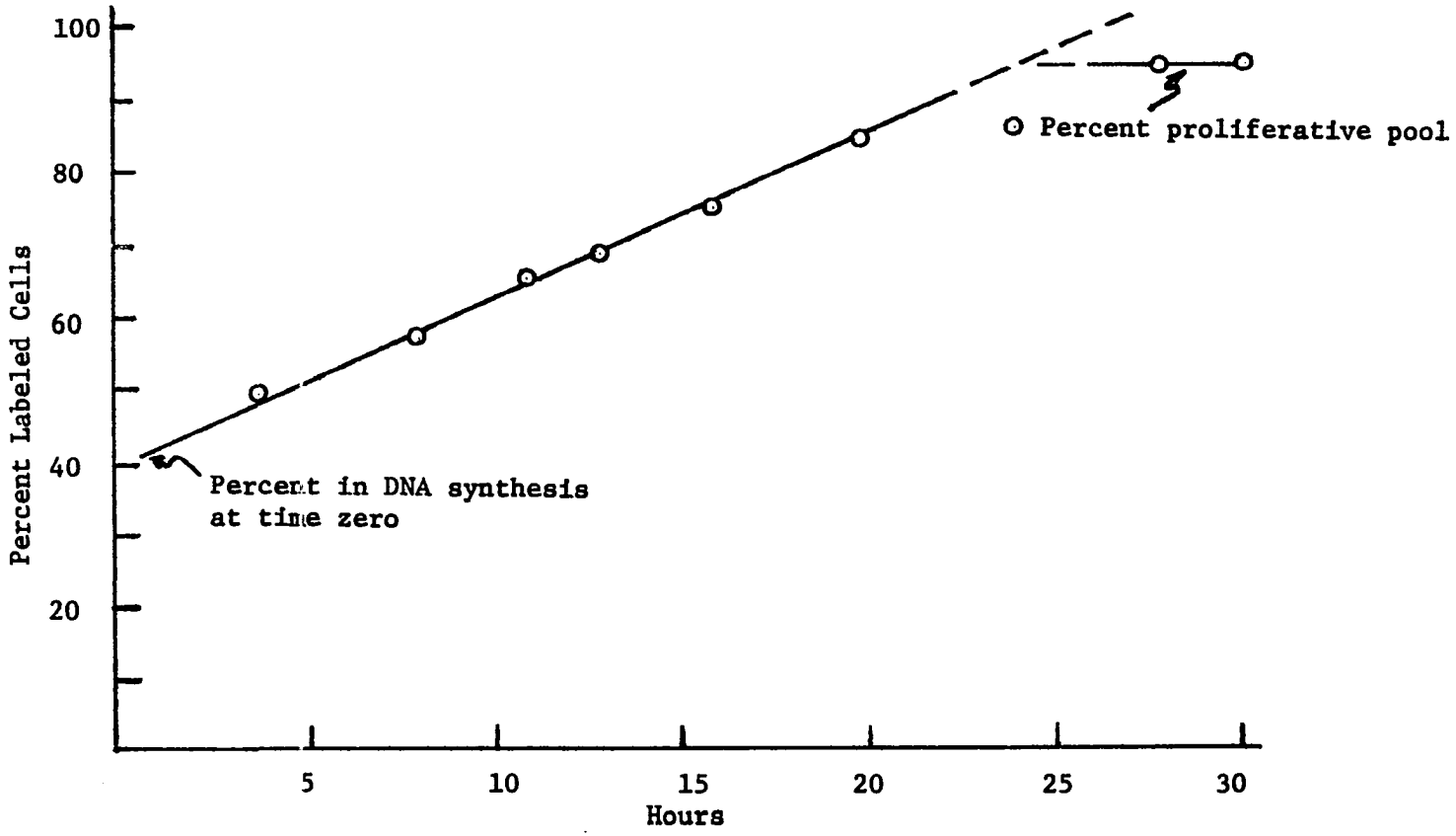

Figure 17. The percent of ^{3}H-labeled PY3T3 cells with time. About 40% are in the S phase of the cell cycle. The flow rate across the G_1 - S border is about 3% per hour. Final labeling indicates about 95% of the cells are in the proliferative pool.

TABLE 14

THE DEGREE OF AGGLUTINATION OF 3T3 CELLS WITH CON A

Con A (μg/ml)	Degree of Agglutination[a]	% Cell Agglutination
100	+	52
200	+	57
400	+ +	71
600	+ +	71

[a] All controls zero, scores are the means of three experiments using 4.5 X 10^5 cells/ml.

TABLE 15

AGGLUTINATION OF 3T3 CELLS AT VARIOUS IONIC STRENGTHS USING 25 μg/ml CON A

Ionic Strength (mEq/l)	Degree of Agglutination [a]
150	+
100	+
50	+
5	+

[a] All controls zero, scores are the means of three experiments using 4.5 X 10^5 cells/ml. About 50% of the cells agglutinated at each ionic strength.

The controls were scored zero and the experiment (and each of the following agglutination experiments) was performed three times, with replicates. The effect of varying ionic strength was studied using 25 and 200 μg/ml Con A. Table 15 indicates there was little change in the agglutinability of 3T3 cells at the lower concentration of Con A when the ionic strength was changed from 150 mEq/l to about 5 mEq/l. There was no pre-incubation of the cells prior to the assay in the respective solutions. About 50% of the cells were agglutinated at each ionic strength used.

The use of 200 μg/ml Con A clearly showed the effect of low ionic strength on the agglutinability of 3T3 cells. The results are shown in Table 16. When the ionic strength was varied from 150 to 5 mEq/l, a prior incubation of the cells at $35^{o}C$ for thirty minutes resulted in about 95% of the cells being clumped. This is in contrast to the smaller average clump size and less percent of cells agglutinated with no prior incubation.

Agglutination of 3T3 cells was examined using the assay described by Burger (17). Cells were added to the well of a glass coverslip (0.5 ml working volume) at a final cell density of 5×10^{5} cells/ml. Con A was added at either 50 or 200 μg/ml. In addition, ionic strength of the medium was varied from 150 to 5 mEq/l with different preincubation times. The cells were gently rocked for 10 minutes, then scored. Table 17 shows that no agglutination occurred when the cells were assayed by this protocol.

Using the standard assay, Table 18 shows the degree of agglutination for PY3T3 cells for different concentrations of Con A. About 95% of the cells were agglutinated using 800 μg/ml Con A compared to 50% at

TABLE 16

AGGLUTINATION OF 3T3 CELLS AT VARIOUS IONIC STRENGTHS USING 200 μg/ml CON A

Ionic Strength (mEq/l)		Degree of Agglutination[a]	% Cell Agglutination
No preincubation	150	+	56
	100	+	56
	50	+ +	68
	5	+ +	70
(Preincubated 30 minutes)	150	+	60
	100	+ +	76
	50	+ + +	88
	5	+ + +	94

[a] All controls zero, scores are the means of three experiments using 4.5 X 10^5 cells/ml. Preincubation temperature was 35°C.

TABLE 17

AGGLUTINATION OF 3T3 CELLS AT VARIOUS IONIC STRENGTHS USING 50 and 200 µg/ml CON A[a]

Pre-incubation time	Con A (µg/ml)	Ionic Strength (mEq/l)	Degree of Agglutination[b]
zero minutes	50	150	0
		100	0
		50	0
		5	0
30 minutes	50	150	0
		100	0
		50	0
		5	±[c]
zero minutes	200	150	0
		100	0
		50	±
		5	0
30 minutes	200	150	0
		100	0
		50	±
		5	±

[a] Assay was 5 X 10^5 cells/ml in well of glass coverslip for 10 minutes, gentle agitation

[b] Mean of two experiments

[c] Mixed scores of zero and occasional doublets

TABLE 18

THE DEGREE OF AGGLUTINATION OF PY3T3 CELLS WITH CON A

Con A (μg/ml)	Degree of Agglutination[a]
5	+
10	+
25	+
50	+ +
100	+ +[b]
200	+ + +
400	+ + + +
600	+ + + + +
800	+ + + + +

[a] All controls zero, scores are means of three experiments using 2 X 10^5 cells/ml.

[b] 100 μg/ml Con A consistently agglutinated 75% of the cells.

5 to 10 µg/ml. Comparing the PY3T3 and 3T3 cell lines using 75% cell agglutination, about 100 µg/ml Con A was required for PY3T3 cells and 600 µg/ml Con A was needed for 3T3 cells. The PY3T3 also showed enhancement of agglutination using low ionic strength. Table 19 demonstrates that 100% of the cells could be agglutinated using 400 µg/ml Con A at an ionic strength of 5 mEq/l, when the cells were pre-incubated for 30 minutes at 35°C before assay.

The specificity of agglutination using Con A was confirmed for both the 3T3 and PY3T3 cell lines. The hapten-inhibitor, α-methyl-D-Mannoside completely inhibited agglutination at a concentration of 20 mM/l using 200 µg/ml Con A. The addition of the sugar to agglutinated cells dispersed the cell clumps within 30 minutes.

Differential Effect of Native and TRYP-Con A On Cell Growth

The following results on the growth of L5178Y cells demonstrate the monomeric nature of the TRYP-Con A solution. Figure 18 shows the growth of L5178Y cells for 5 days following the addition of 1, 5, 10, 20, and 50 µg/ml native Con A. Trypan blue staining for viable cells indicate that initially, 95% of the cells were killed during the first 48 hours. No cells survived the addition of native Con A at concentrations equal to, or above 10 µg/ml.

In contrast, the addition of TRYP-Con A to the L5178Y cell cultures allowed survival of cell cultures, up to the highest concentration of 50 µg/ml. About 80% of the sensitive cells are killed within 48 hours, but the recovery curves indicate that the growth of viable cells was similar to that of the control cultures at about the fourth day.

TABLE 19

DEGREE OF AGGLUTINATION OF PY3T3 CELLS AT LOW IONIC STRENGTH WITH CON A

Con A (μg/ml)	Degree of Agglutination[a]
25	+ + +
50	+ + + +
100	+ + + +
200	+ + + + +
400	+ + + + + +[b]
800	+ + + + + +

[a] All controls zero, scores are the means of three experiments using 2 X 10^5 cells/ml. Pre-incubation time was 30 minutes.

[b] 100% of the cell agglutinated using this score.

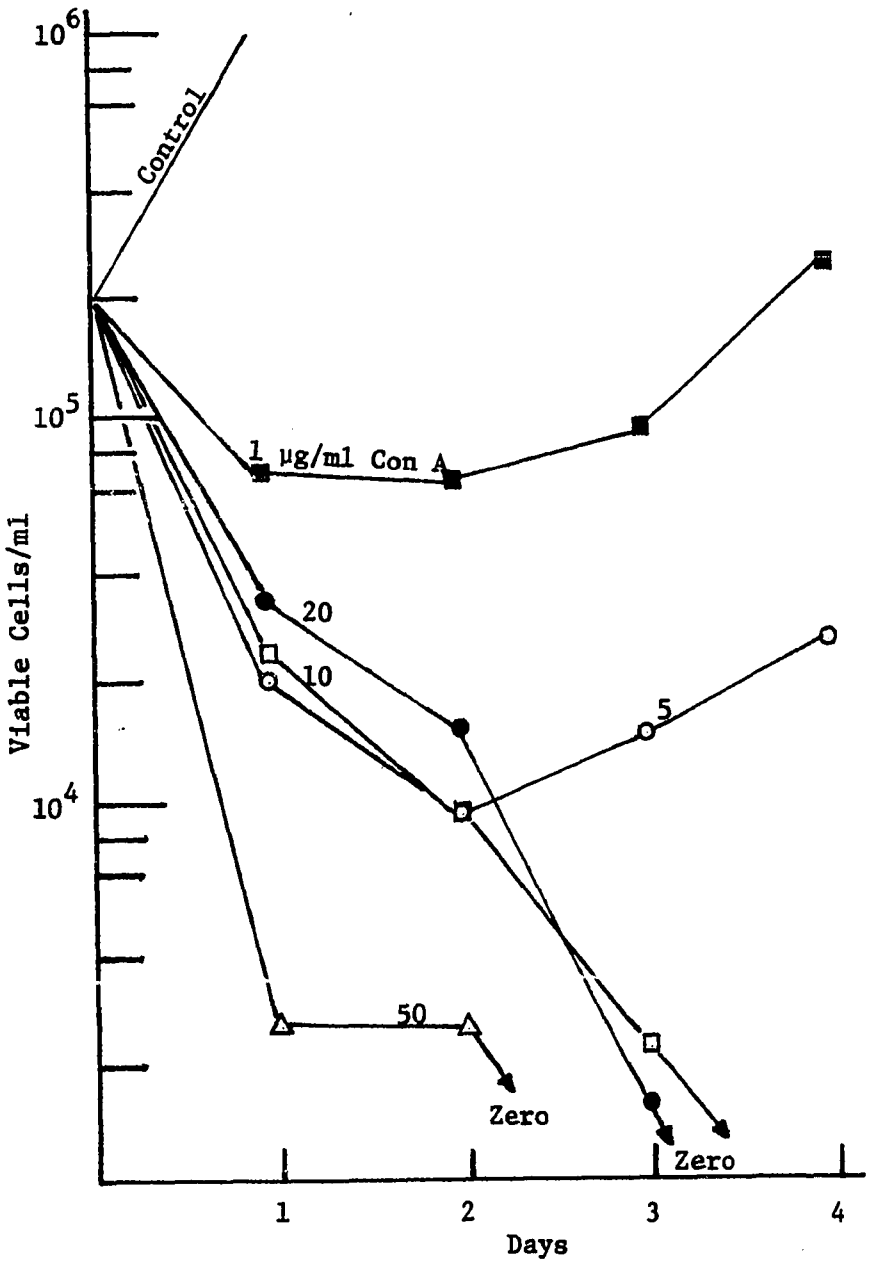

Figure 18. The number of viable L5178Y cells with time, after the addition of various concentrations of native Con A to the medium. No cells survive 72 hours, using 10 µg/ml or greater. Numbers on the curves indicate the concentration of Con A.

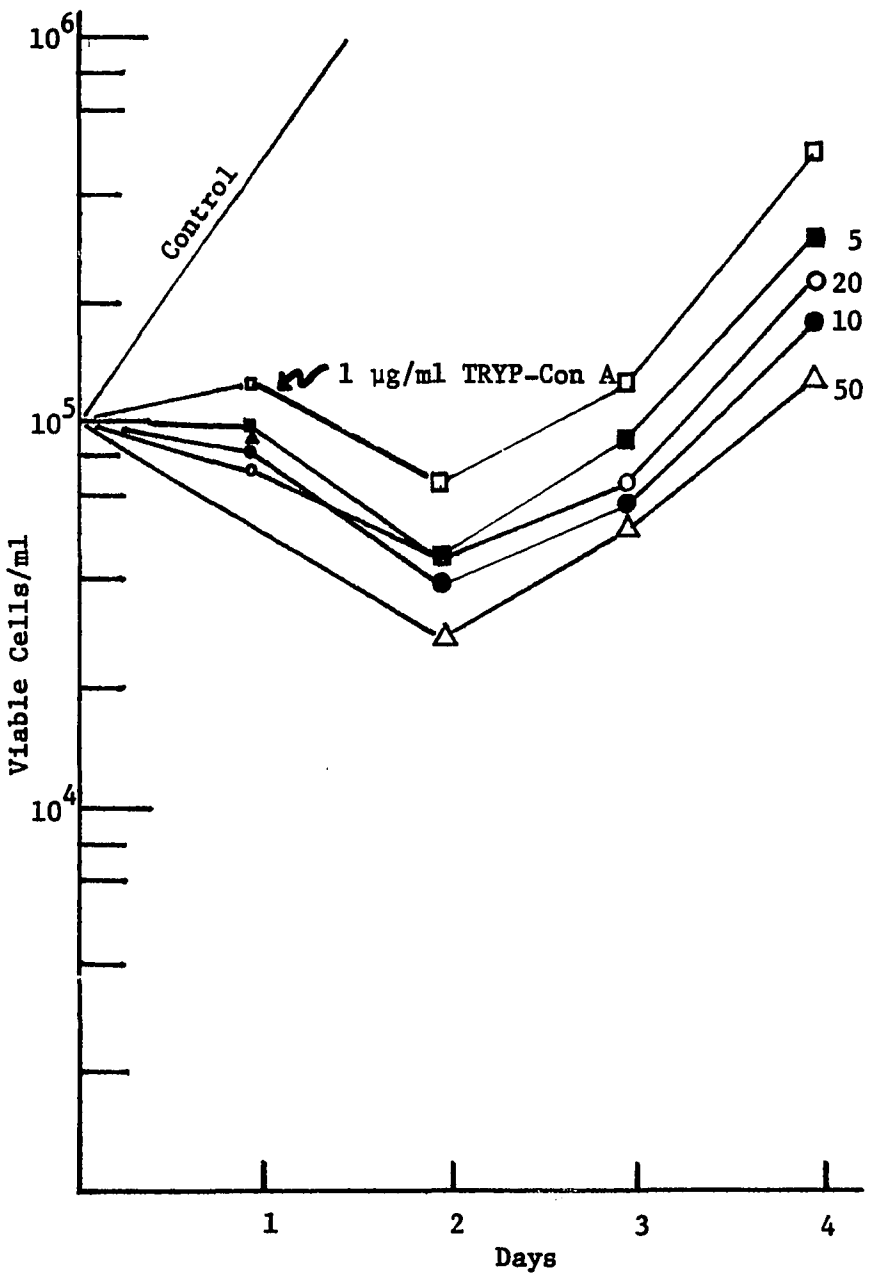

Figure 19. The number of viable L5178Y cells with time, after the addition of various concentrations of trypsinized Con A. All cell cultures survived the doses of TRYP-Con A used.

Growth Parameters of the Chronic TRYP-Con A Treated PY3T3 Cell Line

Morphology

The cells used for the establishment of this line were in their 10th passage in culture. The medium and conditions of culture remained unchanged. Figures 20a, 20b, and 20c show the PY3T3 cells that were continuously treated with 40 μg/ml TRYP-Con A, after 2, 4, and 6 months, respectively. This line was designated PY3T3CCA. The morphology of the PY3T3CCA cell line is comparable to the untreated PY3T3 cells during the first few weeks after the addition of TRYP-Con A. Figure 20a shows that the cells continue to overlap each other which results in the formation of large clones, although by the end of the first month in culture, the saturation density of the PY3T3CCA cultures is the same as the nontransformed 3T3 cells, 6×10^4 cells/cm^2. There are still many cell types visible in these cultures, although the large, flat, multi-nucleated cells do not seem to be as numerous as before the treatment with TRYP-Con A. No changes in cytoplasmic structures, or nuclei was observed.

The cultures are visibly changed by the 4th month. Figure 20b shows the center of a large clone, and it can be seen that although the clone is several layers thick in the center, the cells are flat, and have little overlap in the peripheral region. Discrete regions of the flask have an abundance of only one cell type, and many clones are formed with a monolayer. There is some regularity observed in patterns formed by the elongated, fibroblastic cells. "Swirls" form about the clones with little or no cell overlap from these type of cells.

The center of a clone is shown in Figure 20c. After 6 months of chronic TRYP-Con A treatment, the cells form large clones, but

Figure 20a. PY3T3CCA cells after 2 months of TRYP-Con A treatment. Little change is observed compared to the untreated cells. All photographs in this series are at 300x magnification.



Figure 20b. PY3T3CCA cells after 4 months of TRYP-Con A treatment. Cells appear more ordered within the clone. The extent of cell overlap is reduced. The morphology also appears more uniform.

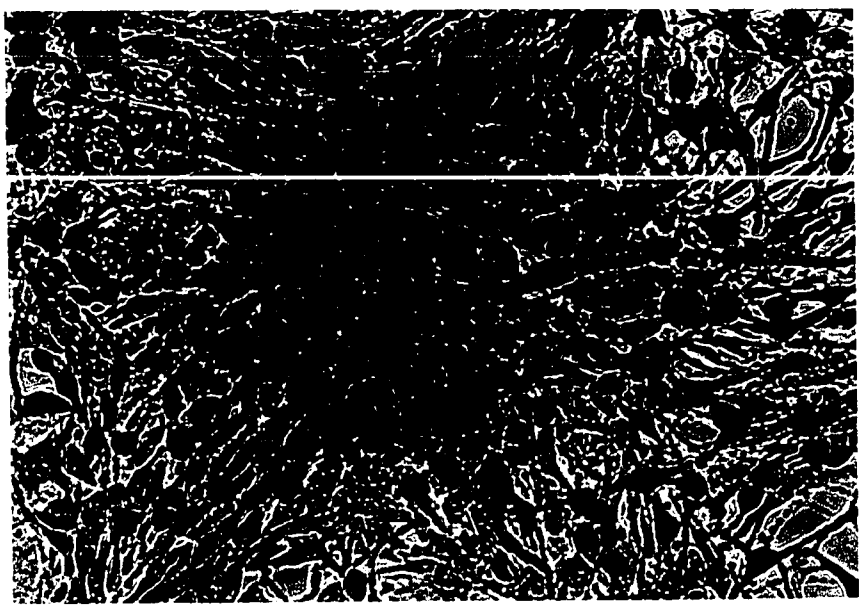

Figure 20c. PY3T3CCA cells after 6 months of TRYP-Con A treatment. The center of the clone appears to be a monolayer but some cell overlap can be observed. The cells appear much like the 3T3 cells at confluency.

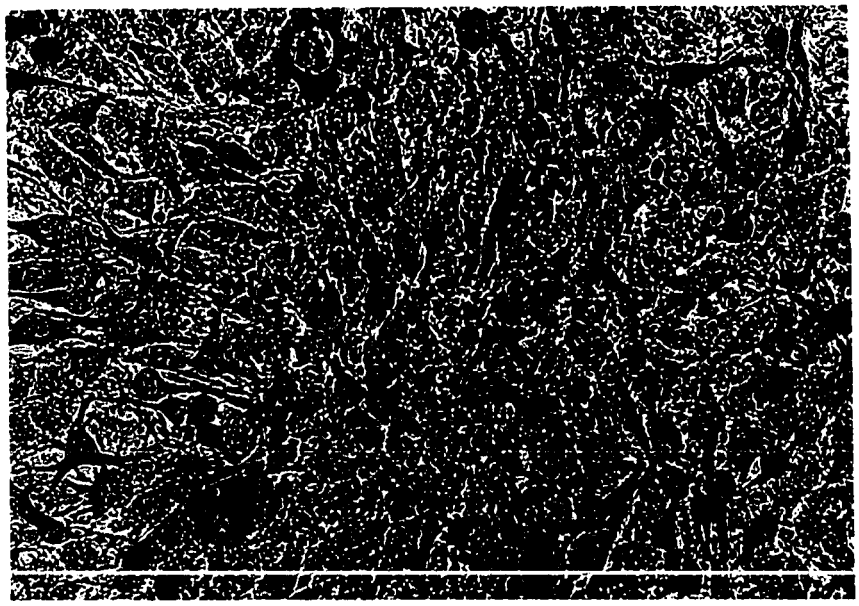

usually with a single layer of cells. Some overlap of cells can be observed, but the appearance of these cultures dramatically change compared to the PY3T3 cells. The dominant cell type is very similar to 3T3 cells, being small, flat, and usually having no extended pseudopodia.

Doubling Time, Saturation Density, and Proliferative Pool of the PY3T3CCA Cell Line

The growth curves of PY3T3CCA cells are shown for the first 6 months in Figures 21 and 22. The number of cells per cm^2 is plotted against time, in days. The doubling time of the cultures increase from 29 hours (untreated PY3T3 cells) to about 75 hours after the first month following treatment with 40 µg/ml TRYP-Con A. The doubling time fluctuates for the next couple of months, then starts to decrease, reaching 41 hours after 6 months in culture.

The saturation densities are comparable to the nontransformed 3T3 cell cultures. All of the PY3T3CCA cell cultures reach about 6×10^4 cells/cm^2. For comparison, the saturation densities and doubling times of the 3T3, PY3T3, and PY3T3CCA cell lines are shown in Table 20.

The acute effect of 40 µg/ml on the growth of PY3T3 cells was studied by examining the growth of the cultures and the proliferative capacity of the attached cells. Figure 23 shows the growth of PY3T3 cells in three experiments, following the addition of TRYP-Con A. Cell death is the dominant feature for the first 72 hours, then the cultures grow with a decreased rate compared to the untreated cells. The incorporation of ^3H-thymidine following TRYP-Con A treatment is demonstrated in Figure 24. The percent of labeled cells is plotted as a function of time, in hours. This curve shows that the kinetics of growth for the PY3T3 cells

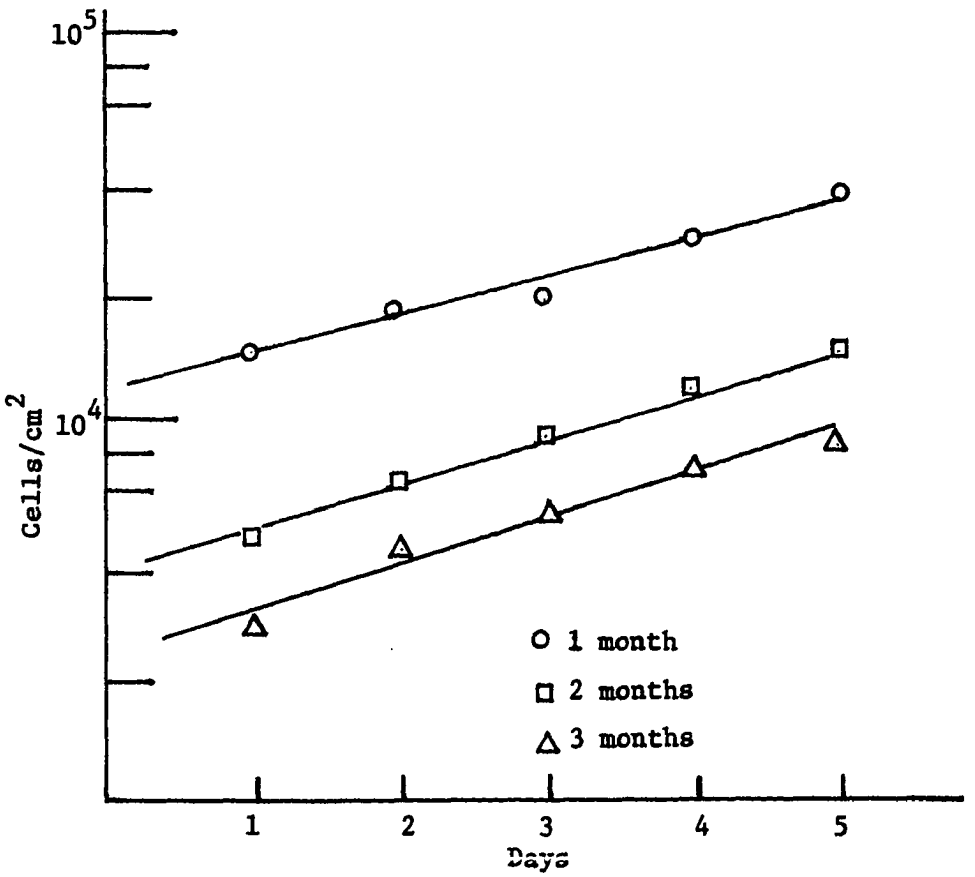

Figure 21. Growth of PY3T3CCA cells after 1, 2, and 3 months in the continuous presence of 40 µg/ml TRYP-Con A.

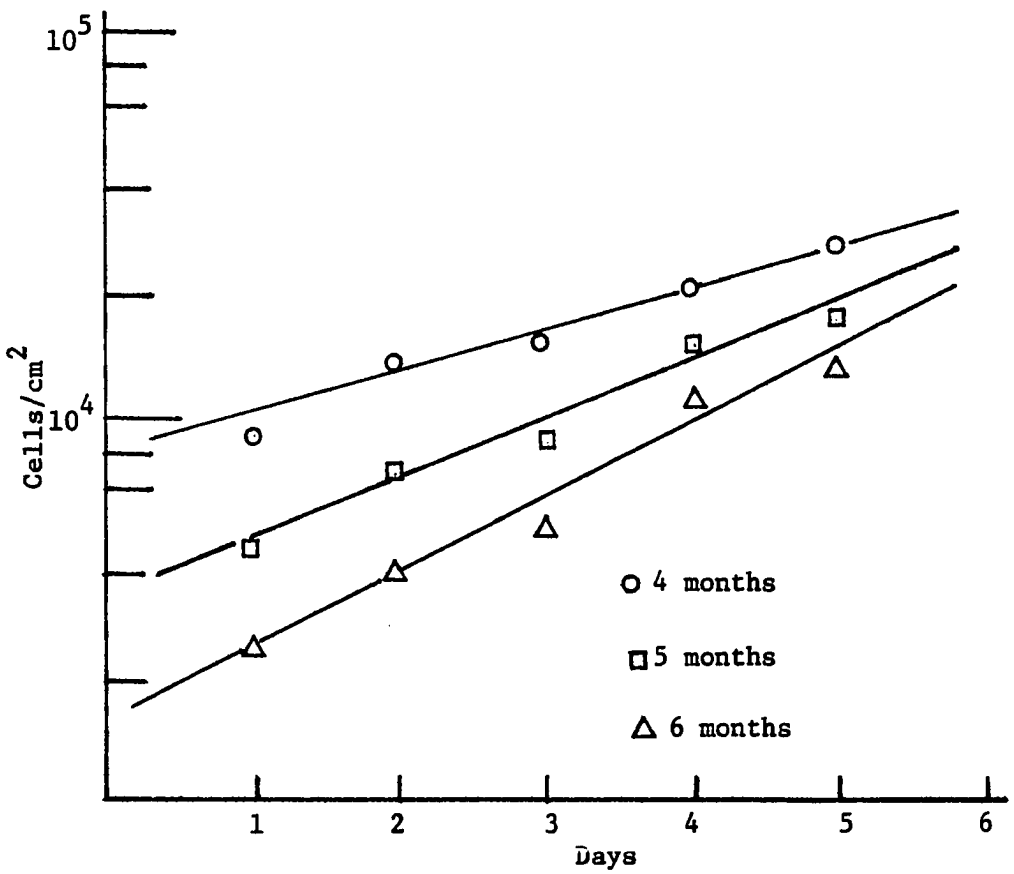

Figure 22. Growth of PY3T3CCA cells at 4, 5, and 6 months of continuous TRYP-Con A treatment with 40 µg/ml.

TABLE 20

GROWTH PARAMETERS AND AGGLUTINABILITY OF 3T3, PY3T3, AND PY3T3CCA CELLS

Cell Line	Doubling Time (hours)	Saturation Density (cells/cm^2)	Degree of Agglutination[a]
3T3	23	6.0×10^4	+
PY3T3	29	8.6×10^5	+ + +
$PY3T3CCA_1$[b]	70	6.1×10^4	0
$PY3T3CCA_2$	58	5.5×10^4	0
$PY3T3CCA_3$	57	5.9×10^4	0
$PY3T3CCA_4$	72	5.8×10^4	0
$PY3T3CCA_5$	47	6.8×10^4	0
$PY3T3CCA_6$	41	6.2×10^4	0

[a] 200 μg/ml Con A, regular ionic strength

[b] Subscript numbers indicate months of treatment with 40 μg/ml TRYP-Con A

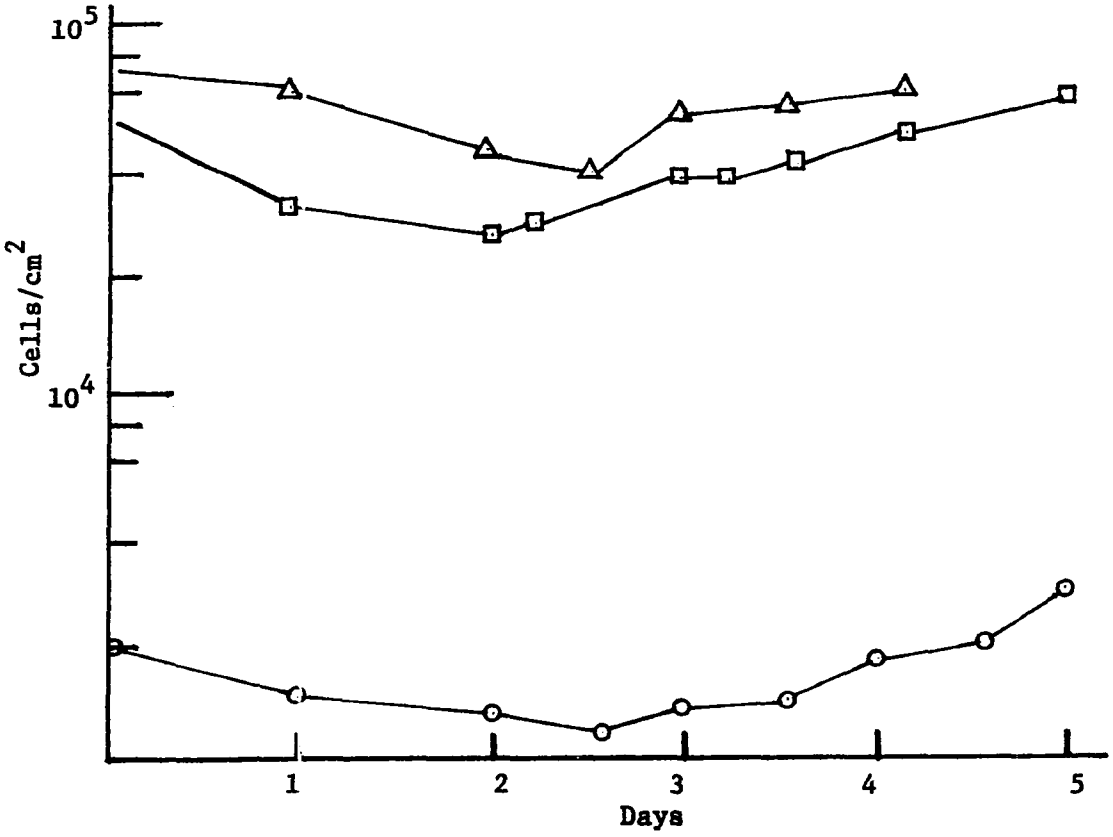

Figure 23. Acute treatment of PY3T3 cells with 40 µg/ml TRYP-Con A. Positive growth rate does not occur until about 72 hours indicating an initial cell killing. Three separate experiments are shown.

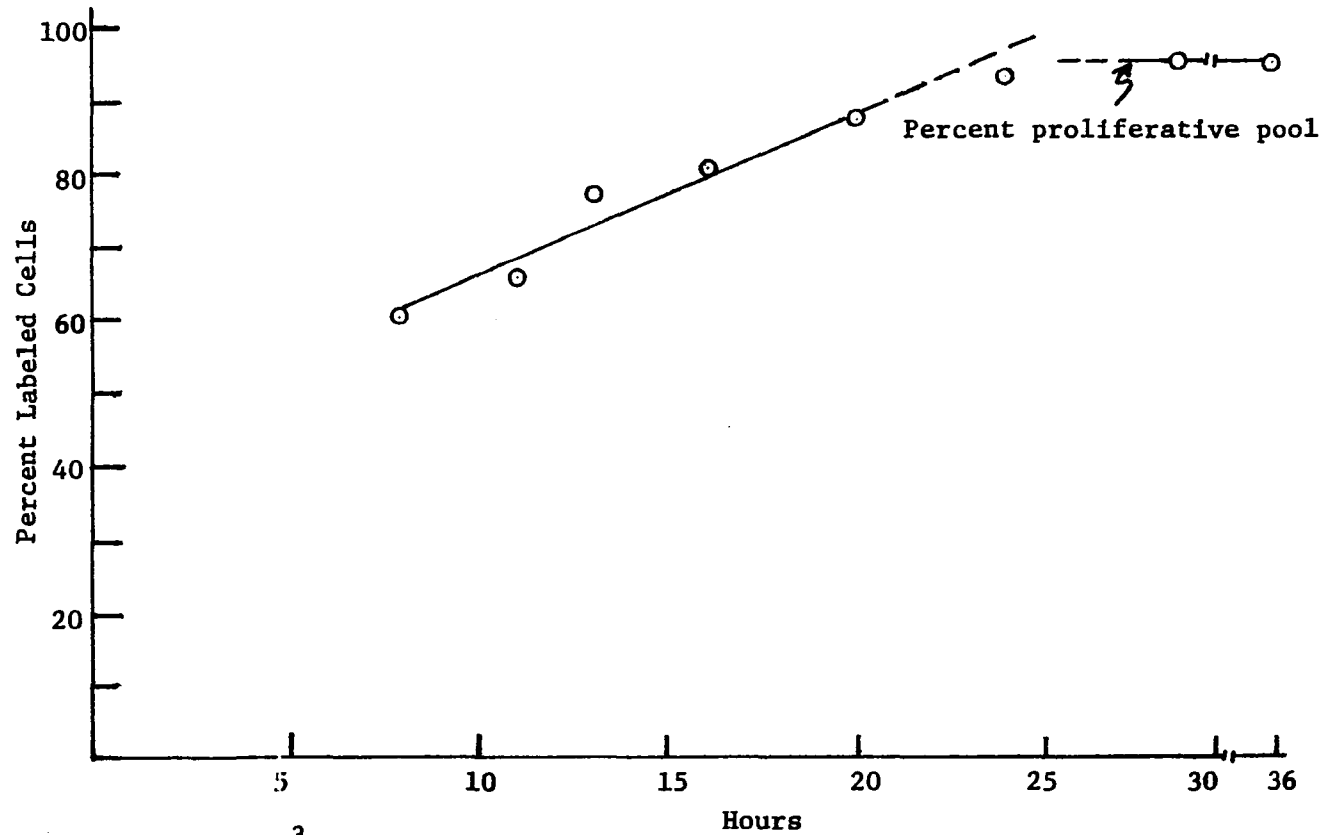

Figure 24. Percent ^{3}H-labeled PY3T3 cells with time, following the addition of 40 µg/ml TRYP-Con A. Final labeling indicates that about 95% of the cells (attached) are in the proliferative pool. The flow rate across the G_1 - S border is about 3% per hour.

treated with TRYP-Con A is not different than the untreated PY3T3 cells. About 95% of the attached cells are labeled within 25 hours, a time consistent with the observed growth of untreated cultures. The medium of the treated cultures contained clumped, granular cells, reflecting the cell death indicated from Figure 23.

The agglutinability of the PY3T3CCA cell line was lost within 4 weeks of culture. The TRYP-Con A was dissociated by a one-hour incubation with 50 mM/l α-methyl-D-Mannoside. The cells were washed, resuspended with native Con A, and assayed for agglutination. Assays were performed on PY3T3CCA cultures from 1 month to 6 months treatment with TRYP-Con A. The degree of agglutination was zero for all cells tested, even using concentrations of Con A as high as 1000 μg/ml.

Microelectrode Properties and Cell Penetration

The physical description of microelectrodes fabricated with the Chowdhury Pipette-Puller has been published (123).

The change in the tip potential and DC resistance when the ionic environment of the tip is changed (e.g. when impaling the cell cytoplasm) was estimated using 32 microelectrodes. Figure 25 shows the change in tip potential, ΔV_T, in mV, as a function of the tip potential when the microelectrode is immersed first in a 140 mM NaCl - 10 mM KCl solution, then changed to a 140 mM KCl - 10 mM NaCl solution. The best-fit linear regression line yields the equation for ΔV_T;

$$\Delta V_T = 0.2\ V_T + 0.1\ mV$$

i.e. an inherent tip potential of 5 mV will usually be associated with a 1.0 mV change, to 6 mV when the microelectrode is inserted into an environment of low Na^+ and high K^+ concentrations. Figure 26 demonstrates

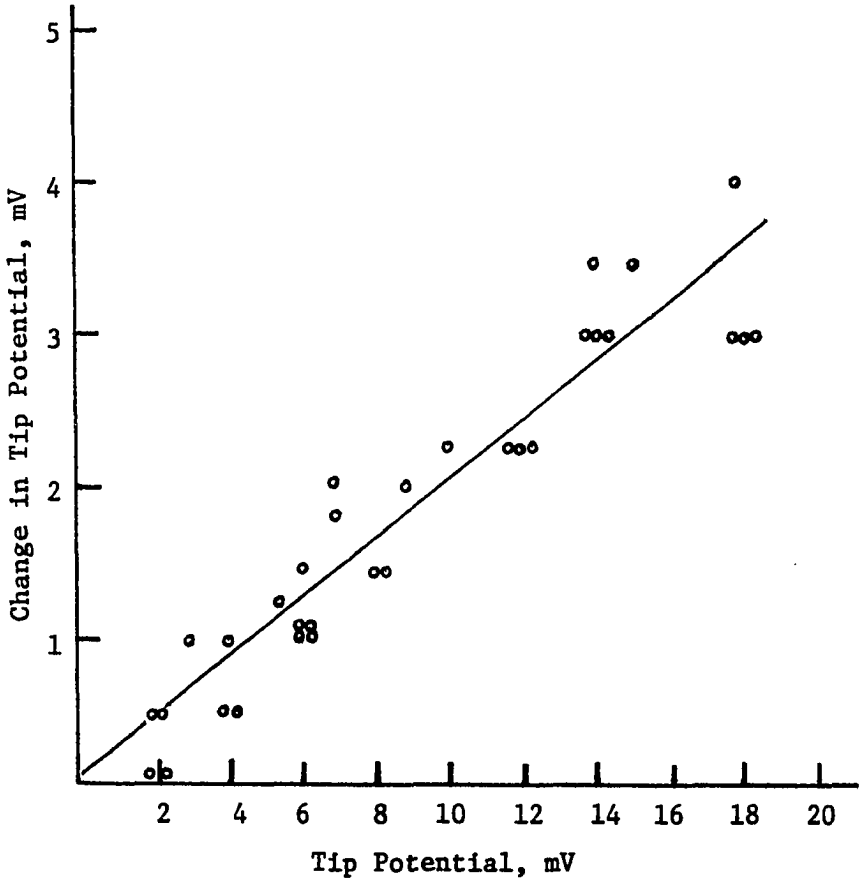

Figure 25. The change in tip potential as a function of the tip potential in 140 mM NaCl-10 mM KCl solution. This graph allows an estimate for the change in tip potential of the microelectrode upon entry into the cellular environment. The data were obtained by immersion of the microelectrode into a 10 mM NaCl-140 mM KCl solution. The linear regression is shown by the solid line, having the equation $\Delta V_T = 0.2\ V_T + 0.1$.

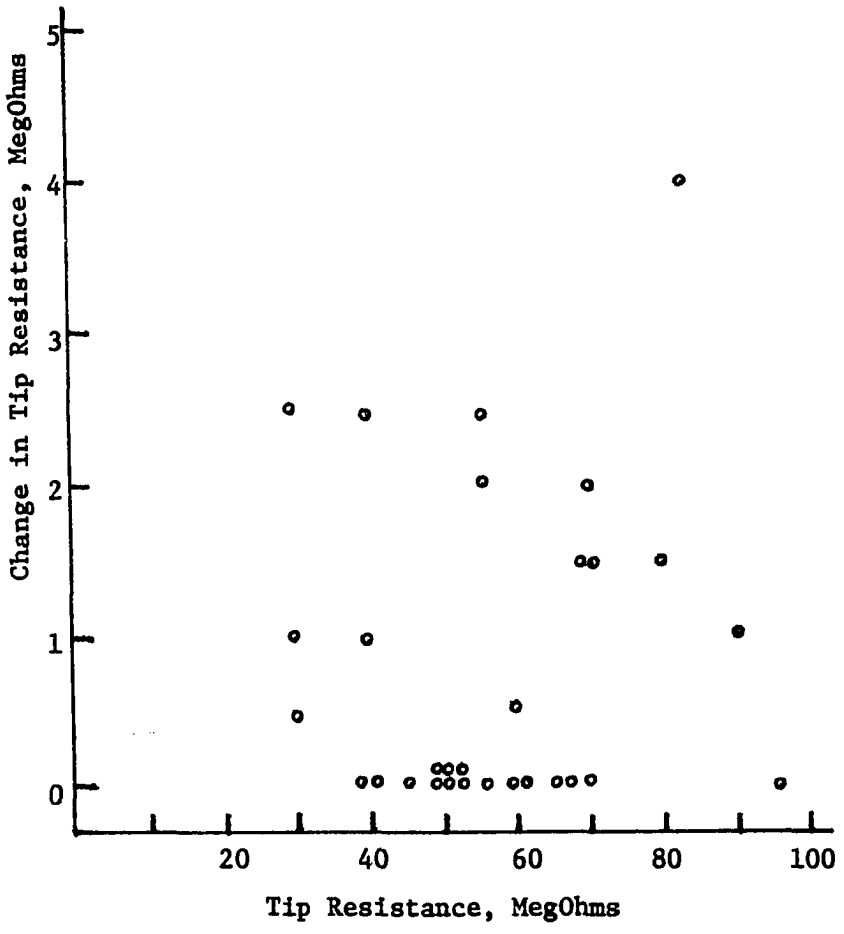

Figure 26. The change in tip resistance as a function of the tip resistance in 140 mM NaCl-10 mM KCl solution. There appears to be little correlation between the change in resistance, ΔR_T, and the original resistance, R_T. The data were obtained by immersion of the microelectrode into a 10 mM NaCl-140 mM KCl solution.

that there is little correlation between the original tip resistance, R_T, in MegOhms, and ΔR_T, the change in resistance following immersion of the electrode into the 140 mM KCl - 10 mM NaCl solution. Therefore, no statistical analysis was attempted. Figure 27 shows that when ΔR_T is plotted against the tip potential of the microelectrode, there is little change in R_T when the tip potential is less than 10 mV. It was decided therefore, to have a zero correction for R_T when measuring the membrane resistance, since all microelectrodes used had less than a 10 mV tip potential. All intracellular potential measurements were corrected for the individual ΔV_T associated with the tip potential of the measuring microelectrode. In no instance was the correction greater than 2 mV and most corrections were zero.

A successful intracellular measurement of potential and resistance is shown in Figure 28. This is an enlarged tracing of an actual recording. The tip potential is shown by the displacement above the baseline. There was a positive deviation of the tip potential as the microelectrode was brought into position against the cell. This positive pre-potential was due to dimpling of the cell and occurred only before the membrane was penetrated. Upon insertion of the microelectrode, the potential reading changed in a single step to the final value, in this case, -37 mV. The height AB represents the uncorrected intracellular potential. The corrected potential is obtained by adding to this value, the proper ΔV_T obtained from Figure 25. In this illustration, the tip potential is +5 mV, ΔV_T is therefore taken to be + 1.0 mV due to intracellular insertion. The final value for V_m, the transmembrane potential is -38 mV. The DC membrane resistance measurement is indicated by the

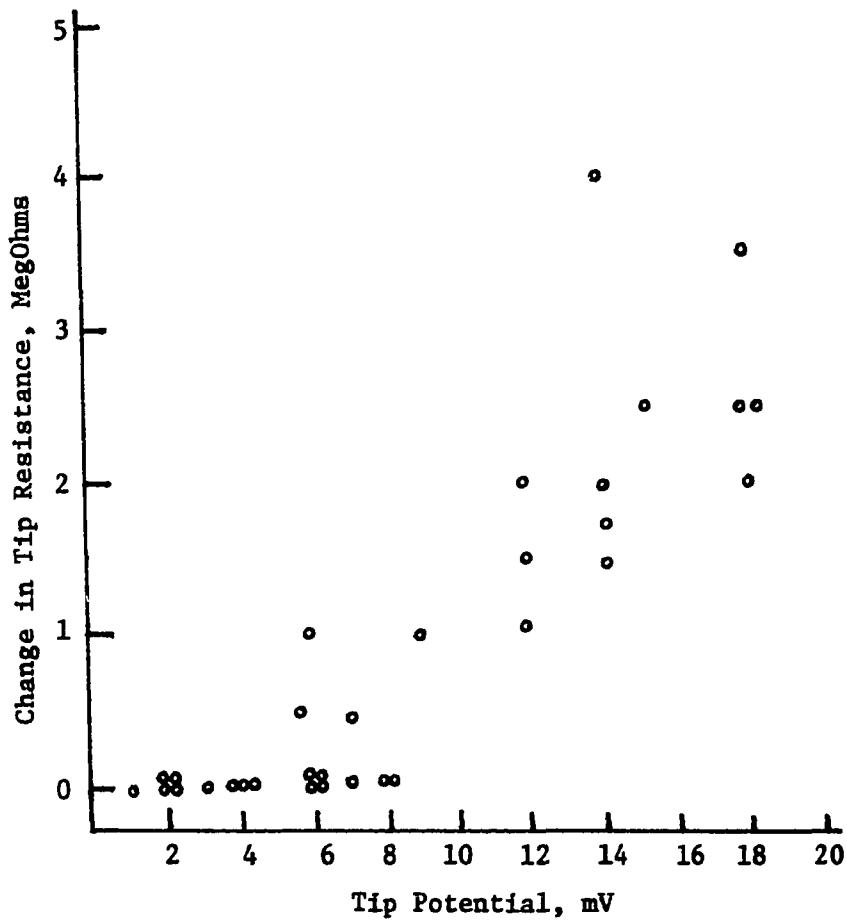

Figure 27. The change in tip resistance plotted as a function of the tip potential in 140 mM NaCl-10 mM KCl solution. The data were obtained by immersion of the electrode into a 10 mM NaCl-140 mM KCl solution. Based on this graph, a zero correction for resistance was used, since all microelectrodes used had less than a 10 mV tip potential.

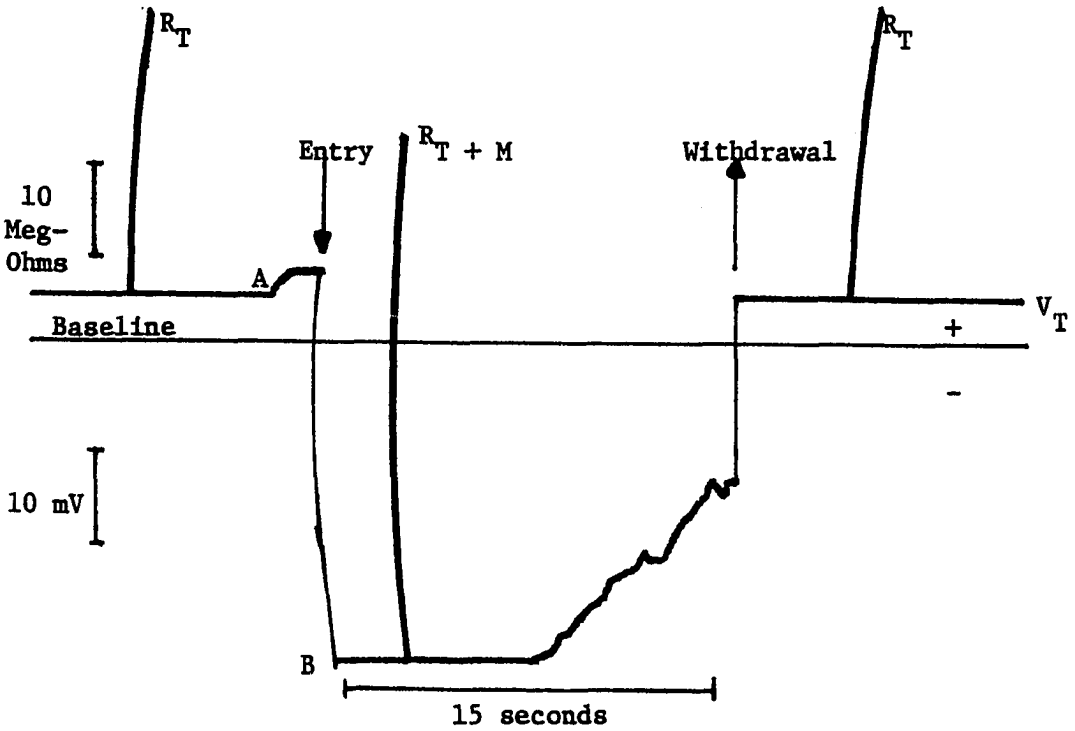

Figure 28. An example of a successful cell puncture. The tip potential, V_T, is 5 mV, as shown by the upward deviation from the baseline. R_T is 30 MegOhms. At point A, the microelectrode is positioned against the cell, giving rise to a transient positive deflection. The sharp fall in potential to point B represents the uncorrected intracellular potential difference. In this example the value is -37 mV. Adding a -1.0 mV correction for the tip potential change upon insertion, the final value is -38 mV and this is taken to be the transmembrane potential. R_{T+M} measures 55 MegOhms and by subtraction, the membrane resistance is computed to be 25 MegOhms.

intermittent upward deflection of the pen. Inside the cell, this deflection represents the sum of the tip resistance, R_T, and the membrane resistance, R_M, hence the designation R_{T+M}. R_T is 25 MegOhms, R_{T+M} is 55 MegOhms, so in this example, R_M is 30 MegOhms. The potential often decayed shortly after impalement due to vibration of the microelectrode tip within the cell, leading to damage and subsequent loss of the potential difference. Some potential measurements were stable for several minutes.

The Effect of Cell Density, Ions, and Temperature on the Transmembrane Potential and Resistance

Effect of Cell Density

The PY3T3 cell line was used to determine whether the transmembrane potential (TMP) and membrane resistance (MR) were functions of the cell density. Figure 29 illustrates the marked change in the TMP as the cell density of the culture increases. The TMP is expressed in mV (the cell interior being negative with respect to the bathing solution). Each point on the graph is the mean of at least 30 measurements. In a sparse culture ($<10^5$ cells/cm^2) the membrane potential averages to -22.7 + 1.6 mV. The TMP becomes more negative as cell density increases and becomes -46.1 ± 2.4 mV at saturation density. Cells growing within clones had the same average value of TMP as isolated cells. The changes in membrane resistance with cell density are shown in Figure 30. The MR is expressed in MegOhms and is plotted as a function of cell density. The MR increases from 23.6 ± 1.6 MegOhms at a cell density of 5×10^3 cells/cm^2 to an average value of 34.8 ± 2.4 MegOhms for the higher cell densities examined. The TMP and MR of 3T3 cells were measured at a cell

density of 5 X 10^4 cells/cm^2, about 90% confluency. The average values are also shown in Figures 29 and 30. The TMP was -12.3 ± 0.9 mV and the MR was 14.4 ± 1.3 MegOhms. Comparing the TMP and MR (in KRSS bathing solution), between the 3T3 and PY3T3 cell lines at the constant cell density of 5 X 10^4 cells/cm^2, both parameters are found to be significantly different ($P<.05$).

Figures 31 and 32 are histograms of the data described above and allow the range of values to be examined for each cell density studied.

Effect of External Ions

Changes of the bathing solutions with various ionic compositions were accomplished within 30 seconds and the first several measurements were made within 30 seconds later. All experiments were carried out at a constant cell density for each cell line. When more than one preparation was used the results were pooled, as average values were not statistically different between preparations. The first ten impalements were compared to the last ten impalements of given preparations and were found not to significantly differ in average value. This rules out the possibility of the TMP to vary in time following the change of solution. All values were corrected for estimated changes in microelectrode tip potential upon insertion into the cell interior. The results of all studies are shown in Tables 21 and 22. N represents the number of measurements and the error given is one standard error of the mean. The asterisks indicate a statistical significance ($P<.05$) when compared to the KRSS bathing solution.

The effects of increasing external potassium $(K)_o$, was studied by replacing NaCl with KCl on a molar basis. The 3T3 cells were in-

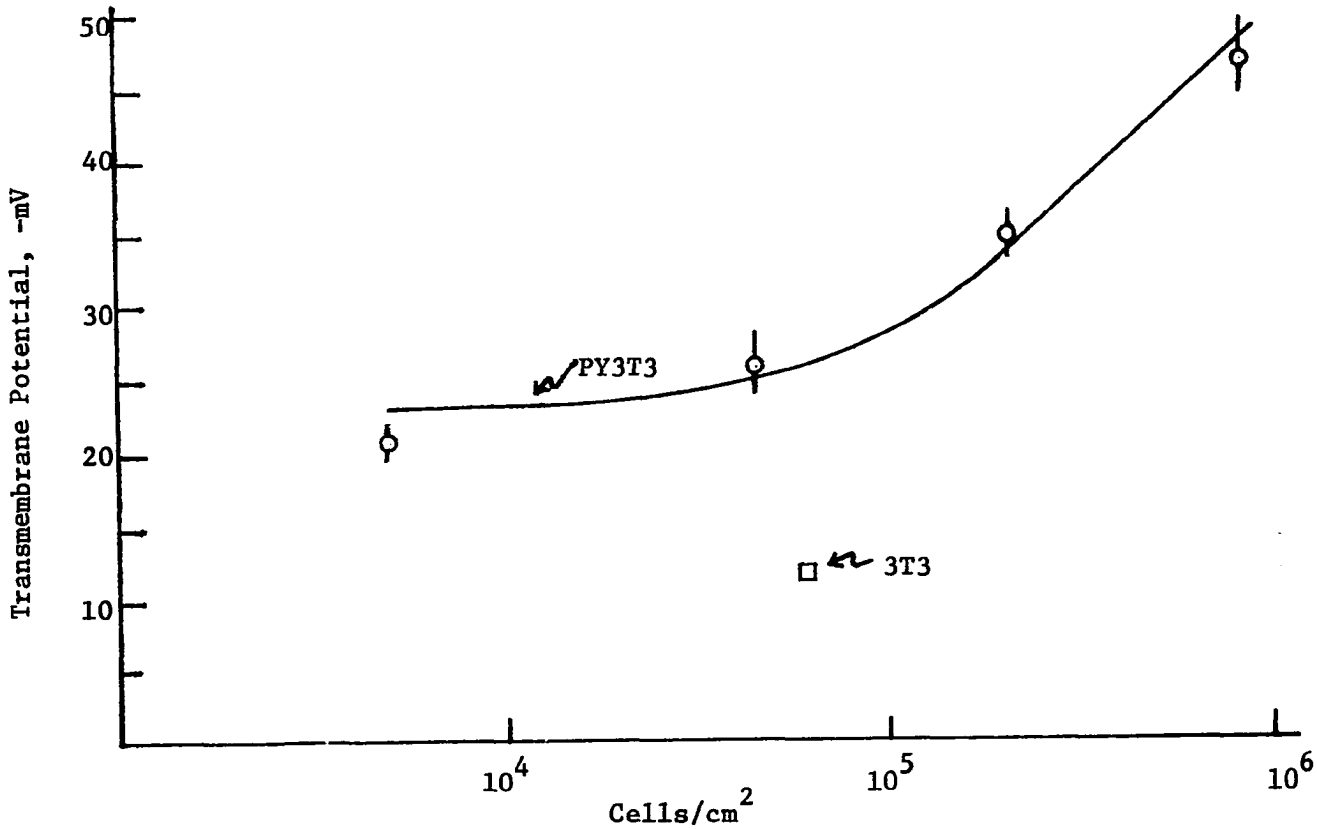

Figure 29. The transmembrane potential as a function of the cell density for PY3T3 cells. The bars represent one standard error of the mean. Each point is the mean of at least 30 measurements. The corresponding value for the 3T3 cells is indicated.

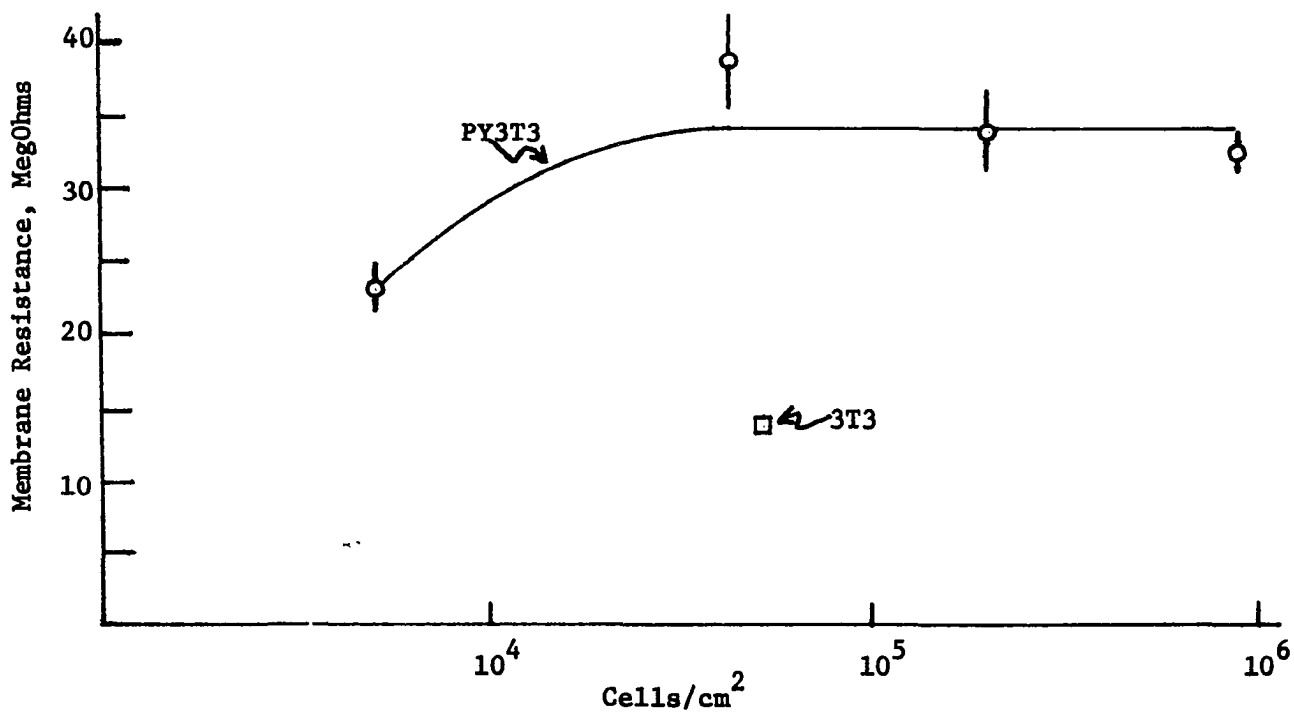

Figure 30. The DC membrane resistance as a function of cell density for the PY3T3 cells. Each point represents the mean of at least 30 measurements. The bars represent one standard error of the mean. Note that the membrane resistance increases prior to any significant change in the transmembrane potential (see Figure 29).

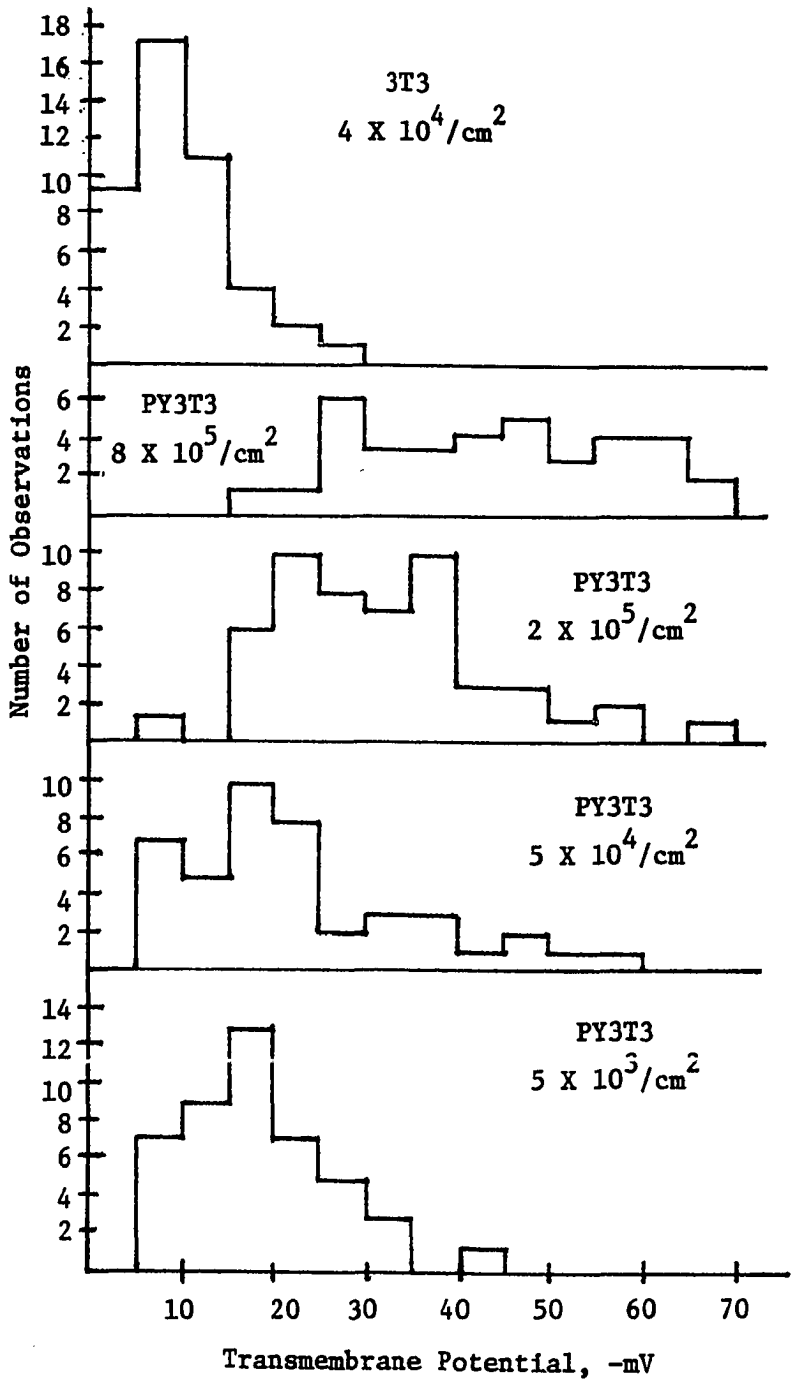

Figure 31. Histograms of the variation in transmembrane potential with cell density

Figure 32. Histograms of the variation in membrane resistance as a function of cell density.

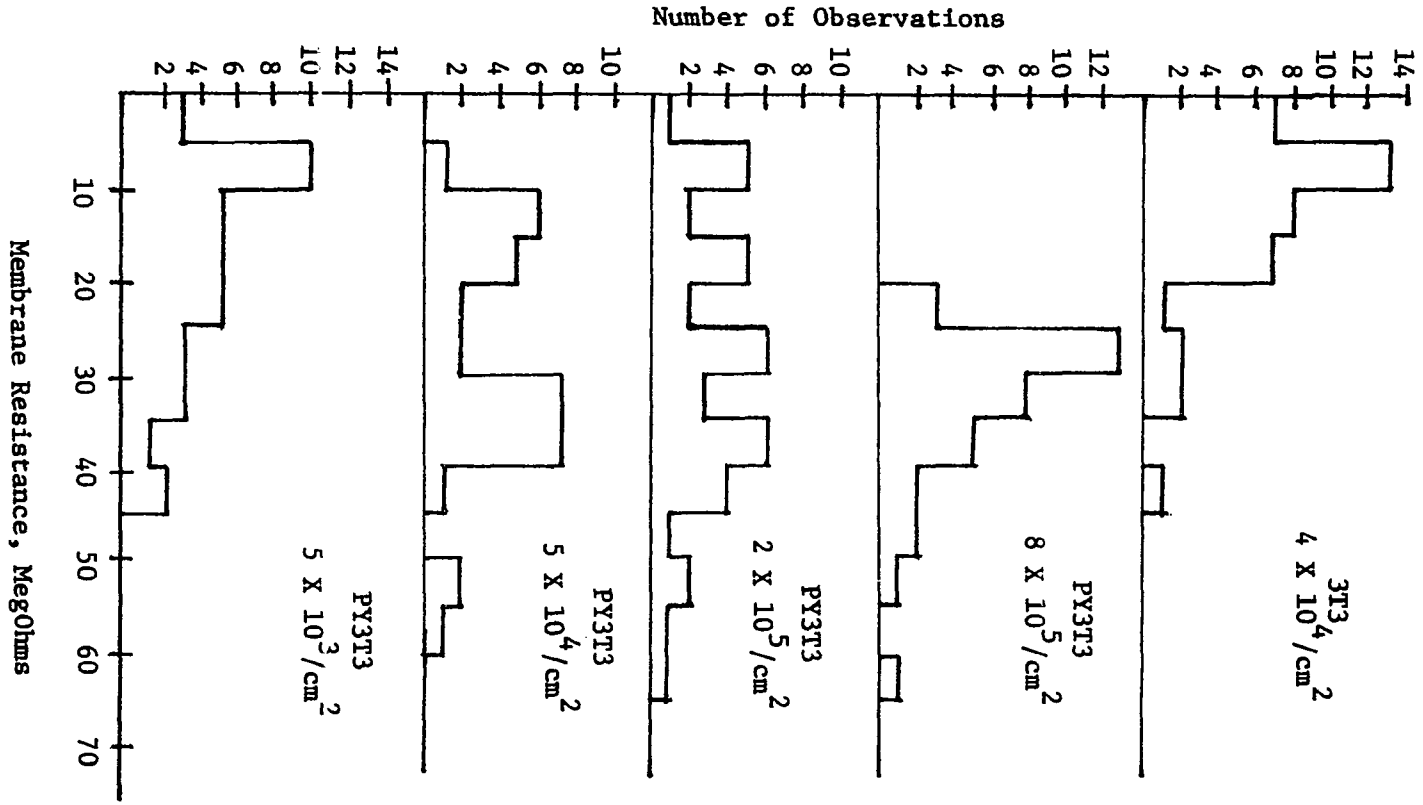

TABLE 21

THE EFFECTS OF EXTERNAL IONS ON THE TRANSMEMBRANE POTENTIAL AND MEMBRANE RESISTANCE OF 3T3 CELLS

Solution	I[d]	TMP (-mV)[a]	N[c]	MR (MegOhms)[b]	N
KRSS		12.3 ± 0.9	44	14.4 ± 1.3	41
K_1	21	10.3 ± 0.6	33	13.4 ± 1.8	21
K_2	53	11.2 ± 0.6	32	14.0 ± 2.2	24
K_3	93	6.3 ± 0.3*	30	8.6 ± 0.7*	22
Cl_1	53	10.9 ± 0.9	43	14.2 ± 3.6	36
Cl_2	32	5.9 ± 0.4*	40	11.0 ± 1.6	37
Cl_3	17	7.4 ± 0.5*	37	8.5 ± 0.9*	33
Na_1	87	8.0 ± 0.6*	33	10.5 ± 1.4*	23
Na_2	44	11.8 ± 0.9	28	12.4 ± 1.1	20
Na_3	11	7.7 ± 0.6*	24	7.3 ± 0.6*	21
Na_4	1	5.3 ± 0.5*	31	5.1 ± 0.6*	24

[a] Transmembrane potential, cell density 5 X 10^4 cells/cm^2

[b] DC membrane resistance

[c] Number of measurements, asterisks denote significance ($P<.05$)

[d] Concentration of the indicated ions, mM/l

TABLE 22

THE EFFECTS OF EXTERNAL IONS ON THE TRANSMEMBRANE POTENTIAL AND MEMBRANE RESISTANCE OF PY3T3 CELLS

Solution	I[d]	TMP(-mV)[a]	N	MR(MegOhms)	N
KRSS		35.2 ± 1.6	52	34.0 ± 2.8	42
K_1	21	14.6 ± 0.9*	45	9.6 ± 0.7*	37
K_2	53	7.8 ± 0.8*	30	8.7 ± 1.4*	21
K_3	93	7.2 ± 0.7*	31	7.0 ± 0.6*	23
Cl_1	53	26.9 ± 2.1*	40	22.5 ± 2.2*	25
Cl_2	32	28.3 ± 1.8*	42	19.3 ± 1.7*	36
Cl_3	17	32.5 ± 2.7	30	32.8 ± 3.4	17
Na_1	87	29.5 ± 1.4*	47	18.3 ± 2.0*	28
Na_2	44	25.1 ± 2.0*	27	16.7 ± 1.6*	21
Na_3	11	29.5 ± 1.8*	30	21.0 ± 1.9*	15
Na_4	1	16.1 ± 0.8*	59	10.0 ± 1.8*	40

[a] Transmembrane potential, cell density 2 X 10^5 cells/ cm^2

[b] DC membrane resistance

[c] Number of measurements, asterisks denote significance ($P<.05$)

[d] Concentration of the indicated ions, mM/l

sensitive to increasing $(K)_o$, until $(K)_o$ was about 90 mM/1. The cells then depolarized to -6.3 mV compared to the control value of -12.3 mV at a $(K)_o$ of 5.4 mM/1. The membrane resistance also showed no change until the $(K)_o$ reached about 90 mM/1 where the MR was 8.6 MegOhms compared to 14.4 MegOhms in the KRSS solution. In contrast, the PY3T3 cells showed a significant depolarization of the TMP starting with 21 mM/1 for $(K)_o$. The TMP changed from -35.2 to -14.6 mV. A further decrease in magnitude was observed at a $(K)_o$ of 53 mM/1, of -7.8 mV, and this value is not significantly different from -7.2 mV obtained for $(K)_o$ being 93 mM/1. The MR of the PY3T3 cells decreased from the control value of 34.0 MegOhms to 9.6, 8.6, and 7.0 MegOhms when the $(K)_o$ was 21, 53, and 93 mM/1, respectively. No unusual morphological changes were observed in either cell line during the time the cells were incubated with high potassium solutions. Rounding was observed in some cells.

External sodium, $(Na)_o$, was decreased by replacement of NaCl with tetramethylammonium chloride and ammonium bicarbonate. External potassium and chloride ions were held constant at their respective KRSS values of 5.4 and 120 mM/1. The 3T3 cells demonstrated a diphasic response in TMP and MR values to lowering $(Na)_o$. The TMP magnitude was lowered to -8.0 mV when $(Na)_o$ was 87 mM/1, but then no change from the control value of -12.3 mV was observed when $(Na)_o$ was lowered to 44 mM/1. Further depolarization to -7.7 and -5.3 mV occurred when $(Na)_o$ was 11 and 1 mM/1, respectively. Membrane resistance was also diphasic, decreasing to 10.5 MegOhms at a $(Na)_o$ of 87 mM/1, returning to a value not significantly different from the control when $(Na)_o$ was 44 mM/1. Lowering $(Na)_o$ to 11 and 1 mM/1 resulted in MR values of 7.3 and 5.1 MegOhms, respectively.

When $(Na)_o$ was lowered for the PY3T3 cells, there was a depolarization to an average value of -27.8 mV for $(Na)_o$ values of 87, 44, and 11 mM/1 (the values shown in Table 22 for Na_1, Na_2, and Na_3 do not statistically differ from each other at the 5% level of significance). The TMP magnitude fell to -16.1 mV when $(Na)_o$ was further lowered to 1 mM/1. The membrane resistance decreased to an average value of 18.7 MegOhms for $(Na)_o$ values of 87, 44, and 11 mM/1. For the $(Na)_o$ of 1 mM/1, the MR decreased to 10.0 MegOhms compared to the control value of 34.0 MegOhms. Both cell lines exhibited almost immediate vacuole formation within the cytoplasm when external sodium was lowered. These dark, globular structures appeared to line the nucleus and seemed to decrease in number after 5-10 minutes exposure to the altered solution. Many cells would appear more refractile and rounded, although thin cytoplasmic extensions would remain attached and continuous with the cells.

External chloride, $(Cl)_o$, was decreased by replacing NaCl with Na_2SO_4 as required to maintain $(Na)_o$ constant at 153 mM/1. Potassium was also held fixed at the KRSS level of 5.4 mM/1. Lowering $(Cl)_o$ to 53 mM/1 did not change the TMP of 3T3 cells ($P>.05$). Further decreases in $(Cl)_o$ to 32 and 17 mM/1 gave decreases in the TMP to -5.9 and -7.4 mV, respectively. No significant change in the membrane resistance was observed until $(Cl)_o$ was lowered to 17 mM/1, when the MR was 8.5 MegOhms, compared to the control value of 14.4 MegOhms. The PY3T3 cells depolarized to -26.9 and -28.3 mV for $(Cl)_o$ values of 53 and 32 mM/1, respectively. Lowering $(Cl)_o$ to 17 mM/1 did not significantly change the TMP from the control value of -35.2 mV. The MR of PY3T3 cells fell to 22.5 MegOhms when $(Cl)_o$ was lowered to 53 mM/1. No further change

occurred when $(Cl)_o$ was 32 mM/1. Lowering $(Cl)_o$ to 17 mM/1 resulted in no significant change in the MR from the control value of 34.0 MegOhms. Similar morphological changes of the cell lines were observed for lowering external chloride as when $(Na)_o$ was decreased. The time course of the changes was not as rapid, and the rounding up of the cells was not as pronounced when $(Cl)_o$ was lowered from the KRSS concentration of 120 mM/1.

Effect of Temperature

Measurements of the TMP and MR were made on both cell lines following a 30 minute incubation at 23°C. The KRSS solution was used. Table 23 gives the values of the TMP and MR for 35° and 23°C. Also shown is the computed Q_{10} value for the TMP measurements. N indicates the number of measurements. The average TMP of 3T3 cells was -10.8 mV at 23°C, which yields a Q_{10} value of 1.13 ± .22 (95% confidence limits). The MR increased to 19.9 MegOhms. The TMP for PY3T3 cells decreased to -13.4 mV, giving a Q_{10} of 2.62 ± 0.22. In contrast to the 3T3 cells, the MR of the PY3T3 cells decreased to 8.9 MegOhms. No morphological changes were observed in either cell line when incubated at 23°C.

The Effect of Acute and Chronic TRYP-Con A Treatment On the Transmembrane Potential and DC Resistance of PY3T3 Cells

The acute effect of 40 µg/ml TRYP-Con A on the TMP and MR of PY3T3 cells is shown in Figure 33. The cells were incubated for one hour with TRYP-Con A added to the culture medium. The flasks were changed to the KRSS solution and measurements made. Results were pooled from three preparations since no significant differences were observed between prepa-

TABLE 23

THE EFFECT OF TEMPERATURE ON THE TRANSMEMBRANE POTENTIAL AND DC MEMBRANE RESISTANCE OF 3T3 AND PY3T3 CELLS

Cell Line	T(°C)	TMP[a](-mV)	N[d]	MR[b](MegOhms)	N	Q^{c}_{10}
	35	12.3 ± 0.9	44	14.4 ± 1.3	41	
3T3						1.13 ± 0.22
	23	10.8 ± 0.7	33	19.9 ± 2.0	21	
	35	35.2 ± 1.6	52	34.0 ± 2.8	42	
PY3T3						2.62 ± 0.58
	23	13.4 ± 1.0	41	8.9 ± 0.4	34	

[a] Transmembrane potential, KRSS solution

[b] DC membrane resistance

[c] Computed ratio $\frac{TMP_{35}}{TMP_{23}}$ at 95% confidence limits

[d] Number of measurements

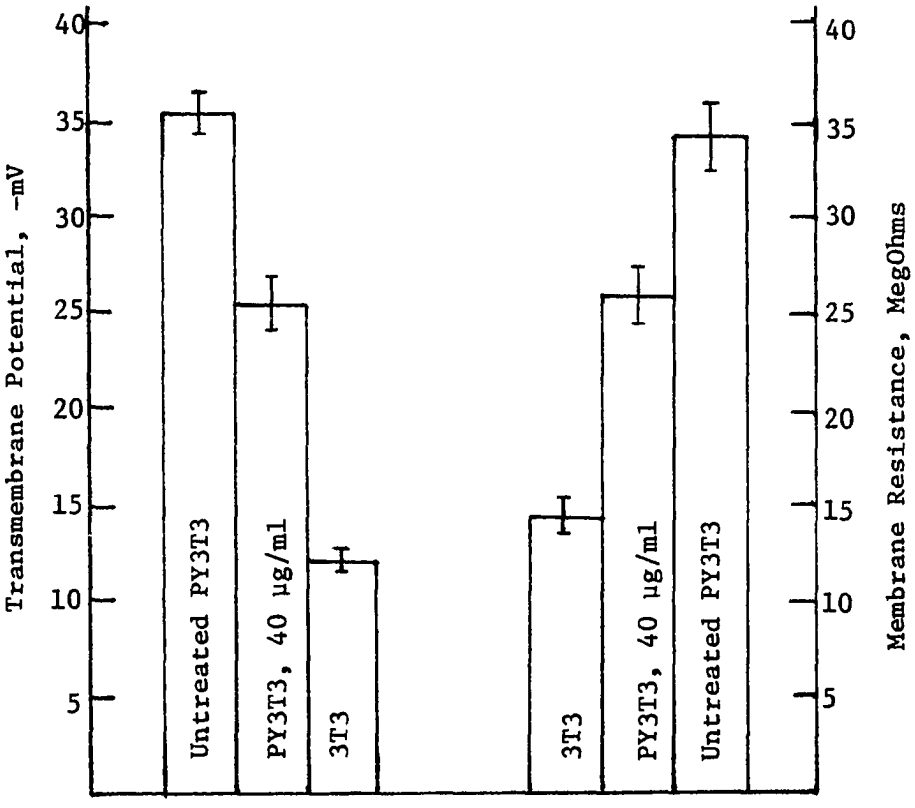

Figure 33. The effect of a one hour incubation of 40 µg/ml TRYP-Con A on the transmembrane potential and membrane resistance of PY3T3 cells. Results were pooled from three preparations. The 3T3 cell values are shown for comparison. Bars represent one standard error of the mean of at least 30 measurements.

rations (P>.05). The cell density was 2 X 10^5 cells/cm^2, the same as all experiments performed on PY3T3 cells. The results show a significant depolarization in the TMP to -25.2 mV compared to the control value of -35.2 mV. A decrease in the MR also was observed, 26.2 MegOhms from 34.0 MegOhms. For comparison, the values for the TMP and MR of 3T3 cells is also shown. No morphological changes were observed during the acute TRYP-Con A experiments.

Figure 34 shows the effect of chronic TRYP-Con A treatment on PY3T3 cells. The measurements of the TMP and MR on the PY3T3CCA cell line were made over a period of six months. The curve for the TMP shows that the cells were depolarized to an average value of -24 mV for the first two months of treatment, which was not different than the acute change described above. After four months of treatment, the TMP magnitude was further decreased to about -9 mV and remained stable through the sixth month. The dashed curve shows the MR was significantly decreased to 20 MegOhms by the second month, then further, to about 10 MegOhms at four months. The MR increased to 20 MegOhms after the sixth month of treatment.

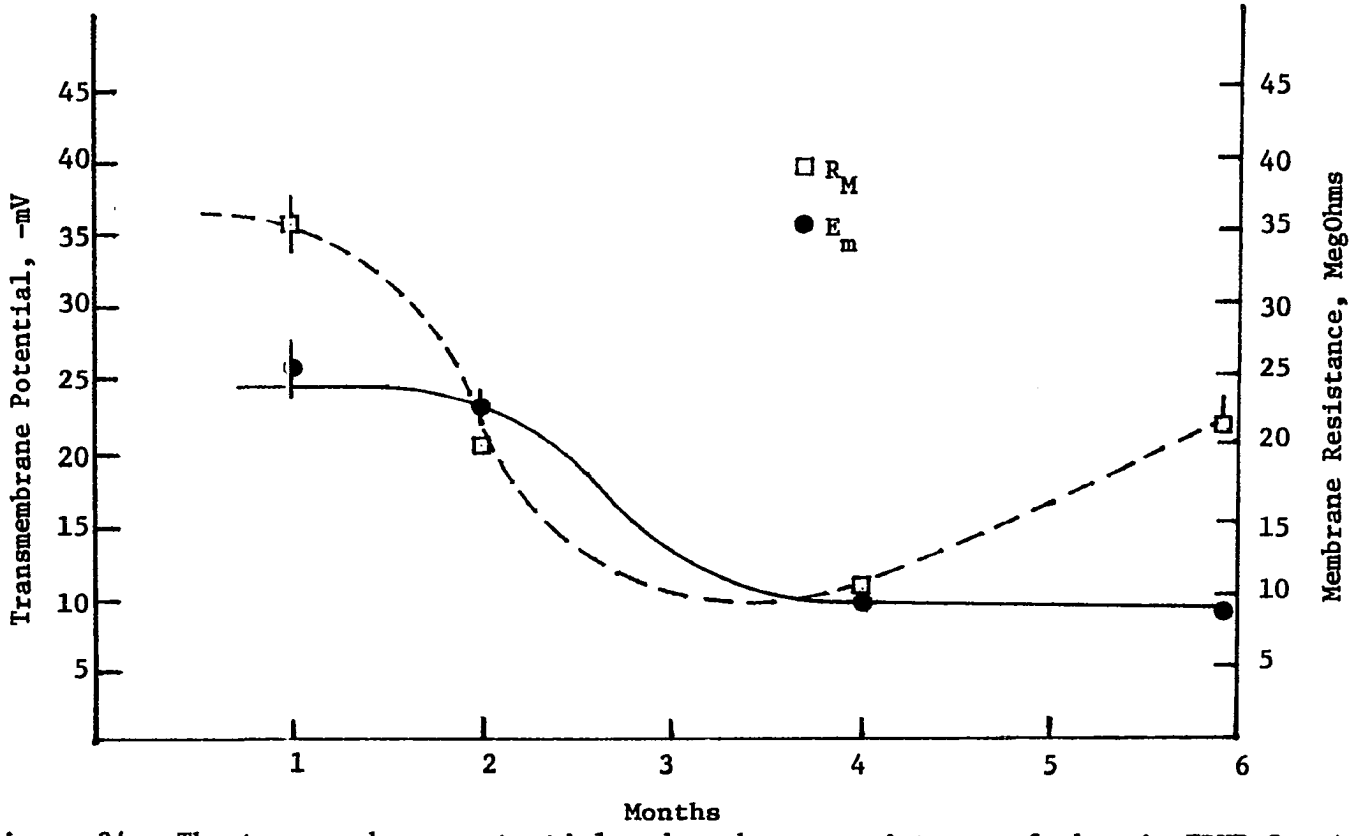

Figure 34. The transmembrane potential and membrane resistance of chronic TRYP-Con A treated cells. Bars represent one standard error of the mean of at least 30 measurements. Note that the membrane resistance change precedes the change in transmembrane potential.

CHAPTER IV

DISCUSSION

The present study was done to examine some membrane properties associated with polyoma virus-transformation of 3T3 mouse fibroblasts. In addition, these properties were studied after treatment of the transformed cells with TRYP-Con A. These properties were the transmembrane potential, DC membrane resistance, and agglutinability with intact Con A.

The discussion of the results from these studies and their interpretations has been divided into several sections. The agglutinability of 3T3, PY3T3, and PY3T3CCA cells was examined after the experimental conditions were standardized. The parameters that affect the assay are first discussed, then the differences in agglutinability between the cell lines can be properly compared.

The effect of altering the ionic composition of the bathing solution on the TMP and MR yields insight into the nature of these parameters for 3T3 and PY3T3 cells. The two lines also showed marked differences in the temperature dependence of the TMP and MR. Therefore, it would be useful to establish some quantitative comparisons between the 3T3 and PY3T3 cells with regard to specific membrane properties before any discussion of the changes in TMP and MR due to cell density and TRYP-Con A treatment. This allows the latter phenomena to be examined in greater detail, and affords some opportunities to offer plausible explanations.

Finally, a sequence of events that probably occur following the treatment of PY3T3 cells with TRYP-Con A can be proposed. The morphology and growth studies, added to the studies on thymidine incorporation indicate that TRYP-Con A treatment selects for cells having membrane characteristics of nontransformed cells. Thus, further experiments can be proposed, using the PY3T3CCA cells. A necessary question to ask, is whether these membrane alterations are required for the in vitro regulation of growth?

Physico-Chemical Factors of Agglutination Using Con A

Agglutination of cells has been used as a technique to demonstrate topological differences between transformed and nontransformed cells. Standardization of the experimental conditions for the assay of agglutination is quite important with the increasing use of plant lectins to examine surface alterations following neoplastic transformation (24-26, 112, 113). It was decided to examine some physico-chemical factors that affect agglutination using Con A, since the assay techniques described in the literature were not consistent as to experimental conditions (17, 25, 28,102).

The present study demonstrates that the scoring for agglutinability is affected by time, cell density, Con A concentration, and ionic strength. The experimental protocol used constant temperature and shaker table frequency. The results indicate that agglutination increases with time after the addition of Con A, reaching a plateau in about thirty minutes (Fig. 3). This result is in aggreement with Powell's data that showed the binding of Con A to human lymphocytes was not at equilibrium until thirty minutes (114). The semi-log plot of Figure 6 shows that the agglutinability increased at about the same rate whether 200, 500, or

1000 μg/ml Con A was used. This finding is consistent with the view that agglutinability measures the distribution of binding, rather than the amount of Con A bound to the cell (28-30). Since the amount of Con A bound to the cell is dependent upon the concentration of Con A (55-57, 97,) agglutination was concentration dependent, as expected, the main effects showing up at low Con A concentrations. All other factors held constant, the agglutinability appears to be solely dependent upon the concentration of Con A. The scoring of the assay tends to plateau at higher concentrations, partly because of the logarithmic nature of the scoring scheme (an increase in a scoring unit of one represents about a three-fold increase in the average clump size), and also due to the statistical nature of agglutination. Free cells are usually visible, even at higher concentrations of Con A, which may reflect the heterogeneity in membrane characteristics of a tumor cell population. The cell density affects agglutinability, so the assay requires that the cell density be reasonable, in the sense that using too high of cell density gives non-specific aggregation very quickly, and too low of cell density yields assays that are difficult to reproduce. The range of 10^5 to 10^6 cells/ml gives consistent results over a wide range of Con A concentrations and since many cell lines differ in their response to Con A, this cell density seems desirable.

The ionic strength dramatically affected the agglutinability of the cell lines used in this study. The enhancement of agglutination when cells were incubated in low ionic strength solutions (LIS) compared to the normally used, high ionic strength solutions (RIS) was shown to be specific for Con A hapten-inhibition experiments with α-methyl-D-

Mannoside. It was found that the LIS effect was maximal with about a thirty minute pre-incubation of the cells at LIS. Furthermore, it was demonstrated that the effect was not due to the absence of the cations, Na^+, K^+, or Ca^{++} used in RIS solutions. Since the enhancement was qualitatively similar to the higher agglutinability of some cells following proteolytic treatment (24,25,30), this suggests that alterations may have occurred at the surface of cell when incubated at LIS. This idea was examined more closely by performing experiments involving certain permutations on pre-incubation in LIS and RIS solutions, with and without the presence of Con A.

It is not required that the cells be in a LIS environment during the agglutination assay for enhancement to occur. This was shown by incubating the cells at LIS without Con A, then washing, resuspending at RIS, and assayed for agglutination. In another experiment, the cells were pre-incubated at RIS with Con A, then transferred to LIS with no additional Con A. Enhancement of agglutination did not occur.

This result implies that if the sites bound by Con A at RIS are also responsible for the enhanced agglutination, then rearrangement of these sites may be inhibited by the binding of Con A. The mixed agglutination experiment strongly suggests that it is not necessary for the cells to bind more Con A to demonstrate enhanced agglutination. When cells were incubated at LIS without Con A, mixed with cells that had incubated at RIS with Con A (the final mixture being at RIS), enhancement was observed. Although more binding sites for Con A may have been exposed on the cells from their LIS incubation, only rearrangement of existing sites would be needed for the observed enhancement of ag-

glutination. This explanation seems reasonable in light of the recent finding that the act of binding Con A to the surface of transformed cells can lead to shifts in the topological distribution Con A-bound sites (115). Furthermore, the quantitative inhibition study for RIS and LIS agglutination using α-methyl-D-Mannoside (in excess) shows that the enhanced agglutinability probably does not involve more Con A bound to the cell. Since the complete inhibition of agglutination occurred at both levels of ionic strength with about 10 mM/l of the sugar, it is unlikely that the cell at LIS binds a substantial amount of Con A compared to the cell in a RIS solution. This assumes that the hapten-inhibition is not affected at LIS, which seems reasonable, as Atchely et al. showed that antigen-antibody reactions were greatly enhanced at low ionic strength (116). In addition, the sugar used for inhibition completely dissociated agglutinated cells at 20 mM/l concentration.

In a series of elegant experiments, Pollack et al. showed that the agglutination of red blood cells was dependent upon the zeta potential (117). This surface potential represents a major repulsive force between cells. Since the zeta potential can be lowered by either raising the ionic strength or lowering the dielectric constant of the medium, then he demonstrated that higher ionic strength favored agglutination of cells. The results of the present study can not be explained satisfactorily by consideration of the zeta potential. Lowering the ionic strength would tend to increase the surface change, which would not favor agglutination, and further, it was not required that the cells be present in a low ionic strength solution to have enhanced agglutination.

The results of the present study on the agglutination of 3T3 cells differ somewhat from those reported in the literature. The 3T3 cells did agglutinate less than the PY3T3 cells, but the difference was not as striking (24-27). Using a value for Con A that agglutinated 75% of the cells, the 3T3 cells required about 600 µg/ml compared to 75 µg/ml for PY3T3 cells. This is in contrast to Burger's report of 1500 µg/ml Con A needed to agglutinate 75% of the 3T3 cells (17). His protocol used the same cell density and ionic strength, so it was decided to use his procedure of incubating 0.5 ml of the cell suspension in the well of a glass coverslip, while gently rocking on the shaker table for 10 to 15 minutes. The results agreed in that using 50 and 200 µg/ml Con A, no agglutination occurred. This can be compared to a score of 1+ with about 60% of the cells agglutinated using a thirty minute incubation of the cells in centrifugation tubes and a horizontal frequency of 150 per minute on the shaker table. The difference in results presented here and Burger's report can be attributed to the short incubation time used for his assay, in addition to the lower frequency of shaking the cell suspension. The present study has shown that agglutinability is time-dependent, and this parameter should not be neglected in assays for agglutination. Both the 3T3 and PY3T3 cells were equally agglutinabile using 200 µg/ml Con A and low ionic strength. The average clump size was 10 to 30 cells per group and about 90% of the cells were agglutinated. However, this degree of agglutination represented about a 30% increase in the number of 3T3 cells participating agglutination, whereas the percentage of PY3T3 cells agglutinated did not change from as assay at regular ionic strength, just the average clump size increas-

ed. This may reflect inherent differences at the cell surface for the nontransformed and transformed cells. The 3T3 cells were more "sensitive" to the decrease of ionic strength than the PY3T3 cells. This may be due to the presence of sites that are cryptic in nature on the surface of nontransformed cells. Whether the mechanism of increased agglutination at low ionic strength for 3T3 cells is the same as PY3T3 cells strength remains unanswered, but the results of the present study suggest that 3T3 cells may have additional sites exposed and an increased density of binding sites when exposed to a low ionic strength environment.

Effects of External Ions on the Transmembrane Potential and Membrane Resistance

The response of the transmembrane potential (TMP) and membrane resistance (MR) was strikingly different for the two cell lines, when external potassium, $(K)_o$, was raised above the normal value of 5.4 mM/l. The TMP of the 3T3 cells was unchanged until $(K)_o$ approached 90 mM/l, in contrast to the depolarization observed for PY3T3 cells when $(K)_o$ was 21, 53, and 93 mM/l. Parallel changes in the membrane resistance with the respective TMP values occurred for both cell lines. We may investigate the nature of these responses by using the Goldman equation (118). This equation relates the transmembrane potential, Na^+, K^+, Cl^-, P_{Na}, P_K, and P_{Cl} in the following form, with the assumption that the ions are passively permeable through the membrane with constant mobilities (118, 119):

$$E_m = \frac{RT}{F} \ln \frac{P_K (K)_o + P_{Na} (Na)_o + P_{Cl} (Cl)_i}{P_K (K)_i + P_{Na} (Na)_i + P_{Cl} (Cl)_o} \quad (1)$$

R, T have their usual thermodynamic meanings, and F is the Faraday. The notation $(X)_i$ and $(X)_o$ denotes the internal and external concentrations

of the ion X, respectively. P_X is the permeability of the X ion through the membrane (defined on page 120). At 35°C, $\frac{RT}{F}$ has the value 26 mV. Data available from the literature show that chloride appears to be passively distributed across the membrane of most cells (71,74,75,83,121,125, 126). Assuming this to be true for mouse cells, in vitro (74), then equation 1 can be rewritten,

$$E_m = 26 \ln \frac{(K)_o + P_{Na}/P_K(Na)_o}{(K)_i + P_{Na}/P_K(Na)_i} \qquad (2)$$

If the membrane were permeable only to K^+, i.e., $P_{Na}/P_K \ll 1$, then equation 2 reduces to the form of the Nernst equilibrium diffusion potential,

$$E_m = 26 \ln \frac{(K)_o}{(K)_i} = 60 \log \frac{(K)_o}{(K)_i} \qquad (3)$$

A plot of the TMP against $\log(K)_o$ should yield a straight line with slope of 60 mV per ten-fold increase in $(K)_o$ and an intercept of $(K)_i$. Figure 35 shows such a plot of the data obtained on 3T3 and PY3T3 cells. The Nernst plot of equation 3 is indicated. It is obvious that neither cell line obeys equation 3, but the PY3T3 cells do have a $(K)_o$-dependence that approaches the slope of the Nernst plot at low values of external K^+. The effect of Na^+ ions on the TMP can be examined by rewriting equation 2,

$$\exp(E_m F/RT) = \frac{(K)_o(1-\alpha) + \beta\alpha}{(K)_i} \qquad (4)$$

where $\alpha = P_{Na}/P_K$, $\beta = (K)_o + (Na)_o$, and $\alpha(Na)_i \ll (K)_i$. If we now plot $\exp(E_m F/RT)$ as a function of $(K)_o$, we will obtain a straight line of slope $\frac{(1-\alpha)}{(K)_i}$ and an intercept of $\frac{\beta\alpha}{(K)_i}$, if equation 4 is valid. These parameters

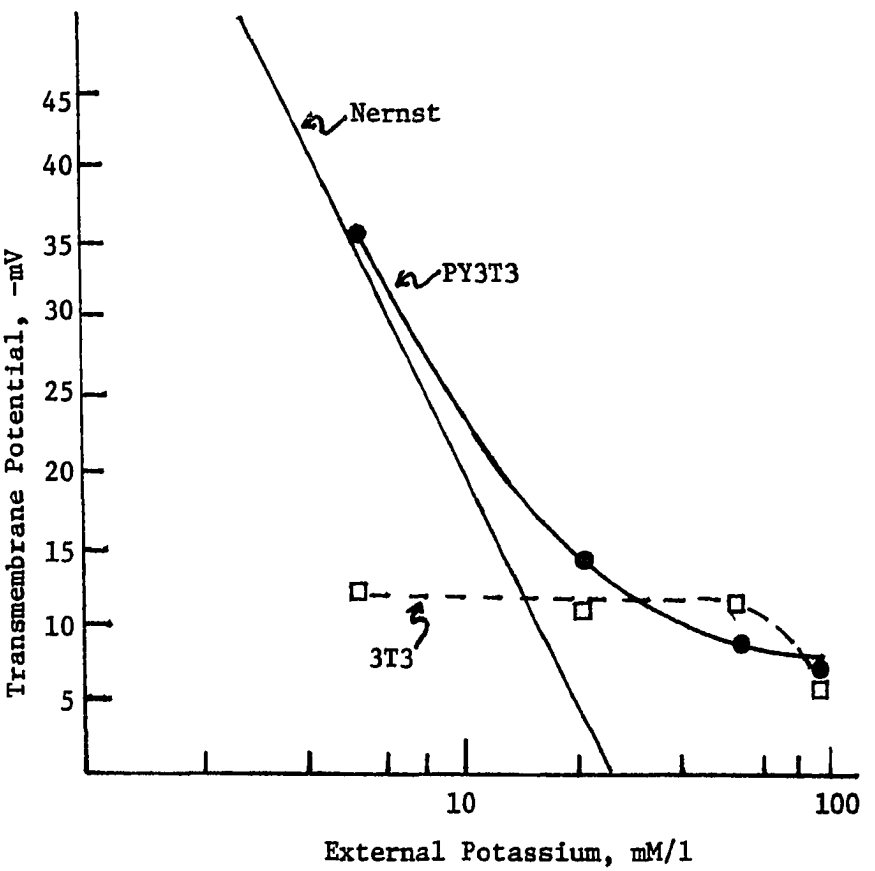

Figure 35. The transmembrane potential of 3T3 and PY3T3 cells as a function of the external potassium concentration. The 3T3 cells are insensitive to increasing $(K)_o$ until about 90 mM/l, compared to the immediate depolarization of the PY3T3 cells. The Nernst line for a potassium electrode is indicated. Standard error bars are omitted for clarity.

allow the determination of P_{Na}/P_K and $(K)_i$. Such a plot is displayed in Figure 36 for the potassium dependence of the 3T3 cells where the slope is zero, hence $\alpha_{3T3} = 1.0$. Borle reported a P_{Na}/P_K value of 0.57 for HeLa cells (82) while Lamb reported a ratio of 0.7 for mouse L cells (74). However, a quite different value of 0.08 has been reported by McDonald et al. (65). The average value of the three data points gives an intercept of 0.66. With $\beta = (K)_o + (Na)_o = 158$ mM/l, then the y-intercept yields $(K)_i = 237$ mM/l. This value is close to that reported by Cone for 3T3 cells (89,90). He estimated this concentration to be 205 mM per liter of cell volume. If a correction is made for the actual volume of cell water, $(K)_i$ can then become as high as 250 mM/l. On the other hand, if some of the internal potassium is bound, say 30%, then $(K)_i$ can be as low as 175 mM/l. High intracellular potassium is common to cultured cells; the reported values ranging from 150 to 206 mM/l (65,74,75,82,119,127).

The value of P_{Na}/P_K for the PY3T3 cells may be approached with the same analysis. A plot of the data shown in Figure 37 indicates that equation 4 is not obeyed (linearity). As a possible explanation for this, it is proposed that the ratio P_{Na}/P_K itself may be a function of the internal and external Na^+ and K^+ concentrations. Figure 38 shows the expimenatal data fitted to the empirical equation given by,

$$\exp\frac{E_m F}{F} = 0.24\sqrt{(K)_o} - 0.014(K)_o - 0.24 \qquad (5)$$

The solid line indicates the curve given by equation 5 and the points represent experimental values. Using the permeability ratio P_{Na}/P_K as a function $\alpha(c)$, the Goldman equation can be rewritten as,

$$E_m = \frac{RT}{F} \ln \frac{(K)_o + \alpha(c)(Na)_o}{(K)_i + \alpha(c)(Na)_i} \qquad (6)$$

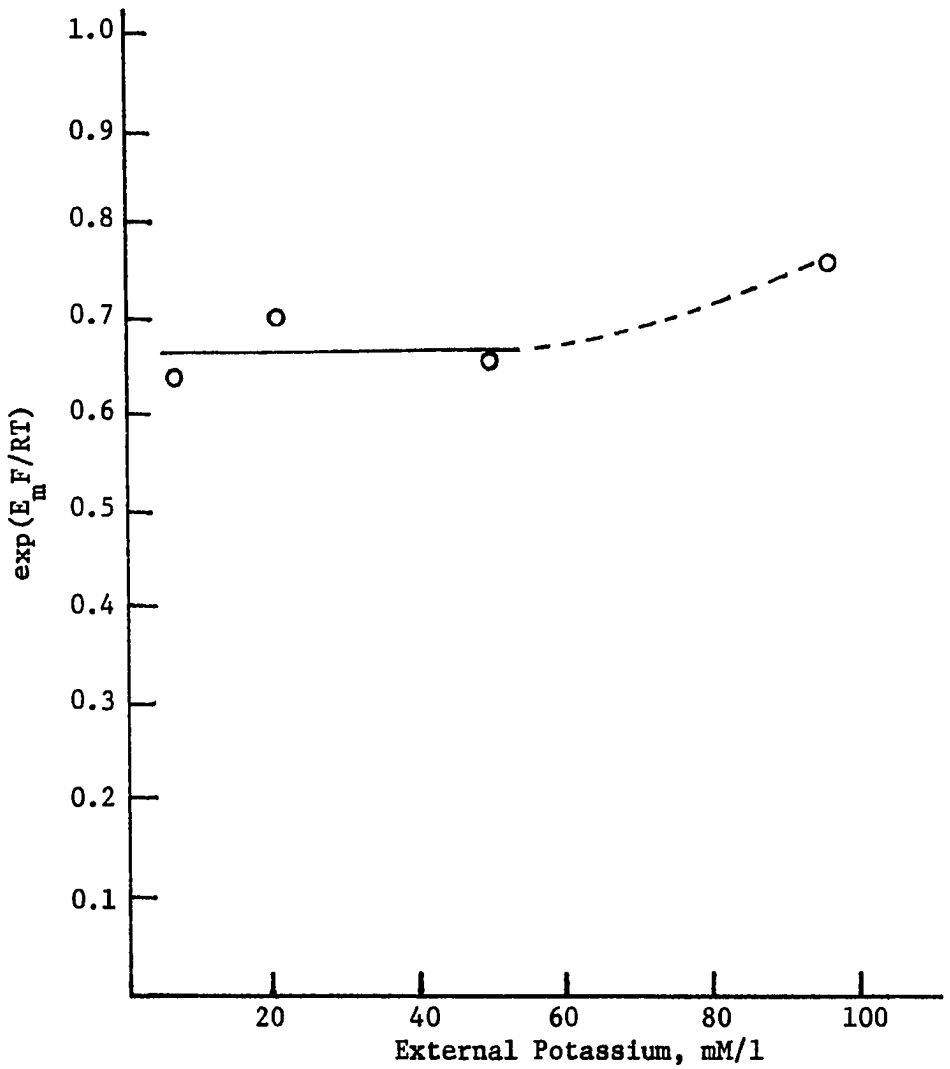

Figure 36. The value of $\exp(E_m F/RT)$ as a function of the external potassium concentration. The slope is taken to be zero and the y-intercept is 0.66.

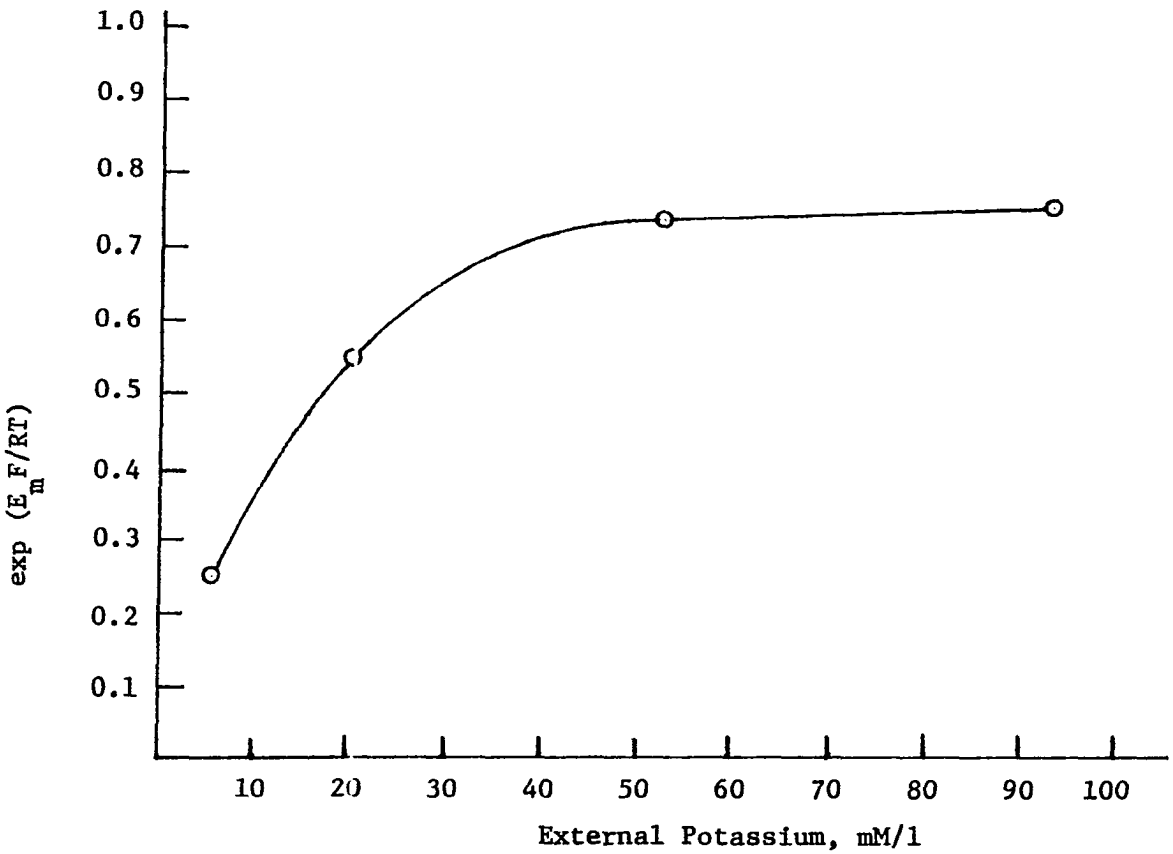

Figure 37. The value of exp (E_mF/RT) for PY3T3 cells as a function of the external potassium concentration. This relation is not linear using a constant P_{Na}/P_K ratio in the Goldman equation.

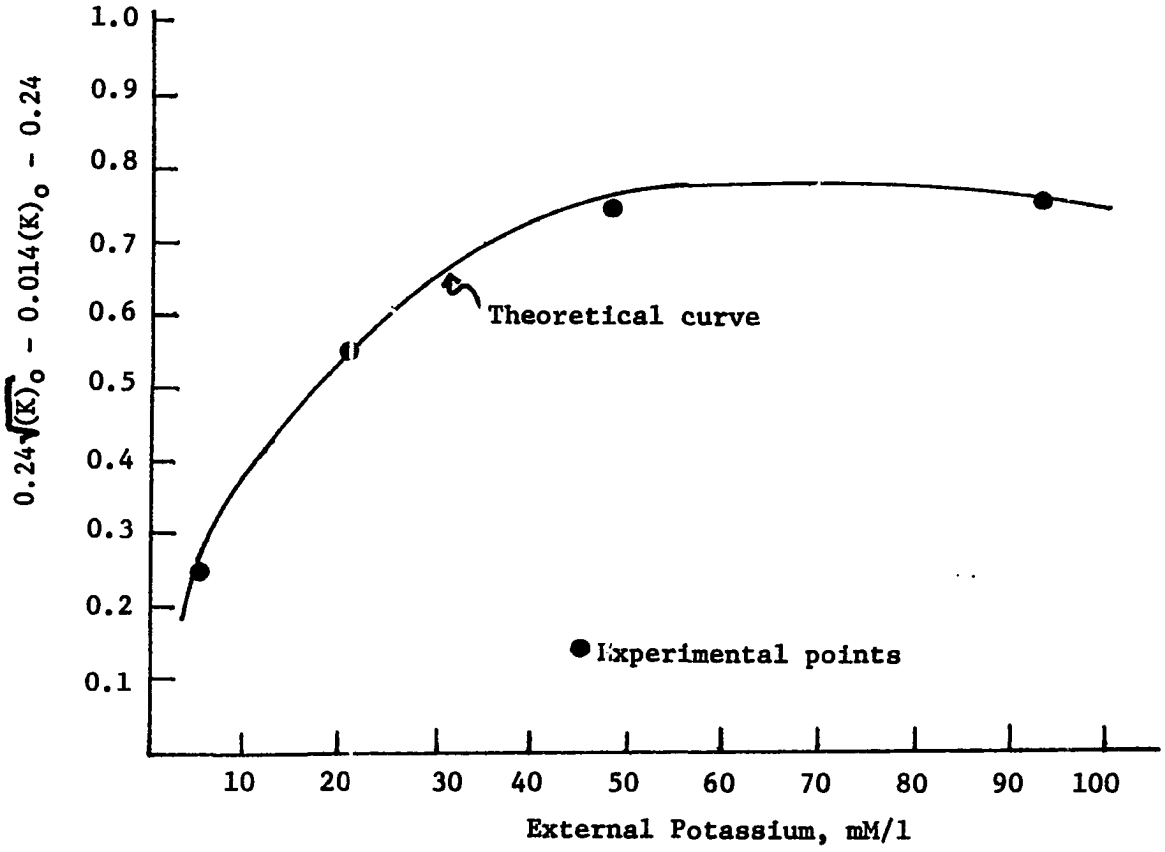

Figure 38. The experimentally-determined data on the potassium dependence of the PY3T3 cells. The solid line indicates the theoretical curve obeying the equation, $0.24\sqrt{(K)_o} - 0.014(K)_o - 0.24$.

where $\alpha(c)$ represents the ratio P_{Na}/P_K as a function of the concentrations of Na^+ and K^+. We can determine the function $\alpha(c)$, by using the fitted curve and equation 6,

$$\alpha(c) = \frac{\gamma(K)_i - (K)_o}{(Na)_o - \gamma(Na)_i} \qquad (7)$$

where $\gamma = 0.24\sqrt{(K)_o} - 0.014(K)_o - 0.24$. Solving for P_{Na}/P_K using the concentrations $(K)_i = 205$, $(Na)_i = 18$, $(K)_o = 5.4$, and $(Na)_o = 153$ mM/l, then equation 5 yields $\alpha_{PY3T3} = 0.27$. Permeability changes for K^+ with varying $(K)_o$ appears in the reports of Claret et al. (73), Noble (140) and Hodgkin and Horowicz (75). The suggestion of membrane permeability to K^+ changing as a function of $(K)_o$ is consistent with the data obtained in this study, and the evidence for such changes is substantial in excitable cells (72). Figure 39 shows the predicted changes in P_{Na}/P_K as a function of $(K)_o$ for PY3T3 cells. It is interesting to note that the ratio does not exceed the value 1.0, and approaches the maximum value at a value of $(K)_o$ which is optimal for the growth of some tissue cultured cells (53,65).

With the use of the computed values of P_{Na}/P_K for the 3T3 and PY3T3 cells, we can now estimate the ratio P_{Cl}/P_K for both cell lines. Substitution of $P_{Na}/P_K = 1.0$ into equation 1 yields

$$E_m = \frac{RT}{F} \ln \frac{(K)_o + (Na)_o + \xi(Cl)_i}{(K)_i + (Na)_i + \xi(Cl)_o} \qquad (8)$$

Where $\xi = P_{Cl}/P_K$. If the chloride ion is passively distributed then we may solve for $(Cl)_i$ and ξ using the conditions,

$$\begin{aligned} (K)_o + (Na)_o &= \xi(Cl)_i \\ (K)_i + (Na)_i &= \xi(Cl)_o \end{aligned} \qquad (9)$$

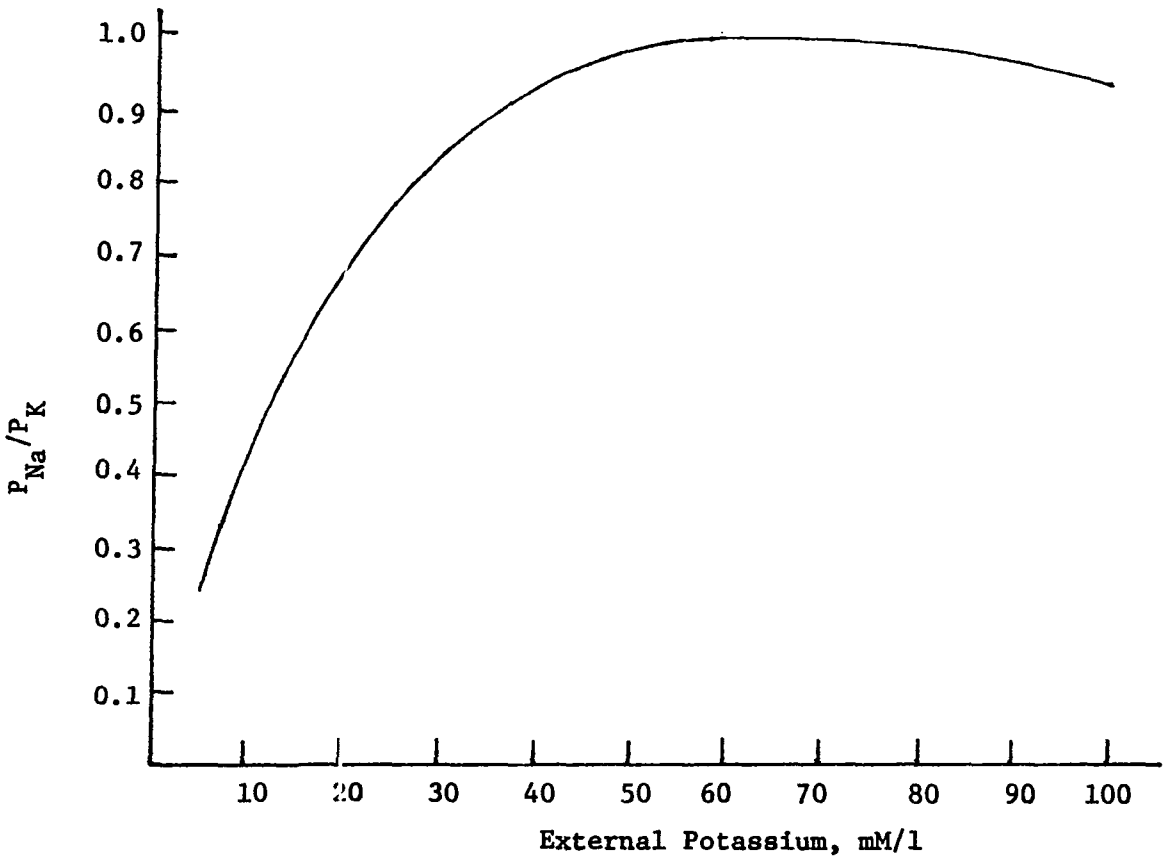

Figure 39. The permeability ratio, P_{Na}/P_K as a function of the external potassium level for PY3T3 cells. Note the ratio does not exceed the value 1.0. This function was derived from a modified form of the Goldman equation.

Solving these two equations containing two unknowns yields $P_{Cl}/P_K = 1.88$ and $(Cl)_i = 83$ mM/l for the 3T3 cells. A similar calculation for the PY3T3 cells using $P_{Na}/P_K = 0.27$, gives $P_{Cl}/P_K = 1.75$ and $(Cl)_i = 28$ mM/l. The proper values for $(Cl)_i$ may be obtained by use of the following equation,

$$E_{Cl} = \frac{-RT}{F} \ln \frac{(Cl)_o}{(Cl)_i} \qquad (10)$$

Using -12.3 mV, $(Cl)_o = 120$ mM/l for 3T3 cells, then $(Cl)_i = 80$ mM/l. For the PY3T3 cells, with a resting potential of -35.2 mV, solution of equation 10 yields $(Cl)_i = 30$ mM/l. The values of P_{Cl}/P_K show that for both cell lines, the decreasing order of permeabilities is $P_{Cl} > P_K > P_{Na}$. This finding is in agreement with the relative permeabilities reported for rat liver cells (75) and mouse L cells (74). The ratio P_{Na}/P_{Cl} may be estimated by using P_{Na}/P_K and P_{Cl}/P_K. The values of P_{Na}/P_{Cl} are 0.53 and 0.15 for the 3T3 and PY3T3 cells, respectively. These values may be compared to 0.54 obtained by Schaefer et al. for the chloroleukemic cell (121) and 0.34 reported by Aull for Ehrlich ascites tumor cells (79).

The transmembrane potential of the 3T3 and PY3T3 cells differs in the resting state of the cells and with increasing the external potassium concentration. The above analysis can explain these observations by considering the ratio P_{Na}/P_K to be quite different. Furthermore, this ratio may increase for PY3T3 cells when $(K)_o$ is raised above the normal level of 5.4 mM/l. A comment should be made as to the validity of using equation 6 containing $\alpha(c)$. As originally developed by Goldman (118) and adapted by Hodgkin and Katz for excitable membranes (128), the permeability, P_{Xi}, of a monovalent ionic through the membrane is given by,

$$P_{Xi} = \frac{U\ R\ T\ Y}{F\ \Delta X} \qquad (11)$$

Where U is the mobility of the ion, Y is the proportionality constant for the X_i ion concentration at a membrane of thickness ΔX. There is no restriction on having the mobility or conversion factor change as the concentration changes. These factors remain constant at given concentrations but may change value as the concentration is changed. Essentially, the success of the Goldman equation for describing the relationship between the major monovalent ions and the potential difference across biological membranes motivates the use of the equation for examining the transmembrane potential of 3T3 and PY3T3 cells. In the present study, the form of the equation can be used where $\alpha(c)$ is interpreted as the ratio P_{Na}/P_K. The agreement of the values for P_{Na}/P_K, P_{Na}/P_{Cl}, P_{Cl}/P_K, and the apparent order of permeabilities compared to other studies is quite acceptable.

Compared to the low value of P_{Na}/P_K for excitable cells ($\simeq$.01), the large values for α_{3T3} and α_{PY3T3} may reflect changes in the absolute permeabilities of either sodium or potassium, or changes in both. Data available from the literature does not present a likely possibility, though it has been argued that non-excitable cells have a high absolute Na^+ permeability (78,82,129). In contrast, there is evidence that the Na^+ permeability of mouse L cells is the same as excitable cells but K^+ permeability is an order of magnitude lower (74). Lowering the external sodium concentration resulted in about a 7 mV depolarization for both cell lines, which suggests that the cells used in the present study have a low absolute permeability to sodium. Assuming the reduced values in the TMP was not due to a high permeability to the substituting cation

(tetramethylammonium), then it is likely the high values of α_{3T3} and α_{PY3T3} may be due to a lowered permeability of K^+ compared to excitable cells, with Na^+ permeability unchanged. Depolarization of rat liver cells was reported by Claret et al. (75) when $(Na)_o$ was decreased.

The use of equation 8 to describe the TMP for these cells allows us to predict the effect of decreasing the external chloride concentration. Using $P_{Na}/P_K = 1.0$ and $P_{Cl}/P_K = 1.88$ for 3T3 cells, and lowering $(Cl)_o$ from 120 to 30 mM/l, substitution into equation 8 yields a value of -7 mV. The observed value of -5.9 ± 0.4 mV is not significantly different from this potential difference ($P>.05$). For the PY3T3 cells, with $P_{Na}/P_K = 0.27$ and $P_{Cl}/P_K = 1.75$, a similar computation gives -26 mV. This value is not significantly different compared to -28.3 ± 1.8 mV, the experimentally determined potential difference. When $(Cl)_o$ was further reduced to 17 mM/l, the 3T3 cells depolarized about 5 mV, and there was no change in the TMP of the PY3T3 cells. This effect may be due to permeation of the sulfate anion, $SO_4^=$, or may be related to the observation of a low P_{Cl} when $(Cl)_o$ is low (75).

The 3T3 cells demonstrated only little change in transmembrane potential or membrane resistance between 35°C and 23°C. The computed value for the Q_{10} is 1.13. In contrast, the TMP of PY3T3 cells had a Q_{10} of 2.62 under the same conditions. This demonstrates another difference between the two cell lines, notably the temperature dependence of the TMP and MR.

If the potential difference across the membrane is due solely to the passive distribution of ions, then the effect of changing temperature should be reflected in coefficient of the equation that describes the

potential. Using the equation 4 from the previous discussion, the ratio of the TMP at 35°C and 23°C is given by,

$$Q_{10} = \frac{E_m(35^oC)}{E_m(23^oC)} = \frac{308}{296} = 1.04$$

which is not significantly different than the 1.13 obtained for the 3T3 cells ($P>.05$). The Q_{10} of 2.62 obtained for PY3T3 cells is not readily explanable, but offers the immediate suggestion that metabolic energy is required for the maintenance of the potential difference, since the Q_{10} of many biochemical reactions is about 2.0 (52). Considering the origin of the TMP to be due to an electrogenic process, it is necessary for the Q_{10} to be considerably higher than 1.04, but not sufficient. Since the permeability of the PY3T3 cell membrane probably changed with varying ionic conditions, then the permeability may change with temperature also. The conductance through the membrane certainly increased by incubating the cells at 23°C, since the MR fell to 9 MegOhms.

If these cells lost potassium and gained sodium at 23°C, this would lower the transmembrane potential. Considering this shift in $(Na)_i$ and $(K)_i$ to be about 50% following a 30 minute incubation at 23°C, with no change in the ratio P_{Na}/P_K, one would expect a depolarization to -23 mV. On the other hand, if there were a 50% increase in the P_{Na}/P_K ratio, from 0.27 to 0.40, the expected TMP for the cells at 23°C would be -31 mV. Neither possibility above can account for the observed TMP alone. If it is considered likely that such a shift in the K^+ and Na^+ distribution could occur and further, that the P_{Na}/P_K ratio could change to a value of 0.40, then the predicted TMP from both of these effects would be -15 mV, a value not significantly different than the observed TMP of -13.4 ± 1.0 mV ($P>.05$). Since cooling cells can lead to a loss of K^+

and Na^+ - loading (130,131) and the MR indicated an increased ion permeability, then a possible explanation for the observed Q_{10} of 2.62 might be due to the situation described above. Borle reported a similar temperature effect for HeLa cells (82) and suggested that changes in membrane permeability might account for his observations. A loss of K^+ and a gain of Na^+ was previously reported for HeLa cells when the cells were cooled (132).

Electrical Properties of 3T3 and PY3T3 Cells

Examination of Figures 29 and 30 point out another difference between 3T3 and PY3T3 cells, with regard to some electrical parameters. Either at the stage of confluency or at a given cell density, the transmembrane potential, as well as the DC membrane resistance, are quite different ($P<.01$). In the late log-phase of growth, the average TMP of 3T3 cells is -12 mV whereas that of the PY3T3 cells is -40 mV. The corresponding values for MR are 14 and 34 MegOhms, respectively. On the other hand, if comparison is made at the same cell density, about 5×10^4 cells/cm^2, then the TMP and MR values for the 3T3 cells are -12 mV and 14 MegOhms, respectively, whereas those for the PY3T3 cells are -25 mV and 35 MegOhms. It seems more meaningful to compare the specific resistances of the membranes, R_{MS}, of these two kinds of cells instead of their total DC resistances. An estimate of this parameter can be made in the following manner.

Morphologically, the 3T3 cells are small, flat, and disc-shaped when attached to the flask. The height of these cells range from 1-4 microns and the diameter is about 40 microns (9). Taking the cells to be discs of height 2 microns, with a radius of 20 microns, the R_{MS} value

is estimated to be 400 ohm-cm^2 for 3T3 cells. Most PY3T3 cells grow as overlapped, thin, fibroblastic appearing cells, with increasing thickness near the center. Approximating the shape of these cells as two right cones, continuous at the base having a radius of 15 microns and a height of 30 microns, then the estimated value for R_{MS} is about 1100 ohm-cm^2 for PY3T3 cells. The values of R_{MS} can actually be a factor of two or four-fold low if the cells have microfilopodia extending from their surface, as described for mouse L cells (76). The relative values would probably remain the same, which means that the R_{MS} of PY3T3 cells is about twice as high as 3T3 cells. These values can be compared to 5000 ohm-cm^2 obtained for L cells (76) and 700, 2000, 5000, and 4000 ohm-cm^2 for squid axon, lobster nerve, crab nerve, and frog muscle, respectively (72).

In most of the studies on the transmembrane potential of cell lines that grow attached to the culture substrate, only confluent cultures have been used (65,82,83,127). It was not until recently (89,90) that studies are being conducted on the effect of cell density upon the TMP and MR of cultured cells. Sachs and McDonald mentioned that confluent cultures seem to yield more electronegative TMP's than sparse cultures (127), but provided no detailed results.

In undertaking the present study it was felt that the PY3T3 cell line offered a good opportunity to test Cone's hypothesis that the TMP should become more negative as proliferative activity decreases (88). If the electrical parameters vary with cell density, then these would indeed prove to be some useful electrophysiological parameters for any comparative study of normal and tumorous cells. The proliferative activity of cultured cells does decrease with increasing cell density,

so alterations in the TMP should be expected in terms of Cone's theory. The results presented in Figures 29 and 30 demonstrate that as the cell density changed by about three orders of magnitude, the TMP and MR of PY3T3 cells also changed with density, the potential increasing from -20.5 to -46.1 mV and R_{MS} increasing from 850 ohm-cm^2 to 1500 ohm-cm^2. This relation for the TMP has recently been shown for 3T3 cells (89,90).

The 3T3 cell line was studied at only one cell density for which the TMP was -12.3 mV and the R_{MS} was 400 ohm-cm^2. Cone obtained a value of -12.2 mV for the TMP of 3T3 cells in late log-phase growth (90). The agreement is remarkable but he made no measurement of membrane resistance. This latter point is important as the present study shows that the membrane resistance of PY3T3 cells change <u>prior</u> to any significant changes in the TMP, suggesting that permeability alterations precede changes in the TMP. The TMP of the 3T3 cells changed rapidly as the cell culture became confluent, reaching a maximum at about -55 mV. Cone reported the values of $(K)_i$ and $(Na)_i$ at this time to be 197 and 8 mM per liter of cell volume, respectively. If the hyperpolarization of the PY3T3 cells is due to the same mechanisms, the shift in intracellular K^+ and Na^+ can not account for the observed change in TMP, from -35 to -46 mV. However, about a 30% change for the value of α_{PY3T3}, from 0.27 to 0.18 can explain the 11 mV hyperpolarization. The present data are consistent with the ideas set forth by Cone (64,86-88) that the TMP is a measure of the proliferative rate of a cell population. Recalling the doubling times of the two cell lines, i.e. 23 hours for the 3T3 cells and 29 hours for the PY3T3 cells, then the less electronegative TMP for 3T3 cells would have been predicted. Both cell lines had about 95% of the cells in the pro-

liferative pool, as indicated by the incorporation of ^{3}H-thymidine, so the figures for doubling times closely approximate the average cell cycle time for the 3T3 and PY3T3 cell lines.

Membrane alterations with increasing cell density have been reported in the literature. Cass demonstrated fluctuations in the membrane permeability of pig kidney cells with changing cell density (133). She observed that the uptake of uridine, adenine, and thymidine was inversely related to cell density. McDonald and his co-workers showed that ^{3}H-thymidine incorporation in hamster kidney cells was correlated with the TMP (127). Although $(K)_o$ was increased to depolarize the cells, measurement of ^{3}H-thymidine incorporation at 5 or 93 mM/l of external potassium in normal or K^+-depleted cells showed that uptake was related to the TMP and not the increasing level of $(K)_o$. Intracellular levels of cyclic-AMP increase in cultured cells at confluency (49-51) which may reflect changes the in activity of adenyl cyclase, a membrane-bound enzyme. Intracellular ion content can be influenced by changes in the cyclic-AMP concentration (59). The chain of events that lead to a decrease in proliferative activity may include a change in the P_{Na}/P_K ratio. This parameter may have a regulatory function to cellular proliferation, but any causal relationship remains unknown.

It can be argued that the 3T3 cell does not represent the normal cell as mentioned by Cone (88), since the 3T3 cell line was established from dissociated embryonic tissue (9,11). However, the 3T3-PY3T3 cell system represents an adequate comparative system, in which one is non-tumorigenic and the other is highly tumorigenic. The 3T3 line is "transformed" to tissue culture, but lacks murine-associated viruses (134) and

displays characteristics of normal cells, *in vitro*. The polyoma virus-transformed line is tumorigenic (9-11) and does not have the degree of density-dependent growth control observed *in vitro* for nontransformed cells. The observed differences for the TMP and MR values for the two cell lines are indicative of changes that had taken place electrophysiologically following transformation with the polyoma virus. There are also reports that the membrane changes observed are subsequent to this transformation (135-137). It reasons therefore, that this study is indeed examining two cell lines on the basis of malignancy, growth regulation, and oncogenic virus-transformation. One can however raise the question of whether the difference obtained in the TMP or MR values is a consequence of virus infection rather than tumorigenic transformation. Although this study itself does not answer that question, it is interesting to note that infection of cells with herpes virus resulted in a change of the TMP from -20 to +12 mV (77).

An important point to note from this study is that the transmembrane potential of tumor cells is not less electronegative than the nontransformed cells. It can be concluded therefore, that for the *in vitro* situation, no generalization can be made as to whether the TMP of tumor cells is always less negative than normal cells.

The Effect of TRYP-Con A on the Transmembrane Potential and Membrane Resistance

Incubation of the PY3T3 cells with 40 µg/ml TRYP-Con A for one hour depolarized the cells from -35.2 to -25.2 mV. The R_{MS} also decreased, from 1100 ohm-cm^2 to 850 ohm-cm^2. Thus, the acute treatment with TRYP-Con A shifts the TMP and R_{MS} values toward the values observed in

the nontransformed cells. It is tempting to suggest that the observed change in the TMP might have been due to a change in α_{PY3T3}. If the potential is expressed in terms of the modified Goldman equation, then we may ask whether the change in the TMP can be explained by leaving α_{PY3T3} fixed and having the values of $(Na)_i$ and $(K)_i$ change. We consider first if only lowering $(Na)_i$ could be responsible. Using $(K)_o$ = 5.4, $(K)_i$ = 205, $(Na)_o$ = 153 mM/1, α_{PY3T3} = 0.27, and E_m = -25.2 mV, and solving for $(Na)_i$ we find that the cell content of sodium must be negative. A similar calculation for a loss of potassium from the cells requires a reduction from 205 to 120 mM/1. This is unlikely if it is true that these cells maintain high levels of K^+. Of course, a combination of these two events is more likely but a substantial reduction in intracellular K^+ and Na^+ must occur. If we hold $(K)_i$ and $(Na)_i$ constant and calculate the required change in α_{PY3T3} needed to obtain -25 mV, this yields a value of 0.48, compared to 0.27. This increase may be unlikely, but it has been shown that TRYP-Con A treatment of $SV_{40}3T3$ cells does affect the $Na^+ - K^+$ ATPase activity (53). If the potential across the membrane is maintained by metabolic energy, as suggested by the large Q_{10} for the TMP of these cells, then TRYP-Con A might have immediate effects upon enzymatic systems which could alter membrane permeability.

It may be argued that the acute studies on the TMP and MR were done on cells that were cytotoxically affected by the TRYP-Con A. Hence, the observed decrease in the TMP might be attributed to a "slow death". Four major pieces of evidence argue against this line of thought.

1. The dead cells tend to become rounded, granular in appearance, detach from the substrate, and float. None of these cells were

prevalent after the one hour incubation with TRYP-Con A. The attached cells had no morphological distinction from untreated cells. Furthermore, the incorporation of ^{3}H-thymidine into the attached cells indicated that 95% entered DNA synthesis within a time consistent with the observed doubling time of untreated cells.

2. The PY3T3CCA cell line was cultured in the continuous presence of 40 μg/ml TRYP-Con A. The TMP and R_{MS} was much lower than that observed in the acute electrical studies. The attached cells of this line show greater than 90% viability after 9 months of culture.

3. The membrane resistance of dead cells would be expected to approach zero, following a loss of membrane integrity. The acute treatment with TRYP-Con A resulted in an R_{MS} of about 850 ohm-cm^2, a value two-fold above that found for viable 3T3 cells.

4. Finally, using Trypan blue vital stain after a one hour incubation of PY3T3 cells with 40 μg/ml TRYP-Con A, less than 10% of the cells were stained. This is no different from any untreated PY3T3 culture.

The chronically treated PY3T3 cells showed a dramatic decrease in the values of the TMP and R_{MS}. After 6 months, the TMP was -9 mV and the R_{MS} about 350 ohm-cm^2. These values are comparable to the values observed in the nontransformed 3T3 cells. Again, the basis for this restoration is unknown. It is possible that chronic treatment with TRYP-Con A selects for cells that have membrane characteristics similar to 3T3 cells. Based on the following observations, the dominant feature of TRYP-Con A treatment appears to be selection of a particular cell population.

First of all, the growth curves of TRYP-Con A treated PY3T3 cells show an immediate drop in cell count, followed by a very slow recovery. This acute treatment could have features of adaptation and selection, but as 95% of the attached cells do incorporate ^{3}H-thymidine, this certainly implicates selection as the dominant feature of the acute treatment. The acute study with L5178Y cells show the effect more clearly. A substantial population was killed within the first 24-48 hours, and those that survived the addition of TRYP-Con A grew as untreated cells.

Secondly, the observed characteristics of the chronic PY3T3CCA cell lines were consistent with a selection process. The doubling times of the cells increased two-fold over the untreated cells for the first 3-4 months of treatment, then started decreasing toward the value of untreated cells. This observation, added to the demonstration that PY3T3CCA cells no longer agglutinate, even at 1000 µg/ml Con A concentration, suggests the following sequence of events probably took place in this study.

Upon the addition of TRYP-Con A, the PY3T3 cells had immediate changes in membrane characteristics due to binding TRYP-Con A fragments. This was borne out by the electrical data, and the studies of Yoshikawa-Fudaka on Na^{+} - K^{+} ATPase and adenyl cyclase (53). Cell division continued at the normal rate, but since mitosis invovles rounding-up and becoming detached, then a certain portion of the floating cells that became agglutinated with the TRYP-Con A fragments subsequently died, (or reattachment was prevented). As this process continued, agglutinated cells were poured off during medium changes, and those cells that did

not agglutinate continued through mitosis, reattached, and continued growth. This would explain the drop in cell number following addition of TRYP-Con A and the 95% proliferative pool as measured by ^{3}H-thymidine incorporation.

Since the tumor cell population is made up of a spectrum of cells having different morphological characteristics, the continuation of this growth pattern and the continued presence of TRYP-Con A caused the above process to be repeated through each cell generation. The result of this repeated operation would be an increased doubling time (as a smaller fraction of the cells actually contribute to the growth of the population), and this was observed. In this study, agglutinability was lost in the first 4 weeks of TRYP-Con A treatment, but only the agglutinability of those cells attached was measured. If this repeated process allowed selection for a population of cells having lower agglutinability then the population would finally consist of predominately that cell type. Hence, the doubling time would start to decrease, since agglutinable progeny were no longer being produced at the same amount, hence more cells contributed to cell growth. This is what was observed from 4-6 months, (i.e., the doubling time decreased to 40 hours). In addition, the morphology of the cell population would become more uniform, if certain cell types were being excluded by selection. This also was observed.

The question that arises from the above discussion is whether the selected cells bind Con A at all. This was not studied, but does not affect the general conclusions. Nontransformed cells do bind Con A, but have little agglutination (10-13,34).

To summarize the overall findings of the electrical studies on PY3T3CCA cells, it was observed that chronic treatment with TRYP-Con A did return the transmembrane potential and membrane resistance to values observed in the nontransformed 3T3 cells. The acute treatment also shifted the TMP and MR values toward the corresponding values of the nontransformed cell. For the chronic-treated cell line, those cells were probably obtained by a slow, yet effective selection process. The acute studies indicate that selection is not necessary to have membrane changes associated with binding TRYP-Con A fragments.

An important series of studies would be to examine the PY3T3CCA line with respect to altering ionic composition of the bathing medium and measuring the TMP and MR to examine whether the response is the same observed for the 3T3 cell line. This would further establish whether the membrane properties of the PY3T3CCA are similar to 3T3 cells. For instance, are PY3T3CCA cells as insensitive to changing $(K)_o$ as observed for the 3T3? Does this imply that the P_{Na}/P_K ratio is shifted toward the value of 1.0 obtained in this study of 3T3 cells? Are these membrane alterations necessary for the observed change in growth behavior?

Summary

The present study was done to answer the questions stated within the Introduction. Taking the questions separately:

1. The results demonstrate that time, cell density, Con A concentration, and ionic strength affect agglutination to such an extent that standardization of the assay conditions are necessary for proper comparisons between cell lines. There are differences in the agglutinability of 3T3 and PY3T3 cells. Furthermore, the agglutinability of PY3T3CCA cells

was lost within the first 4 weeks of TRYP-Con A treatment.

2. The TMP and MR do change as a function of cell density. The TMP becomes more electronegative and the MR increases as the cell density increases. This effect can not be accounted for in terms of reported shifts in ion distribution. This change in TMP may be due to a change in membrane properties, resulting in an alteration of the ratio, P_{Na}/P_K.

3. The TMP of 3T3 cells is less electronegative than the PY3T3 cells. No generalization can be drawn as to the predicted TMP values of transformed cells compared to nontransformed cells. The estimated value for the specific resistance, R_{MS}, of PY3T3 cells is about two-fold higher than the R_{MS} of 3T3 cells.

4. The response of the TMP for the two cell lines are quite different when external potassium is raised. This is explained in terms of the P_{Na}/P_K ratio using a modified form of the Goldman equation. The estimated values of P_{Na}/P_K, P_{Cl}/P_K, and P_{Na}/P_{Cl} are 1.0, 1.88, and 0.53 for 3T3 cells, respectively. The corresponding values for the PY3T3 cells are 0.27, 1.75, and 0.15. The use of the modified Goldman equation also explained the data obtained when external chloride was decreased by a factor of four. Both cell lines have a decreasing order of permeability, $P_{Cl} > P_K > P_{Na}$. The small depolarization observed when external Na^+ was decreased suggests that both cell lines have an absolute sodium permeability comparable to excitable cells, and that the high value for P_{Na}/P_K may be due to a lowered K^+ permeability. The temperature dependence of the TMP for the two cell lines markedly differs. Metabolic energy may be required to maintain the TMP of PY3T3 cells. A 50% increase in the P_{Na}/P_K ratio plus loss of intracellular K^+ and Na^+ can account for the

observed depolarization of the PY3T3 cells at 23°C.

5. The TMP and MR returned to the values observed for the non-transformed cells after 6 months of TRYP-Con A treatment. It is argued that selection of cells having membrane characteristics similar to the 3T3 cells probably occurs. This is supported by the observations on the lack of agglutinability and growth behavior of the PY3T3CCA cells. Acute treatment with TRYP-Con A shifts the TMP and MR toward the values observed for 3T3 cells. Evidence indicates that this was not a cytotoxic effect of the TRYP-Con A.

BIBLIOGRAPHY

1. Rubin, H. 1970 Growth-Regulating Interactions Among Cultured Animal Cells. in Permeability and Function of Biological Membranes. North-Holland Publishing Co., Amsterdam.

2. Culp, L.A. and Black, P.H. 1972 Contact-Inhibited Revertant Cell Lines Isolated from Simian Virus 40-Transformed Cells. J. of Virology 9: 611.

3. Martz, E. and Steinberg, M.S. 1972 The Role of Cell-Cell Contact In "Contact" Inhibition of Cell Division: A Review and New Evidence. J. Cell Physiol. 79: 189.

4. Abercrombie, M. 1970 Contact Inhibition In Tissue Culture. In Vitro 6: 128.

5. Burger, M.M. 1971 The Significance of Surface Structure Changes For Growth Control Under Crowded Conditions. CIBA Foundation Symposia.

6. Weber, J. 1973 Relationship between Cytoagglutination and Saturation Density of Cell Growth. J. Cell Physiol. 81: 49.

7. Abercrombie, M. and Ambrose, E.J. 1958 Interference Microscope Studies of Cell Contacts In Tissue Culture. Exptl. Cell. Res. 15: 332.

8. Abercrombie, M. and Ambrose, E.J. 1962 The Surface Properties of Tumor Cells: A Review. Cancer Research 22: 525.

9. Todaro, G.J., Green, H., and Goldberg, B.D. 1964 Transformation of Properties of an Established Cell Line by SV40 and Polyoma Virus. Proc. Nat. Acad. Sci. 51: 66.

10. Holley, R.W. and Kiernan, J.A. 1968 "Contact Inhibition" of Cell Division in 3T3 Cells. Proc. Nat. Acad. Sci. 60: 300.

11. Pollack, R.E., Green, H., and Todaro, G.J. 1968 Growth Control In Cultured Cells: Selection of Sublines With Increased Sensitivity to Contact Inhibition and Decreased Tumor-Producing Ability. Proc. Nat. Acad. Sci. 60: 126.

12. Sanford, K.K. 1968 in Cancer Cells In Culture, Univ. of Tokyo Press and University Park Press.

13. Purdom, L., Ambrose, E.J., and Klein, G. 1958 A Correlation Between Electrical Surface Charge and Some Biological Characteristics During the Stepwise Progression of a Mouse Sarcoma. Nature 181: 1586.

14. Ambrose, E.J., James, A.M., and Lowick, J.H.B. 1956 Differences Between the Electrical Charge Carried by Normal and Homologous Cells. Nature 177: 576.

15. Heard, D.H., Seaman, G.V.F., Simon-Reuss, I., and Doljanski, F. 1961 Electrophoretic Mobility of Cultured Mesodermal Tissue Cells. Nature 190: 1009.

16. Mayhew, E. and MacKinnon, M.G.A. 1966 Cellular Electrophoretic Mobility and the Mitotic Cycle. J. Gen. Physiol. 49: 717.

17. Burger, M.M. and Noonan, K.D. 1970 Restoration of Normal Growth by Covering of Agglutinin Sites on Tumour Cell Surface. Nature 228: 512.

18. Ben-Or, S., Eisenberg, S., and Doljanski, F. 1960 Electrophoretic Mobility of Normal and Regenerating Liver Cells. Nature 188: 1200.

19. Kraemer, P.M. 1967 Configuration Change of Surface Sialic Acid During Mitosis. J. Cell Biol. 33: 197.

20. Malenkov, A.G. 1972 Electroconductivity Changes During the Mitotic Cycle In Ehrlich Ascites Tumour Cells. Biochim. Biophys. Acta 255: 304.

21. Weiss, L. and Zeigel, R. 1972 Heterogeneity of Anionic Sites at the Electrokinetic Surface of Fixed Ehrlich Ascites Tumor Cells. J. Theor. Biol. 34: 21.

22. Weiss, L. 1970 Cell Adhesion and Some Ionized Groups at the Cell Surface. in Permeability and Function of Biological Membranes. North-Holland Publishing Co., Amsterdam.

23. Ohta, N., Pardee, A., McAuslan, B.R., and Burger, M.M. 1968 Sialic Acid Contents and Controls of Normal and Malignant Cells. Biochim. Biophys. Acta 158: 98.

24. Burger, M.M. 1969 A Difference In The Architecture of the Surface Membrane of Normal and Virally Transformed Cells. Proc. Nat. Acad. Sci. 62: 994.

25. Sela, B., Lis, H., Sharon, N., and Sachs, L. 1970 Different Locations of Carbohydrate-Containing Sites in the Surface Membrane of Normal and Transformed Mammalian Cells. J. Membrane Biol. 3: 267.

26. Sheppard, J.R. and Lehman, J.M. 1972 Agglutinability by Plant Lectins Increases After RNA Virus Transformation. Virology 49: 339.

27. Burger, M.M. and Martin, G.S. 1972 Agglutination of Cells Transformed by Rous Sarcoma Virus by Wheat Germ Agglutinin and Concanavalin A. Nature New Biol. 237: 9.

28. Nicolson, G.L. 1971 Difference In Topology of Normal and Tumor Cell Membranes Shown by Different Surface Distributions of Ferritin-Conjugated Concanavalin A. Nature New Biol. 233: 244.

29. Revel, J. and Smith, S.B. 1972 Mapping of Concanavalin A Binding Sites on the Surface of Several Cell Types. Develop. Biol. 27: 434.

30. Nicolson, G.L. 1972 Topography of Membrane Concanavalin A Sites Modified by Proteolysis. Nature New Biol. 239: 193.

31. Haughton, G. and Amos, D.B. 1968 Immunology of Carcinogenesis. Cancer Research 28: 1840.

32. Basombrio, M.A. 1970 Search for Common Antigenicities among Twenty-Five Sarcomas Induced by Methylcholanthrene. Cancer Research 30: 2458.

33. Mann, D.L., Haltermann, R., and Leventhal, B.G. 1973 Crossreactive Antigens on Human Cells Infected with Rauscher Leukemia Virus and on Human Acute Leukemia Cells. Proc. Nat. Acad. Sci. 70: 495.

34. Burger, M.M. 1973 Surface Changes In Transformed Cells Detected by Lectins. Federation Proc. 32: 91.

35. Warren, L., Fuhrer, J.P., and Buck, C.A. 1972 Surface Glycoproteins of Normal and Transformed Cells: A Difference Determined by Sialic Acid and a Growth-Dependent Sialyl Transferase. Proc. Nat. Acad. Sci. 69: 1838.

36. Warren, L., Fuhrer, J.P., and Buck, C.A. 1972 Surface Glycoproteins of cells before and after transformation by oncogenic viruses. Federation Proc. 32: 80.

37. Yogeeswaran, G., Sheinin, R., Wherrett, J.R., and Murray, R.K. 1972 Studies on the Glycosphingolipids of Normal and Virally Transformed 3T3 Mouse Fibroblasts. J. Biol. Chem. 247: 5146.

38. So, L.L. and Goldstein, I.J. 1967 Protein-Carbohydrate Interaction. V. Application of the Quantitative Precipitin Method to Polysaccharide-Concanavalin A Interaction. J. Biol. Chem. 242: 1617.

39. Poduslo, J.F., Greenberg, C.S., and Glick, M.C. 1972 Proteins Exposed on the Surface of Mammalian Membranes. Biochemistry 11: 2616.

40. Wallach, D.F. 1968 Cellular Membranes and Tumor Behavior: A New Hypothesis. Proc. Nat. Acad. Sci. 61: 868.

41. Mosser, A.G., Janoff, A., and Blondin, J. 1973 Increased Concanavalin A-dependent Agglutinability of Mouse Fibroblasts After Treatment with Leukocyte Lysosomal Preparations. Cancer Research 33: 1092.

42. Ambrose, E.J. 1961 The Inhibition of Tumor Growth by Enzymes In Tissue Culture. Exptl. Cell Res. 24: 220.

43. Goto, M., Kataoka, Y., and Sato, H. 1972 Decrease of Saturation Density In Cultured Tumor Cells by Dextran Sulfate. Gann 63: 371.

44. Briscoe, W.T., Taylor, W.A., Duff, R., and Rapp, F. 1972 Aspartyl Transfer RNA Profiles In Normal and Cancer Cells. Cancer Research 32: 1753.

45. Bissell, M.J., Hatie, C., and Rubin, H. 1972 Patterns of Glucose Metabolism in Normal and Virus-Transformed Chick Cells In Tissue Culture. J. Natl. Cancer Inst. 49: 555.

46. Fishman, P.H., McFarland, V.W., Mora, P.T., and Brad, R.O. 1972 Ganglioside Biosynthesis In Mouse Cells: Glycosyltransferase Activities In Normal and Virally-Transformed Lines. Biochem. Biophys. Res. Commun. 48: 48.

47. Burger, M.M. 1970 Proteolytic Enzymes Initiating Cell Division and Escape from Contact Inhibition of Growth. Nature 227: 170.

48. Schnebi, P.H. and Burger, M.M. 1972 Selective Inhibition of Growth of Transformed Cells by Protease Inhibitors. Proc. Nat. Acad. Sci. 69: 3825.

49. Hsie, A.W. and Puck, T.T. 1971 Morphological Transformation of Chinese Hamster Cells By Dibutyrl Adenosine Cyclic 3':5'-Monophosphate and Testosterone. Proc. Nat. Acad. Sci. 68: 358.

50. Johnson, G.S., Friedman, R.M., and Pastan, I. 1971 Restoration of Several Morphological Characteristics of Normal Fibroblasts in Sarcoma Cells Treated with Adenosine-3':5'-Cyclic Monophosphate and It's Derivatives. Proc. Nat. Acad. Sci. 68: 425.

51. Otten, J., Bader, J., Johnson, G.S., and Pastan, I. 1972 A Mutation in a Rous Sarcoma Virus Gene That Controls Adenosine 3',5'-Monophosphate Levels and Transformation. J. Biol. Chem. 5: 1632.

52. White, A., Handler, P., and Smith, E.L. 1968 in Principles of Biochemistry, McGraw-Hill Book Co., N.Y.

53. Yoshikawa-Fukada, M. and Jojima, T. 1973 Biochemical Characteristics of Normal and Virally Transformed Mouse Cell Lines. J. Cell. Physiol. 80: 421.

54. Barat, N. and Avrameas, S. 1973 Surface and Intracellular Localization of Concanavalin A In Human Lymphocytes. Exptl. Cell Res. 76: 451.

55. Keller, R. 1973 Concanavalin A, A Model "Antigen" For The In Vitro Detection of Cell-Bound Reaginic Antibody In The Rat. Clin. Exp. Immunol. 13: 139.

56. Ono, M., Maruta, H., and Mizuno, D. 1973 Mitogenic Activity of a Sepharose-Concanavalin A Complex on Rabbit Spleen Cells. J. Biochem. 73: 235.

57. Sallstrom, J.F. and Alm, G.V. 1972 Binding of Concanavalin A To Thymic and Bursal Chicken Lymphoid Cells. Exptl. Cell Res. 75: 63.

58. McMrery, J.E. and Rigby, P.G. 1972 Lymphocyte Stimulation by Cyclic AMP, GMP, and Related Compounds. Proc. Soc. Exp. Biol. Med. 140: 1456.

59. Whitfield, J.F., Rixon, R. H., MacManus, J.P., and Balk, S.D. 1973 Calcium, Cyclic Adenosine 3',5'-Monophosphate, and the Control of Cell Proliferation: A Review. In Vitro 8: 257.

60. Cuatrecasas, P. and Tell, G.P. 1973 Insulin-Like Activity of Concanavalin A and Wheat Germ Agglutinin. Direct Interactions with Insulin Receptors. Proc. Nat. Acad. Sci. 70: 485.

61. Husler, D.F. and Peters, J.H. 1972 Contact Cooperation In Stimulated Lymphocytes. Exptl. Cell Res. 74: 319.

62. Kay, J.E. 1971 Lymphocyte Stimulation by Phytohaemagglutinin. Exptl. Cell Res. 71: 245.

63. Quastel, M.R. and Kaplan, J.G. 1968 Inhibition by Ouabin of Human Lymphocyte Transformation Induced by Phytohaemagglutinin in vitro. Nature 219: 198.

64. Cone, C.D., Jr. and Tongier, M. 1970 Control of Somatic Cell Mitosis. Oncology 24: 168.

65. McDonald, T.F., Sachs, H.G., Orr, C.W., and Ebert, J.D. 1972 External Potassium and Baby Hamster Kidney Cells: Intracellular Ions, Growth, DNA Synthesis, and Membrane Potential. Devel. Biol. 28: 290.

66. Lowenstein, W.R. and Kanno, Y. 1967 Intercellular Communication and Tissue Growth. I. Cancerous Growth. J. Cell Biol. 33: 225.

67. Borek, C., Higaskino, S., and Lowenstein, W.R. 1969 Intercellular Communication and Growth. IV. Conductance of Membrane Junctions of Normal and Cancerous Cells in Culture. J. Membrane Biol. 1: 274.

68. Martinez-Palomo, A., Braislovsky, C., and Bernhard, W. 1969 Ultrastructural Modifications of the Cell Surface and Intercellular Contacts of Some Transformed Cell Strains. Cancer Research 29: 925.

69. Lowenstein, W.R. 1972 Cellular Communication Through Membrane Junctions. Arch. Intern. Med. 129: 299.

70. Amos, H. 1970 Introduction to Cell To Cell Communication. In Vitro 6: 1.

71. Williams, J.A. 1970 Origin of Transmembrane Potentials in Non-excitable Cells. J. Theor. Biol. 28: 287.

72. Katz, B. 1966 Nerve, Muscle, and Synapse. McGraw-Hill Book Co., New York.

73. Hodgkin, A.L. and Horowicz, P. 1959 Movements of Na and K in Single Muscle Fibers. J. Physiol. 145: 405.

74. Lamb, J.F. and MacKinnon, M. 1971 The Membrane Potential and Permeabilities of the L Cell Membrane to Na, K, and Chloride. J. Physiol. 213: 683.

75. Claret, M., Coraboeuf, E., and Favier, M.P. 1970 Effect of Ionic Concentration Changes on Membrane Potential of Perfused Rat Liver. Arch. Inter. Physiol. Biochem. 78: 531.

76. Nelson, P.G., Peacock, J., and Minna, J. 1972 An Active Electrical Response in Fibroblasts. J. Gen Physiol. 60: 58.

77. Fritz, M.E. and Nahmias, A.J. 1972 Reversed Polarity in Transmembrane Potentials of Cells Infected with Herpesviruses. Proc. Soc. Exp. Biol. Med. 139: 1159.

78. Johnstone, B.M. 1959 Micro-electrode Penetration of Ascites Tumour Cells. Nature 183: 411.

79. Aull, F. 1967 Measurement of the Electrical Potential Difference Across the Membrane of the Ehrlich Ascites Tumor Cell. J. Cell Physiol. 69: 21.

80. Smith, T.C., Mikiten, T.M., and Levinson, C. 1972 The Effect of Multivalent Cations on The Membrane Potential of the Ehrlich Ascites Tumor Cell. J. Cell Physiol. 79: 117.

81. Lassen, U.V., Nielsen, T., Pape, L., and Simonsen, L.O. 1971 The Membrane Potential of Ehrlich Ascites Tumor Cells. Microelectrode Measurements and Their Critical Evaluation. J. Membrane Biol. 6: 269.

82. Borle, J.B. and Loveday, J. 1968 Effects of Temperature, Potassium, and Calcium on the Electrical Potential Difference in HeLa Cells. Cancer Research 28: 2401.

83. Okada, Y., Ogawa, M., Aok, N., and Izutsu, K. 1973 The Effect of K^+ on the Membrane Potential in HeLa Cells. Biochem. Biophys. Acta 291: 116.

84. Tokuoka, S. and Morioka, H. 1957 The Membrane Potential of the Human Cancer and Related Cells. I. Gann 48: 353.

85. Chowdhury, T.K. and Chou, A. 1973 J. Nat. Can. Inst. (in press)

86. Cone, C.D., Jr. 1971 Unified Theory on the Basic Mechanism of Normal Mitotic Control and Oncogenesis. J. Theo. Biol. 30: 151.

87. Cone, C.D., Jr. 1969 Electroosmotic Interactions Accompanying Mitosis Initiation In Sarcoma Cells In Vitro. Trans. N.Y. Acad. Sci. 31: 404.

88. Cone, C.D., Jr. and Tongier, M. 1970 Control of Cell Division By the Electrical Voltage of the Surface Membrane. Paper, The American Cancer Society, March.

89. Cone, C.D., Jr. and Tongier, M. 1973 Electrical Transmembrane Potential Changes Accompanying Contact Inhibition of Mitosis in Confluent Cultures. A-65: Proc. Tissue Culture Assoc., Inc., In Vitro 8.

90. Cone, C.D., Jr. NASA, Molecular Biology Laboratory, Langley AFB, Virginia. personal communication.

91. Sumner, J.B. and Howell, S.F. 1936 The identification of the Hemagglutinin of the Jack Bean with Concanavalin A. J. Bacteriol. 32: 227.

92. Goldstein, I.J., Hollerman, C.E., and Smith, E.E. 1965 Protein-Carbohydrate Interaction. II. Inhibition Studies on the Interaction of Concanavalin A with Polysaccharides. Biochemistry 4: 876.

93. Sharon, N. and Lis, H. 1972 Lectins: Cell-Agglutinating and Sugar Specific Proteins. Science 177: 949.

94. Edelman, G.M., Cunningham, B.A., Reeke, G.N., Becker, J.W., Waxdal, M.J., and Wang, J.L. 1972 The Covalent and Three-Dimensional Structure of Concanavalin A. Proc. Nat. Acad. Sci. 69: 2580.

95. Waxdal, M.J., Wang, J.L., Pflumm, M.N., and Edelman, G.M. 1972 Isolation and Proteolytic Cleavage of the Intact Subunit of Concanavalin A. Biochemistry 11: 3233.

96. Cunningham, B.A., Wang, J.L., Pflumm, M.N., and Edelman, G.M. 1972 Isolation and Order of the Cyanogen Bromide Fragments of Concanavalin A. Biochemistry 10: 3343.

97. Moller, G., Andersson, J., Pohlit, H., and Sjoberg, O. 1973 Quantitation of the Number of Mitogen Molecules Activating DNA Synthesis in T and B Lymphocytes. Clin. Exp. Immunol. 13: 89.

98. Yuhara, I. and Edelman, G.M. 1972 Restriction of the Mobility of Lymphocyte Immunoglobulin Receptors by Concanavalin A. Proc. Nat. Acad. Sci. 69: 608.

99. Berlin, R.D. 1972 Effect of Concanavalin A on Phagocytosis. Nature New Biol. 235: 44.

100. Friberg, S., Golub, S.H., Lilliehook, B., and Cochran, A.J. 1972 Assessment of Concanavalin A Reactivity To Murine Ascites Tumours by Inhibition of Tumour Cell Migration. Exptl. Cell. Res. 73: 101.

101. Ozanne, B. and Sambrook, J. 1971 in The Biology of Oncogenic Viruses, North-Holland Publishing Co., Amsterdam.

102. Wright, J.A. 1973 Evidence For Pleiotropic Changes In Lines of Chinese Hamster Ovary Cells Resistant To Concanavalin A and Phytohemagglutinin-P. J. Cell Biol. 56: 666.

103. McNutt, N.S., Culp, L.A., and Black, P.H. 1973 Contact-Inhibited Revertant Cell Lines Isolated From SV40-Transformed Cells. J. Cell Biol. 56: 412.

104. Burger, M.M. 1973 Paper, American Association for Cancer Research, March.

105. Weston, J.A. and Hendricks, K.L. 1972 Reversible-Transformation by Urea of Contact-Inhibitied Fibroblasts. Proc. Nat. Acad. Sci. 69: 3727.

106. Burger, M.M. and Goldberg, A.R. 1967 Identification of a Tumor-Specific Determinant on Neoplastic Cell Surfaces. Proc. Nat. Acad. Sci. 57: 359.

107. Akedo, H., Mori, Y., Kobayashi, M., and Okada, M. 1972 Changes of Isoelectric Points of Concanavalin A Induced by the Binding of Carbohydrates. Biochem. Biophys. Res. Commun. 49: 107.

108. Friberg, S., Cochran, A.J., and Golub, S.H. 1971 Concanavalin A Inhibits Tumour Cell Migration. Nature New Biol. 232: 121.

109. Eisenberg, S., Ben-Or, S., and Doljanski, F. 1962 Electrokinetic Properties of Cells In Growth Processes. I. The Electrophoretic Behavior of Liver Cells During Regeneration and Postnatal Growth. Exptl. Cell Res. 26: 451.

110. Whitney, R. B. and Sutherland, R. M. 1972 Enhanced Uptake of Calcium by Transforming Lymphocytes. Cell Immunol. 5: 137.

111. Robbins, E. and Pederson, T. 1971 On the Role of Ions In Mitosis. In Vitro 6: 323.

112. Poste, G. 1972 Changes In Susceptibility of Normal Cells To Agglutination by Plant Lectins Following Modification of Cell Coat Material. Exptl. Cell Res. 73: 319.

113. Moscona, A. A. 1971 Embryonic and Neoplastic Cell Surfaces: Availability of Receptors for Concanavalin A and Wheat Germ Agglutinin. Science 171: 905.

114. Powell, A. E. and Leon, M. A. 1970 Reversible Interaction of Human Lymphocytes with the Mitogen Concanavalin A. Exptl. Cell Res. 62: 315.

115. Rosenblith, J. Z., Ukena, T. E., Yin, H. H., Berlin, R. D., and Karnovsky, M. J. 1973 A Comparative Evaluation of the Distribution of Concanavalin A - Binding Sites on the Surfaces of Normal, Virally-Transformed, and Protease-Treated Fibroblasts. Proc. Nat. Acad. Sci. 70: 1625.

116. Atchley, W. A., Bhagavan, N. V., and Masouredis, S. P. 1964 Influence of Ionic Strength on the Reaction Between Anti-D and D-Positive Red Cells. J. Immunol. 93: 701.

117. Pollack, W., Hager, H. J., Reckel, R., Toren, D., and Singher, H. 1965 A Study of the Forces Involved in the Second Stage of Hemagglutination. Transfusion 5: 158.

118. Goldman, D. E. 1943 Potential, Impedance, and Rectification in Membranes. J. Gen. Physiol. 27: 30.

119. Goldman, D. E. (as presented by Tupper, J. T. 1972 The Ionic Basis of the Membrane Potential in the Early Asterias Embryo. Dev. Biol. 29: 273.)

120. Merchant, D. J., Kahn, R. H., and Murphy, W. H. 1967 in Handbook of Cell and Organ Culture. Burgess Publishing Co., New York.

121. Schaefer, A. E., Hempling, H. G., Handler, E. E., and Handler, E. S. 1972 Measurement of the Electrical Potential Difference and the Distribution of Ions in the Shay Chloroleukemic Tumor Cell. Cancer Research 32: 1170.

122. Kapeller, M. and Doljanski, F. 1972 Agglutination of Normal and Rous Sarcoma Virus-Transformed Chick Embryo Cells by Concanavalin A and Wheat Germ Agglutinin. Nature New Biol. 235: 184.

123. Chowdhury, T. K. 1969 Fabrication of Extremely Fine Glass Micropipette Electrodes. J. Sci. Instruments 2: 1087.

124. Li, J. C. R. 1969 in Statistical Inference I. Edwards Brothers, Inc., Ann Arbor, Michigan.

125. Williams, J. A., Withrow, C. D., and Woodbury, D. M. 1971 Effects of Ouabain and Diphenylhydaution on Transmembrane Potentials, Intracellular Electrolytes, and Cell pH of Rat Muscle and Liver, in vivo. J. Physiol. 212: 101.

126. Baker, P. F., Hodgkin, A. L. and Shaw, T. I. 1962 The Effects of Changes In Internal Ionic Concentrations on the Electrical Properties of Perfused Giant Axons. J. Physiol. 164: 355.

127. Sachs, H. G. and McDonald, T. F. 1972 Membrane Potentials of BHK (Baby Hamster Kidney) Cell Line: Ionic and Metabolic Determinants. J. Cell. Physiol. 80: 347.

128. Hodgkin, A. L. and Katz, B. 1949 The Effect of Sodium Ions on the Electrical Activity of the Giant Axon of the Squid. J. Physiol. 108: 37.

129. Schanne, O. and Coraboeuf, E. 1966 Potential and Resistance Measurements of Rat Liver Cells, in situ. Nature 210: 1390.

130. Cereijido, M. and Rotunno, C. A. 1970 Introduction to the Study of Biological Membranes, Gordon and Breach, Science Publishers, Inc., New York, New York.

131. Thomas, R. C. 1972 Electrogenic Sodium Pump in Nerve and Muscle Cells. Physiol. Rev. 52: 563.

132. Wickson-Ginzburg, M. and Solomon, A. K. 1963 Electrolyte Metabolism in HeLa Cells. J. Gen. Physiol. 46: 1303.

133. Cass, Carol 1972 Density-Dependent Fluctuations In Membrane Permeability In Logarithmically Growing Cell Cultures. Exptl. Cell Res. 73: 140.

134. Aaronson, S. A. and Todaro, G. J. 1968 Basis for the Acquisition of Malignant Potential by Mouse Cells Cultivated in vitro. Science 162: 1024.

135. Salzberg, S. and Raskas, H. J. 1972 Surface Changes of Human Cells Productively Infected with Human Adenoviruses. Virology 48: 631.

136. Yan, T. M. and Weber, M. J. 1972 Changes In Acyl Group Composition of Phospholipids from Chicken Embryonic Fibroblasts After Transformation by Rous Sarcoma Virus. Biochem. Biophys. Res. Comm. 49: 114.

137. Salzman, N. F. 1971 Biochemical Aspects of Viral Transformation. In Vitro 6: 349.

138. Fischer, G. A. and Sartorelli, A. S. 1964 Development, Maintenance and Assay of Drug Resistance. Methods in Med. Res. 10: 247.

139. Smith, J. D., Freeman, G., Vogt, M., and Dulbecco, R. 1960 The Nucleic Acid of Polyoma Virus. Virology 12: 185.

140. Noble, D. 1965 Electrical Properties of Cardiac Muscle Attributable to Inward Going Rectification. J. Cell Comp. Physiol. 66: 127.

141. Lowry, O. H., Rosenbrough, N. J., Farr, A. L., and Randall, K. J. 1951 Protein Measurement with the Folin Phenol Reagent. J. Biol. Chem. 193: 265.